FREEHAND THREE-DIMENSIONAL ULTRASOUND TO EVALUATE SCAPULAR MOVEMENT

by

Lynn A. Worobey

BS, Worcester Polytechnic Institute, 2008

Submitted to the Graduate Faculty of

Swanson School of Engineering in partial fulfillment

of the requirements for the degree of

Doctor of Philosophy

University of Pittsburgh

2013

UNIVERSITY OF PITTSBURGH

SWANSON SCHOOL OF ENGINEERING

This dissertation was presented

by

Lynn A. Worobey

It was defended on

May 7, 2013

and approved by

Jennifer L. Collinger, PhD, Assistant Professor, Physical Medicine and Rehabilitation

Anthony Delitto, PhD, PT, Associate Dean for Research, School of Health and Rehabilitation

Sciences

Shawn S. Farrokhi, DPT, PhD, Assistant Professor, Physical Therapy

Alicia Koontz, PhD, Associate Professor, Rehabilitation Science and Technology

Dissertation Director: Michael L. Boninger, MD, Chair, Physical Medicine and Rehabilitation

FREEHAND THREE-DIMENSIONAL ULTRASOUND TO EVALUATE SCAPULAR MOVEMENT

Lynn A Worobey, PhD

University of Pittsburgh, 2013

Altered scapular kinematics have been linked to increases in shoulder pain and pathology. As such, identifying normal scapular movement is integral to preventing pathology and maintaining health of the joint. Existing methods to evaluate scapular movement are invasive, expensive, require exposure to radiation, suffer skin based motion artifacts, or allow for examination only in static postures. Freehand three-dimensional ultrasound offers the unique ability to image bone while being non-invasive, relatively low cost, and free of radiation. This is a novel application of a technology that in the past has been used for needle guided injections and determining changes in organ volumes, but never for evaluating bone movement. We have developed a custom freehand-ultrasound system that shows high repeatability across trials (SEM < 2°) in evaluating scapular kinematics in static postures with the arm at rest and elevated in the sagittal, frontal and scapular planes. Among manual wheelchair users and able-bodied controls we found scapular kinematics with the arm in an elevated position were predicted by scapular and trunk position at rest. We also found BMI ≥ 25, presence of pathology on a physical exam, shoulder abnormalities on a clinical ultrasound exam, and greater than 10 years of wheelchair use resulted in scapular postures associated with shoulder pathology in previous studies. We found no significant differences between wheelchair users and age-matched controls but attribute this to a lack of difference in pathology between the groups. A learning curve was identified over time for

capturing quality ultrasound images and it is suggested future studies incorporate ample training time and require raters to meet minimum performance measures set forth by this study. In a subsample of subjects we found increases in external rotation, upward rotation and posterior tilting at incremental angles of humeral elevation during dynamic trials indicating that it is feasible to apply our methods to evaluate dynamic scapular movement. Application of these methods may help to identify shoulder pathology and evaluate the efficacy of interventions to correct altered scapular kinematics.

TABLE OF CONTENTS

LIST OF TABLES

LIST OF FIGURES

xiii

ACKNOWLEDGEMENTS

I would first and foremost like to thank my parents, their constant love and support made this journey possible. They have encouraged me through every step of my academic career and instilled in me the ability to 'adapt and overcome'. I would also like to thank to Ben who believed I was capable of far more than I ever thought, spent nights listening to me talk about point cloud transformations, and embraced my excitement for the CAT and desire to pursue PT school. Dr. Boninger has been an outstanding mentor, guiding me through this research process and helping me from 'getting lost in the trees'. I owe him a sincere amount of gratitude and look forward to joining him in the field of rehabilitation. Research is a group effort and my HERL family, study participants, and friends were integral to me learning the ropes, completing this study, and remembering there was a life outside of research. Lastly, I'd like to thank the CAT clinicians for helping lead me to my next stage of life by exposing me to the world of seating mobility and the life changing effects it can have.

1.0 INTRODUCTION

1.1 MOTIVATION

The shoulder is a common site of injury across many populations. As the most mobile joint in the body, it is not surprising that there is a high prevalence of disorders at this joint. Thirty-five percent of those over the age of 65 report shoulder problems. [1-2] Shoulder impingement is found in 16-40% of assembly line workers, steelworkers, and construction workers.[3] Among construction workers, working above shoulder level has shown a dose response with shoulder pain. [4] An epidemiological study of shoulder pain found a prevalence of 29% across athletes.[5] Among wheelchair athletes 33% report chronic shoulder pain.[6] The prevalence of pain is even more concerning when the failure of clinical interventions to resolve pain is taken into account. Across the general population in the Netherlands, 21% of individuals reported shoulder pain to their primary care physician and 40-50% of those reporting continuing unresolved symptoms after prescribed treatment. [7]

Individuals are at increased risk for shoulder pathology when exposed to high forces, awkward postures, and repetitive movements. [7] Wheelchair users are exposed to all of these factors in activities of daily living. The prevalence of shoulder pain is accordingly higher among wheelchair users. Among individuals with spinal cord injury (SCI) 31-73% report shoulder pain.[6, 8-11] For this population shoulder pain limits mobility as well as independence. Shoulder

pain can preclude independence in transfers, dressing, feeding, and hygiene.[12] Impaired

occupational performance in individuals with SCI as well as difficulty with propulsion, transfers,

driving, cleaning, and cooking have been found as a result of shoulder pain.[13] The presence of

shoulder dysfunction among individuals with SCI significantly affects function and has been

shown to decreases quality of life.[14-15]

Unfortunately, surgical intervention can be debilitating in activities of daily living and

mobility and conservative treatment of shoulder pain is not always successful. In the able-bodied

population it is recommended that patients avoid pushing, pulling, reaching and carrying for

several months following surgery.[16] It would be difficult for wheelchair users to avoid these

same activities and maintain and active lifestyle acknowledging the demands of wheelchair

propulsion, transfers, and weight relief lifts. Surgical repair of rotator cuff tears has been

associated with a 2-4 month period following surgery before normal transfers and propulsion

could be presumed.[16] Beyond these extended periods of restriction, surgery is not always

successful. A retrospective study found that rotator cuff repairs did not result in improvements in

function or range of motion.[17] Conservative treatments are also subject to criticism with routine

therapies proving ineffective among individuals with spinal cord injury.[18] As such, it is critical

to emphasize prevention of shoulder pathology and better interventions. Scapular kinematics

have been shown to be related to a multitude of shoulder problems.[3, 19-33] Existing methods to

evaluate scapular kinematics are limited by invasiveness, cost, restricted movement, and

exposure to radiation. Freehand three-dimensional ultrasound has the potential to overcome these

limitations and allow for visualization of scapular movement. The goal of this study is to develop

and validate techniques for use of freehand three-dimensional ultrasound to evaluate scapular

movement during reaching tasks and detect changes in kinematics with pathology.

1.2 SHOULDER DISORDERS

Across general practitioners, shoulder problems follow only the neck and low back in reported frequency.[34-35] Shoulder and neck disorders constitute 18% of disability costs for musculoskeletal problems in Sweden.[36] In the United States the cost of treating shoulder dysfunction in 2000 was $7 billion. [37] A prospective cohort study found that only 20% of shoulder problems had been resolved in 6 months and 50% after 18 months.[38] A separate study on 443 patients found only 32% reported symptom recovery after one year.[39] A prospective descriptive study examined the outcome of individuals treated with NSAIDs, physiotherapy, injection therapy and manipulation therapy as prescribed by a primary care physician found that shoulder problems persisted after 26 weeks for 51% of individuals and after 12-18 months for 41% of individuals.[40] In some instances pain and limited range of motion can be found years after follow up.[41] Among the elderly population 74% face unresolved shoulder problems 3 years after initial diagnosis.[42]

1.2.1 Treatment and Interventions

Shoulder pathology spans a wide range of conditions including bursitis, tendinitis, adhesive capsulitis, impingement, avascular necrosis, glenhohumeral osteoarthritis, and rotator cuff tears. [37, 43] In instances when surgery is required, an anterior acromiplasty or arthroscopy subacromial decompression will generally be performed. [44-46] The goal of these surgical interventions is to increase the subacromial space and avert compression of soft tissues. Surgical

interventions are often associated with poor outcomes and have a significant limiting impact on functioning and activities of daily living among wheelchair users.[6, 16-17] Since surgery is invasive, limits function, and is not always successful, conservative treatments are often pursued. Unfortunately, it has been demonstrated that conservative treatments are not effective in alleviating pain among individuals with SCI and do not have consistent outcomes.[18] As such, prevention is very important. For prevention of shoulder pathology it is recommended individuals avoid repetitive movements, extreme postures and high forces. [47] Unfortunately this is not always possible due to the nature of wheelchair propulsion and transfers. Early intervention has been shown to be associated with a faster recovery so it is critical we are able to identify differences in populations.[48] We will investigate the relation between pain and pathology and scapular kinematics among wheelchair users. Identifying changes in kinematics may allow for earlier detection of pathology.

1.3   SCAPULAR MOVEMENT

The scapula is part of three joint interfaces (scapulothoracic, acromioclavicular, and glenohumeral). The scapula is flat which allows it to glide along the thoracic wall as it translates and rotates.[20] It is a broad bone that provides surface area for the attachment of 17 muscles, 11 of which originate on the scapula. Proper positioning of the scapula is integral to maintain proper length-tension relationships of these muscles. [20] The scapula is able to translate in two directions to produce elevation/depression and abduction/adduction. Additionally, the scapula can rotate about three axes to produce internal/external rotation, upward/downward rotation, and anterior/posterior tilting (Figure 1).
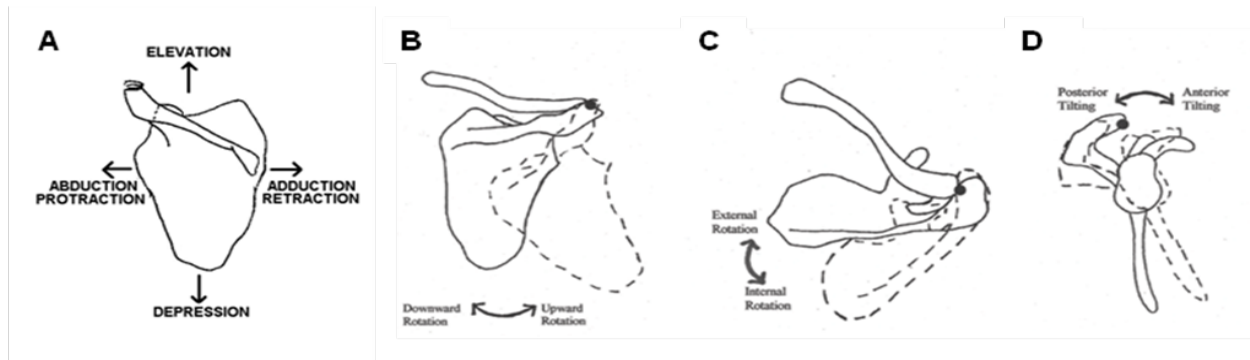
Figure 1: Scapular Translations and Rotations, Adapted From: (54)

During the initial phase of arm elevation the serratus anterior and upper trapezius are the primary scapular movers. As the arm is raised past 80 degrees the lower trapeizus is activated to contribute to elevation.[49] During humeral elevation the scapula will upwardly rotate, posteriorly tilt and externally rotate.[50] These movements move the acromion away from the head of the humerus. As a multi-joint interface and base for so many muscles, abnormal scapular movement has a significant effect on the entire shoulder complex.[51] Altered scapular kinematics have been found to be associated with rotator cuff pathology[19, 21-22], impingement[3, 23-24, 26, 28, 52-54], shoulder instability[24, 29-31], and adhesive capsulitis as is seen with frozen shoulders.[25, 32-33, 55] This pathologic movement can be a result of accommodating pain, muscle imbalance, or altered muscle firing.

Impingement is the compression of the tendons of the rotator cuff against the coracoacromial arch when the arm is elevated.[56] Among the theorized causes of impingement are bony abnormalities, degeneration of the rotator cuff, glenohumeral instability, repetitive stresses, hooked acromial shape, decreased blood supply, thoracic kyphosis, acromioclavicular arthrosis, and altered muscle function.[20, 47, 57-59] Narrowing of the supraspinatus outlet can also result from

altered scapular movement. [20, 58, 60] Individuals with impingement exhibit decreased upward rotation[3, 51], decreased posterior tipping[3, 23, 51] and increased internal rotation of the scapula[3]. In these instances, the scapula does not move properly and the greater tuberosity is not able to achieve the proper clearance, reducing the subacromial space. The subacromial space is a critical area that houses bursa and rotator cuff tendons. Compression of these tendons can cause pain and also lead to tearing. One study showed that increased anterior tilting of the scapula of just 7° can decrease the subacromial space by twenty-five percent.[61] Another study found individuals with impingement demonstrated less posterior tilting ($25.1\pm9°$) than those without impingement ($34.6\pm9.7°$).[23] In contrast, other studies report decreased upward rotation, increased posterior tilting, or no differences between groups.[52, 54 3, 26, 62] The lack of agreement across studies indicates that this topic warrants further investigation. As there is a large prevalence of shoulder pathology among wheelchair users and shoulder pathology has been linked to altered scapular kinematics, we expect to find differences in scapular movement between controls and wheelchair users. We hypothesize wheelchair users will present with increased upward rotation and internal rotation when raising their arm in the scapular plane

1.4   MEASUREMENT OF SCAPULAR KINEMATICS

As the field of biomechanics has grown, the techniques to evaluate scapular kinematics have also expanded. Early studies on scapular movement used x-ray however this method exposes the subject to radiation and requires static positions. [63-64] Further, there may be errors associated with the projection and analysis is limited to only one rotation. Biplanar radiography addresses some of the shortcomings of x-ray but it still exposes the subject to radiation and a short protocol is

required to minimize exposure. [65-66] Magnetic resonance imaging (MRI) is another imaging modality that has been used to evaluate scapular movement.[67] While the images are of high quality and allow for landmark identification, MRI is expensive, not readily available, and the setup may not be compatible to mimic functional tasks. Additionally, MRI does not allow for evaluation of dynamic movement, only static postures can be examined. Bone pins are considered the gold standard for measuring scapular movement but they are highly invasive and usually studies have smaller sample sizes because of this.[68-69]

Goniometers are non-invasive and do not expose subjects to radiation but suffer from measurement inaccuracies. [70-71] One study found that measurements differed by at least 8 degrees across raters.[71] Digitizers have been used that work with optical or electromagnetic sensors have been used to digitize scapular landmarks with palpation.[23, 72-75] This method is limited by the accuracy of the palpation and can only be applied to static postures. Soft tissue located above the scapula can also affect the accuracy of this method. Skin based marker systems consist of acromial sensors[76], an acromial jig with position sensors[76-78], and electromagnetic sensors[3, 21, 51, 79-80]. In a comparative study between an acromial jig, acromial sensors, and bone pins (gold standard) it was found that the jig better estimated posterior tilt external rotation, the acromial method better estimated upward rotation, and both methods were inaccurate at ranges of motion greater than 120 degrees.[76] For skin based methods correction models have been developed to account for movement artifacts that result from the scapula sliding under the skin. However, in some studies the sample sizes are small so the generalizability of these models may be questionable.[76] In contrast to other non-invasive methods for evaluating scapular movement, freehand three-dimensional ultrasound is not subject to skin movement artifacts and is less likely to be affected by varying amounts of soft tissue between the bone and surface of the skin.

Ultrasonography allows for the direct visualization of the scapula provided by biplanar radiography and MRI without the harmful ionizing radiation or high costs. Additional benefits of this method include low cost, wider availability, and potential to evaluate both static and dynamic postures.

1.5   FREEHAND THREE-DIMENSIONAL ULTRASOUND

Freehand three-dimensional ultrasound pairs ultrasound with motion tracking to create a three-dimensional reconstruction. This technology is not a new concept in medical imaging and has been used to image the fetus, heart, gall bladder, kidney and prostate.[81-85] Freehand three-dimensional ultrasound has been primarily used for soft tissue examination or registration of organ volumes and has never been applied to examine bone or joint movement. Despite its lack of use for these applications, this imaging modality presents significant promise for evaluating bone movement.

Ultrasound allows for direct imaging of the bone and is a relatively unexplored modality for analyzing shoulder biomechanics. Ultrasound offers the benefits of being non-invasive and comparatively inexpensive. Bone is easily visualized in musculoskeletal imaging with ultrasound due to its high impedance compared to surrounding tissues (Figure 2). An ultrasound image is composed of grayscale pixels with values ranging from 0 (black) to 255 (white). Bone appears very hyperechoic in images (white) in contrast to surrounding soft tissues, that are fluid filled and appear more hypoechoic. Compared to soft tissues, which are anisotropic and sensitive to probe orientation, the cortical surface of bone is less subject to change in appearance. These properties of bone make it well suited for evaluation with ultrasound.

8
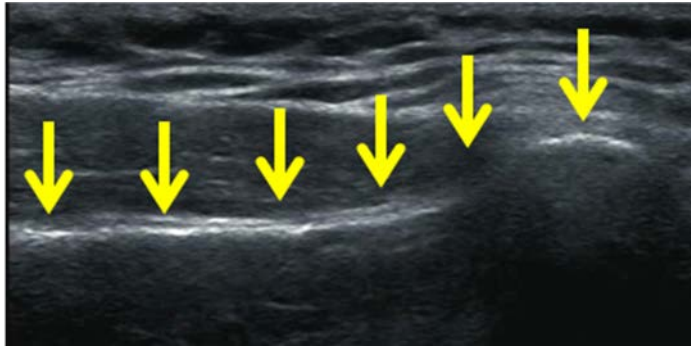
Figure 2: Highly Echogenic Scapula Bone Surface

By pairing ultrasound with motion capture, it becomes a useful tool for evaluating scapular movement. An attached position sensor makes it possible to determine the location of 2D images in global space. The attached position sensor allows for freedom of movement (hence 'freehand') in which there are no restrictions on the path or speed of scanning. Unlike MRI or CT the spacing of the images is not regular and it depends on movement by the operator. The freedom of movement of the probe makes it possible to guide the ultrasound probe along the border of the scapula (Figure 3). The freedom to image along these edges at any probe orientation makes it possible to image not only static positions, but also movement.

Figure 3: Imaging Medial Border of Scapula with Freehand Three-Dimensional Ultrasound

1.6   RESEARCH GOALS

The goal of this study was to develop and validate techniques for use of freehand three-dimensional ultrasound to evaluate scapular movement during reaching tasks and detect changes in kinematics with pathology. A custom system was built and analysis methods were developed to create a reconstructed scapular border in global space from points of interest in two-dimensional ultrasound images. Internal/external rotation, upward/downward tilting, and anterior/posterior tilting of the scapula were determined to characterize scapular position. Chapter 2 describes calibration and components of the system as well as intra-rater reliability and

measurement error of freehand three-dimensional ultrasound to determine scapular rotations. Additionally, this chapter compares our technique to landmark digitization. Chapter 3 compares scapular kinematics between healthy controls and manual wheelchair users. Additionally, this chapter describes how scapular kinematics are related to resting posture and subject characteristics such as shoulder pathology, shoulder pain, age, body mass index, and years of wheelchair use. Further, this chapter also determines the reliability of applying this measurement technique to wheelchair users. Chapter 4 describes the application of freehand three-dimensional ultrasound to evaluate scapular position during dynamic movement in a subsample of healthy controls and wheelchair users.

2.0 RELIABILITY OF FREEHAND THREE-DIMENSIONAL ULTRASOUND TO MEASURE SCAPULAR ROTATIONS

2.1 INTRODUCTION

As the base of the shoulder, the scapula is integral to normal function of the joint. Altered scapular kinematics have been linked to shoulder pathology and impingement syndrome[3, 23-24, 54, 86]. Attempts have been made in the past to move beyond visual observation of shoulder dyskensis to more objective methods that can detect acute changes in movement and identify pathology. The gold standard to evaluate scapular movement has become bone pins. While highly accurate, this method is invasive and studies are generally limited to very small sample sizes.[87-88] Radiography has been used to visualize movement but many studies are limited to one dimension of imaging and subjects are exposed to radiation. MRI allows for three-dimensional reconstruction of the scapula but it is expensive, time consuming, and does not allow for the evaluation of functional movement. Skin based marker systems have been used in the more recent past which do not expose subjects to radiation and allow for evaluation of dynamic postures. Studies using these methods have employed acromial marker clusters, a set of markers placed above each of three bony landmarks that define the scapula local coordinate system, and electromagnetic scapular tracking devices.[23, 78-79, 89-92] Unfortunately, inherent to the scapula gliding under skin and muscle during movement, these skin based systems will always be subject

to error. In validation studies this error has been reported to be particularly pronounced at arm elevation angles above 120°.[88, 93] Digitization techniques have also been used to characterize scapula movement, however they are limited to static postures and affected by the amount of skin, muscle and adipose tissue between the bone and digitizer.[93] Based on the limitations of previous studies, we proposed the novel application of freehand three-dimensional ultrasound to evaluate scapular movement. This method involves no radiation, is comparatively low cost, can be used for evaluation of static and dynamic postures, and allows for direct visualization of the bone.

The main objective of this study was to evaluate the reliability of using freehand three-dimensional ultrasound to measure scapular rotations with the arm held in different static positions (arm at rest and elevated to 120° in the sagittal, frontal, and scapular planes). In order to evaluate the application of this method, it was first necessary to establish the reliability of freehand system. To achieve this we calibrated the system by scanning a phantom. We expected that the root mean square error (RMSE) would be less than 0.1 cm between the known and measured dimensions of the scanned phantom. Manual point selection was used to identify the scapular border in each ultrasound image. To ensure that selection was consistent across raters and within raters, we had two raters analyze 3 trials of images, 3 times each in a randomized order. We hypothesized the intra-rater and inter-rater reliability would both exceed 0.9, indicating excellent agreement.

Next, we wanted to evaluate the reliability of using our freehand system to determine scapular rotations. For this, we had one ultrasonographer perform three scans of healthy able-bodied controls' scapulae in four previously mentioned testing positions. We hypothesized that the intra-rater reliability for each scapular rotation (internal/external rotation, upward/downward

13

rotation, and upward/downward tilting) would have an intraclass correlation coefficient greater than 0.9 in each position, indicating excellent agreement. We also determined the standard error of measurement and minimal detectable difference for each testing position/scapular rotation pairing. We expected this difference would be less than 3° based on error found in previous studies.[72]

Beyond repeatability, we also wanted to evaluate how our method compared to other methods for calculating scapular rotations. As a motion capture system was already being used, we elected to use landmark digitization as our standard to compare our freehand three-dimensional ultrasound measures against. We hypothesized that there would be good reliability with an intraclass correlation coefficient of greater than 0.9. Additionally, we hypothesized there would be good agreement between the two methods as evidence by Bland Altman plots. Scapular position in these trials, determined by freehand three-dimensional ultrasound scanning and landmark digitization, would have been affected by changes in trunk or arm position. We hypothesized that our testing setup would limit these and there were be no significant differences between trials in either trunk or arm position.

2.2   METHODS

2.2.1   Freehand Three-Dimensional Ultrasound System

For this study we created a custom system for freehand three-dimensional ultrasound imaging. Ultrasound imaging was completed using a Philips HD11XE ultrasound machine equipped with

a 5-12MHz linear transducer.[1] This machine was limited to 6s of video recording and trials were approximately 1 to 7.5 minutes in length so an Epiphan Frame Grabber was used to record video collected during the trial, set at a sampling rate of 10Hz.[2] The second component of the freehand three-dimensional ultrasound system was the motion capture of the movement of the probe. In order to track the movement, the ultrasound probe was fitted with a custom orthogonal attachment equipped with Vicon markers (Figure 4).

Figure 4: Ultrasound probe fitted with custom orthogonal attachment and Vicon markers

[1] Philips Medical Systems**,** Bothell, WA

[2] Epiphan Systems, Ottawa, ON, Canada

Movement was recorded using Vicon Nexus software and 10 cameras.[3] Vicon cameras were arranged to maximize visibility of subject makers as well as the ultrasound probe, keeping in mind the need for the ultrasound operator to be in close proximity to the subject during testing (Figure 5). Vicon data was collected at a sampling frequency of 120Hz.
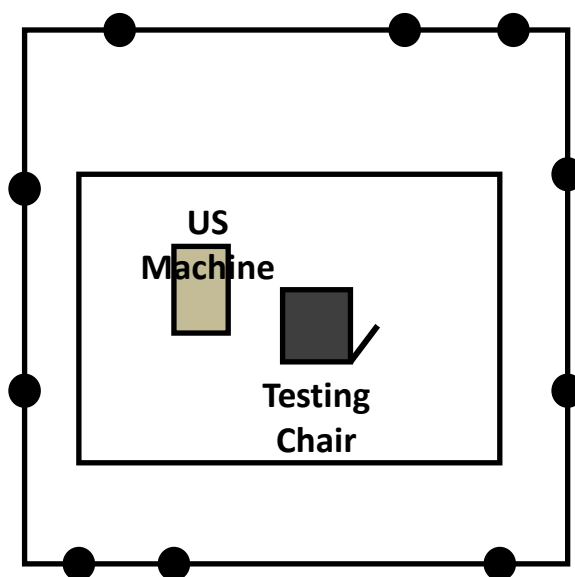
Figure 5: Testing setup with Vicon Camera placement

2.2.1.1 Calibration

Different calibration techniques have been used for freehand three-dimensional ultrasound including imaging a calibration phantom (object with known dimensions). A multi-step process was used for calibration of our freehand three-dimensional ultrasound system. To start, the Vicon motion capture system was calibrated using a standard T-frame calibration wand ensuring camera error below 0.1mm for all cameras

In order to determine the relation between the custom orthogonal attachment and the beam of the probe, 4 Vicon markers were attached to the probe aligned with the plane of the beam of scanning. A static trial was collected in which the custom orthogonal attachment and 4 attached markers were visible (Figure 6). We calculated transformations from the beam to the custom orthogonal attachment and from the custom orthogonal attachment to the global coordinate system (2.2.5).
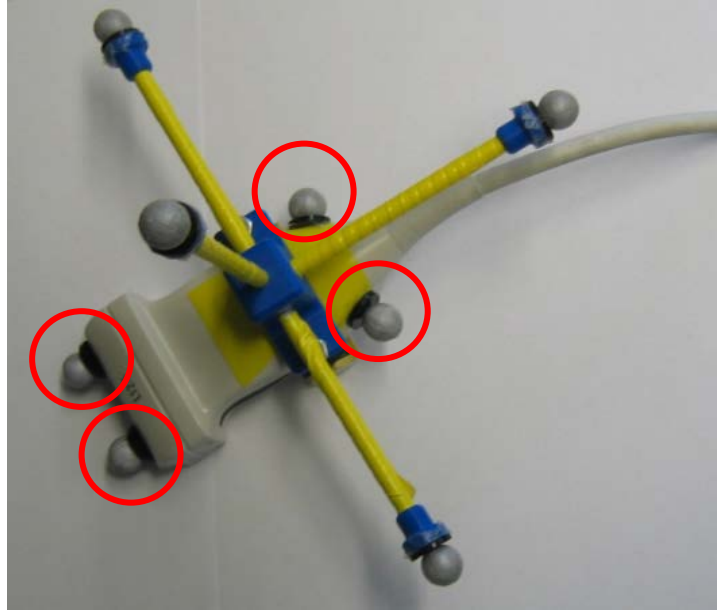
Figure 6: Additional Vicon Markers In-line with the Plane of Scanning

In order to evaluate the accuracy of this calibration method, we used our freehand three-dimensional ultrasound system to image a phantom with known dimensions (Figure 7). The phantom was immersed in water and we scanned two edges of the phantom that were parallel to each other but could not be captured together in the viewing range of the ultrasound probe. These edges were a known distance of 2.5 inches apart. Using two separate sweeps of the ultrasound probe, labeled 1 and 2 in Figure 7, each edge was scanned. This was repeated ten times for each side. Following this, the edges were identified in all images and reconstructed into three-dimensional locations in the global coordinate system. The distance between edges was calculated for each pair of sweeps and the root mean square error (RMSE) between the known and measured distances was determined. We hypothesized the RMSE would be less than 0.1 cm.
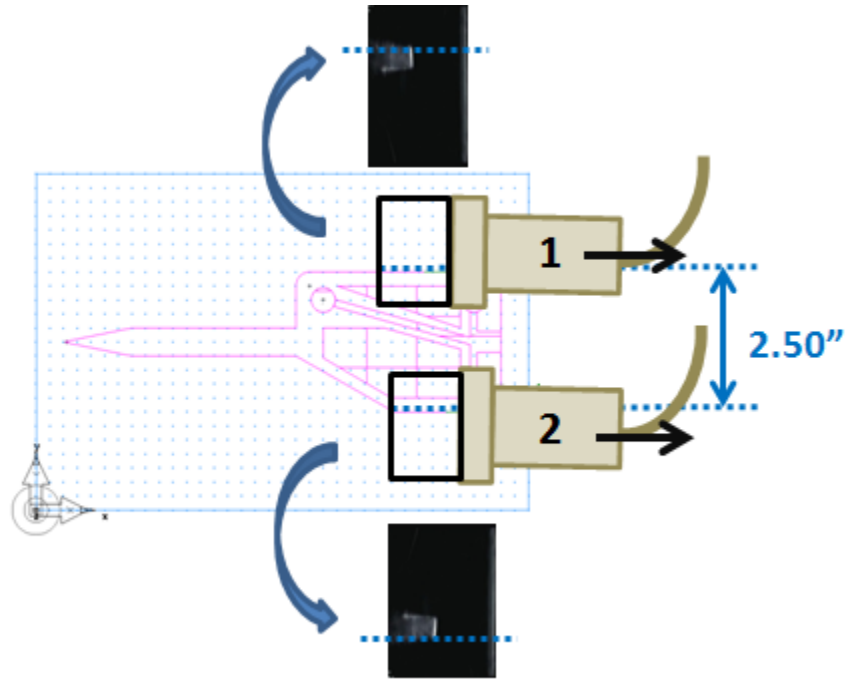
Figure 7: Phantom Scanned for System Calibration

2.2.1.2 Manual Point Selection Reliability

In trials where the scapula was scanned, the scapula was manually identified in each frame of the video. To ensure that there was no variability between raters or between multiple analyses by one rater, a reliability study was performed to determine the inter-rater and intra-rater reliability of manual identification of the scapula in ultrasound images. Three separate freehand three-dimensional ultrasound scans were taken of one individual's scapula by one operator. Two raters then analyzed each of the images from each of the three trials. One rater was experienced with identifying the scapular border and trained the second rater. Ample time was provided for the second rater to practice and view trials from other subjects. The order was randomized and raters were blinded to the trial they were viewing. Scapula identification consisted of selecting an x-y

coordinate in the ultrasound image (Figure 8). To evaluate reliability of selection of this point, the distance between this point and the image origin was determined. The intraclass correlation coefficient was used to determine the inter-rater and intra-rater reliability on manual point selection. We hypothesized that the ICC would exceed 0.90 indicating excellent reliability.
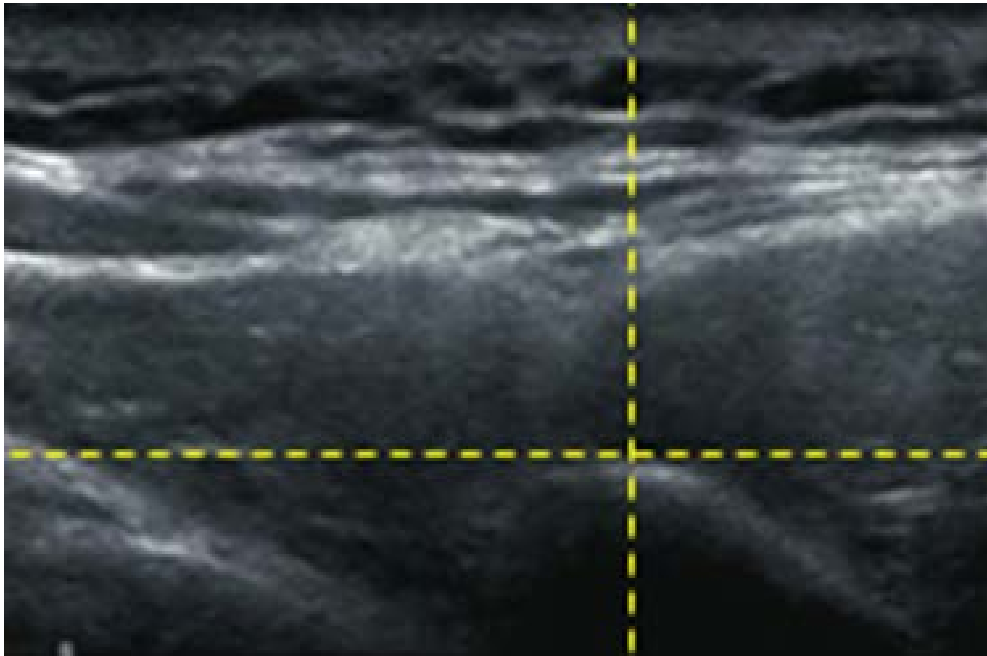
Figure 8: Identification of Scapular Border in Ultrasound Image

2.2.2 Participants

Subjects were eligible to participate in this study if they were over the age of 18, spoke English, and were able to raise their arm above their head. Subjects were excluded from this study if they had a history of fractures or dislocations in the shoulder from which they had not fully recovered,

had upper extremity impairment, weakness or spasticity that prevented smooth movement, or if they could not complete reach tasks while seated with support straps around the trunk.

2.2.3 Testing Setup

A testing chair was designed to isolate scapular movement during testing (Figure 9). The backrest of the chair was height adjustable to accommodate a multitude of torso lengths (Figure 9A). An adjustable pad (height and depth) was also placed behind the contralateral shoulder to provide support (Figure 9B). It was marked on the subject where the contralateral shoulder met the pad so the subject's posture could be readjusted if he/she shifted between trials. Additionally, the contralateral shoulder was held in place by a strap that reached from the shoulder pad, around the anterior portion of the shoulder and down to the seat of the chair (Figure 9C). An adjustable strap was also placed around the subject's trunk to minimize trunk movement (Figure 9D).

Equipped with a guide bar that was angle adjustable to each of the the testing planes (Figure 9E), the testing chair was designed to ensure consistency in holding the arm at the three elevated testing positions. For the first elevation trial, the subject raised his/her arm while maintaining contact with the guide bar until the angle of humeral elevation registered to 120° using a goniometer. A stop marker was placed on the bar and remained at this height for all elevation trials for that subject (Figure 9F). During testing the palm of the dominant hand was against the guide bar and thumb pointed upwards. Participants were also instructed to keep their head facing forward during the trial.
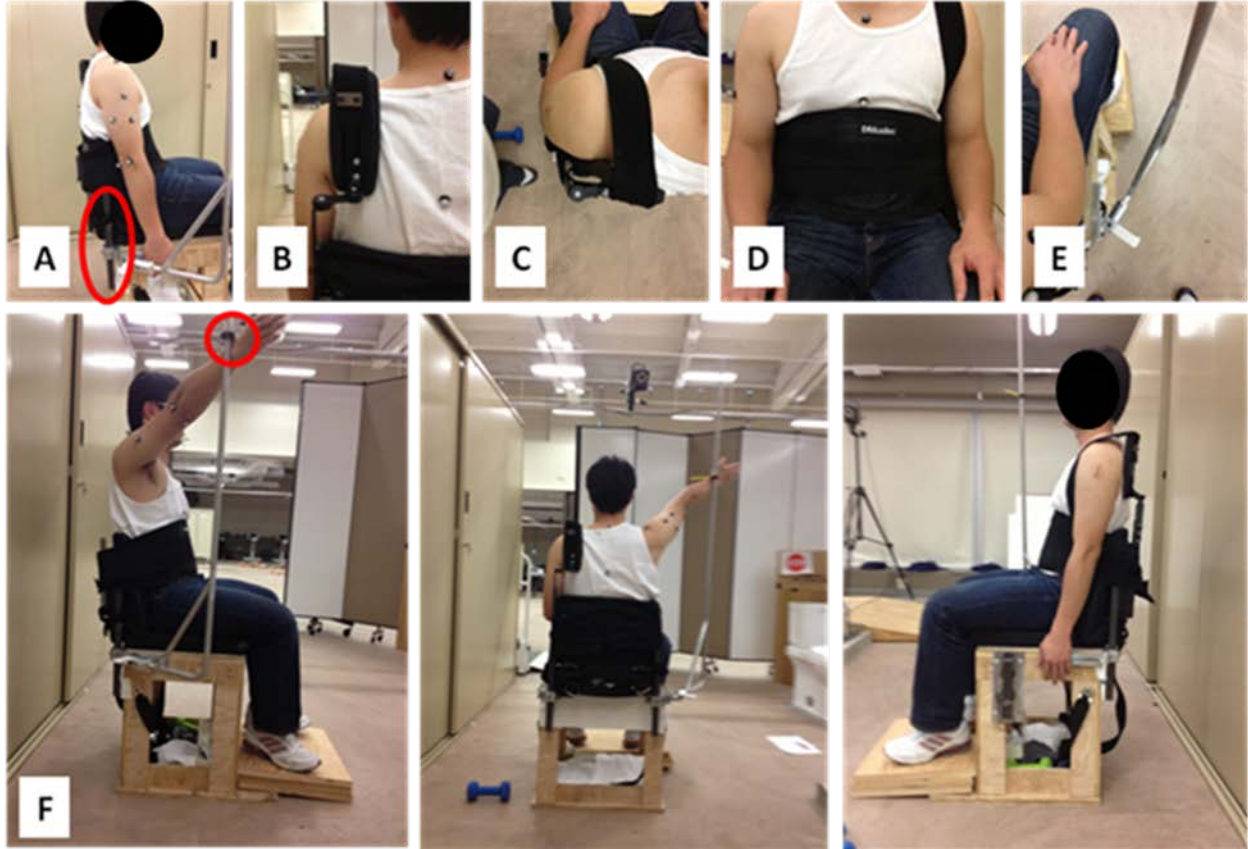
Figure 9: Testing Chair and Setup

During testing participants wore a white tank top or removed their shirt to allow for placement of Vicon markers on the trunk and dominant arm. Marker placement was determined using standards set forth by the International Society of Biomechanics[94] and included the following bony landmarks: C7, T8, anterior sternoclavicular (sternum), processus xiphoidesu (xyphoid), anterior acromioclaviculare (acromion), lateral epicondyle, and medial epicondyle (Figure 10). A triad of markers was also placed on the upper arm in case of marker dropout for the medial epicondyle. These markers allowed us to measure trunk and upper arm movement during trials.
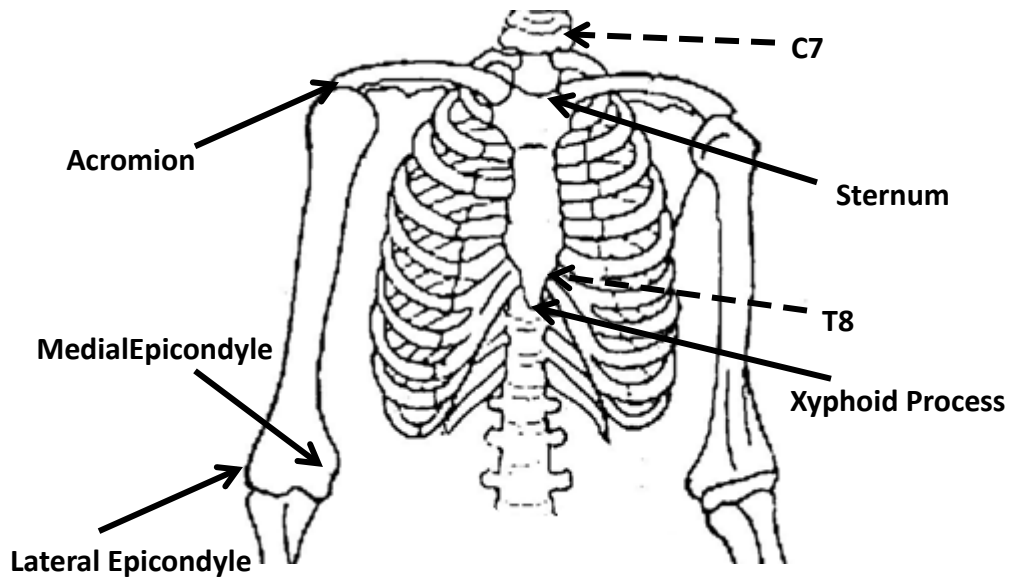
Figure 10: Vicon Marker Placement (Dash line indicates marker placed on subject's posterior)

2.2.4 Testing Procedure

2.2.4.1 Ultrasound Imaging of the Scapula

One operator performed all ultrasound scanning. The depth of the ultrasound imaging was set to 4cm for all participants. Ample ultrasound gel was applied to the skin overlaying the scapula and the probe was oriented to maintain visualization of the border of the scapula in the image. Ultrasound produces a cross-sectional image of the anatomy perpendicular to the surface of the skin.

Figure 11 illustrates a probe orientation and associated ultrasound image of the spine of the scapula. The bone in the image appears bright white and the most posterior aspect of the spine is identified by the intersection of hashed yellow lines.
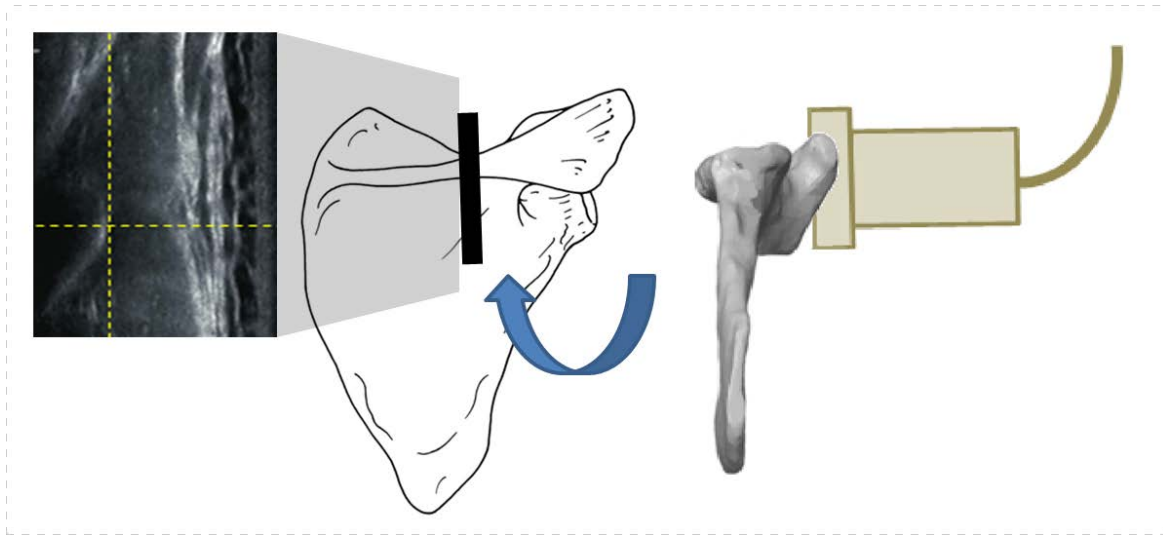
Figure 11: Imaging the spine of the scapula

Participants were imaged in four positions of interest which consisted of the arm by the participant's side at rest and humeral elevation to 120° in the sagittal, frontal, and scapular planes (30° anterior to the frontal plane). The four testing positions can be seen in Figure 12.
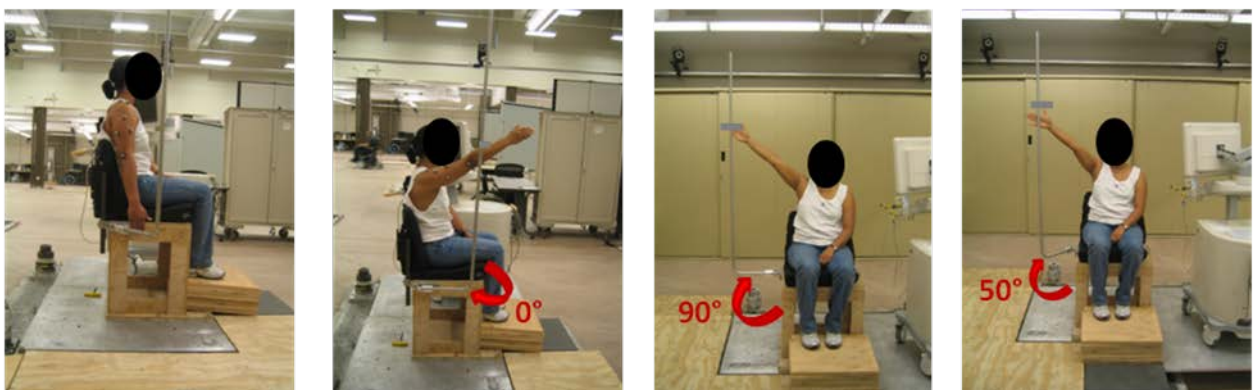
Figure 12: Testing positions: rest, sagittal plane, frontal plane, scapular plane

The scapula was imaged using the custom freehand three-dimensional ultrasound system in each position three times before moving on to the next position to evaluate reliability. A two minute rest period was provided between all trials to prevent fatigue. The subject held each position for one minute during scanning. Scanning during each trial consisted of the following six basic movements (Figure 6):

1. Placement of ultrasound probe on spine of scapula

2. Syncing movement (see: 2.2.5.2)

3. Scanning along spine of scapula

4. Removal/rotation of ultrasound probe from spine to medial border

5. Scanning along medial border of scapula

6. Removal of ultrasound probe from medial border of scapula at completion of scanning

Recording for both Vicon and ultrasound data started prior to the aforementioned steps.
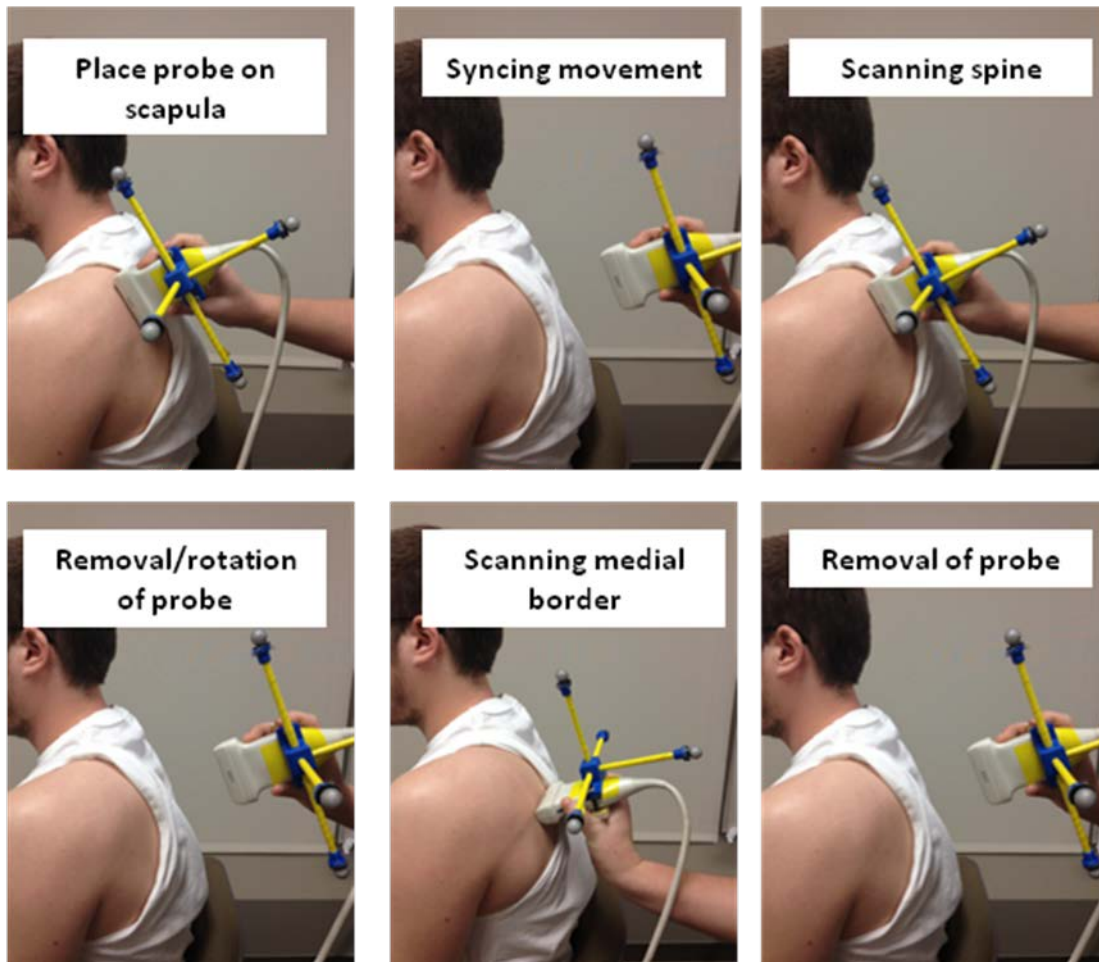
Figure 13: Six Movements during Ultrasound Scanning

2.2.4.2 Scapular Bony Landmarks Digitization

To compare our new method of imaging to current techniques of determing scapular rotations, landmark digitization was also performed. Prior to ultrasound imaging in each position, the angulus acromialis (acromial angle), trigonum spinae scapulae (root of the spine), and angulus inferior (inferior angle) were digitized (Figure 14). Digitization was performed using a custom digitizing stylus fitted with Vicon markers (Figure 15). With the participants arm in the testing position, each landmark was palpated and then digitized.
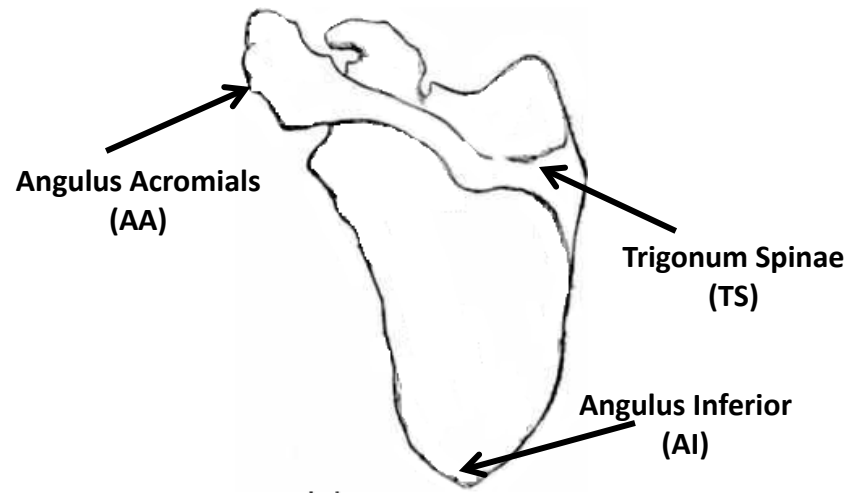
Figure 14: Digitized Scapular Landmarks

Figure 15: Digitizing Stylus with Vicon Markers

2.2.5 Data Processing

2.2.5.1 Data Collection Systems

Ultrasound video files were collected of the trial at 10Hz using an Epiphan DVI2USB Solo frame grabber. Videos were read into Matlab and written to individual image files (Appendix A). Within each image, the scapular border was manually identified as an x-y coordinate or noted as not visible using a custom written Matlab program (Appendix A). In each image, the most posterior aspect of the scapula was selected; an example can be seen in Figure 16. For each set of images, frames were analyzed in sequence to allow tracking of the scapula from one image to the next and prevent misidentification of the scapular border. In the image coordinate system, the top left corner is the origin. X-y coordinates were converted from pixels to centimeters. A reliability study was completed on three sets of videos, each analyzed three times. Two blinded raters analyzed the videos in a randomized order.
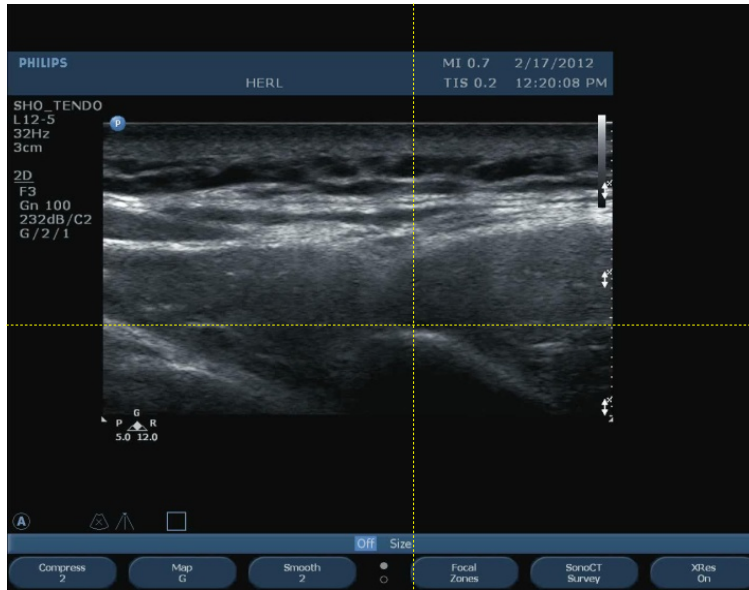
Figure 16: Selection of Scapular Border in 2D Ultrasound

Vicon data collected at 120Hz using Vicon Nexus 1.8 software. Data was exported and smoothed using a 4th order zero-lag Butterworth filter with a cutoff frequency of 5 Hz. Vicon data was converted from mm to cm.

2.2.5.2 Syncing Vicon and Ultrasound Systems

To combine Vicon and ultrasound data, it was first necessary to identify the sync, one of the six movements of the trial previously mentioned. The syncing movement consisted of moving the ultrasound probe quickly off of the surface of the skin; this movement could be detected in both the Vicon and ultrasound data sets as a sharp change in the position of the markers on the probe attachment in three dimensional space (Figure 17A) and a loss of contact with the subject in the ultrasound images (Figure 17B). For the Vicon system both the left and

right markers on the attachment were used to confirm the sync point (A). Data following the sync in each system was used for analysis.
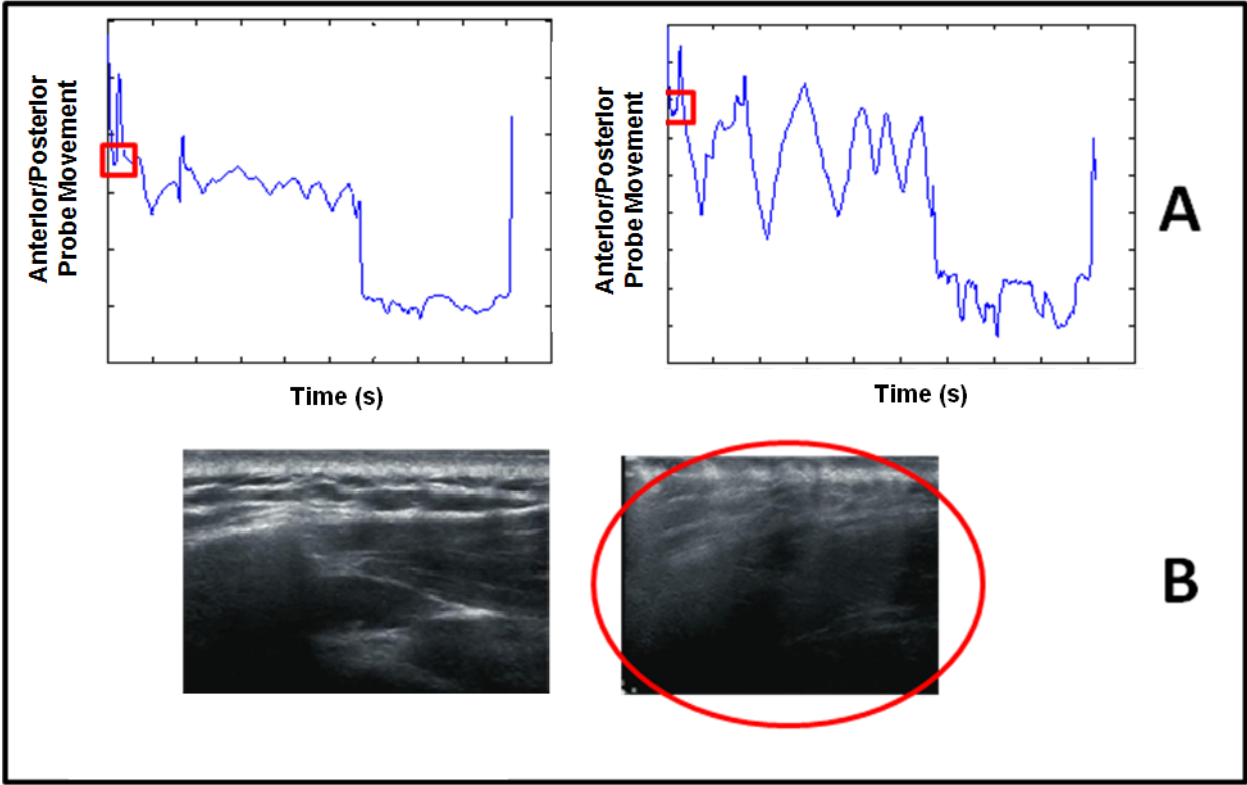
Figure 17: Identifying sync between Vicon motion capture (A) and ultrasound images (B).

It is important to note the Epiphan framegrabber has a dynamic image sampling frequency which means the rate at which it writes the video varies based on the contents of the image.[95] The range of frame rate is defined by the manufacturer based on the screen resolution. The resolution of the ultrasound screen is 1280 x 1040 which should result in a frame rate that ranges from 10-52 frames per second. This range is lower than the Philips ultrasound machine data collection rate, which is 60Hz. The manufacturer was contacted about minimizing this variation and we were advised to set our sampling frequency to be capped at 10Hz. The live sampling frequency is not recorded by the device however it is displayed on the program screen during recording. Despite setting our frame rate at 10Hz, we still discovered variations during testing based on visual observation of frame rate displayed on the screen.

This dynamic sampling frequency results in a misalignment with Vicon's fixed 120Hz sampling rate. Ultrasound images were recorded at a one-second resolution, based on a timestamp of collection embedded in the image (Figure 18). To limit error propagation, this timestamp was used for a resampling between consecutive images within the one-second period. Using optical character recognition methods, a custom Matlab program was written to tally the number of ultrasound images in each one-second time period (Appendix A). This count was used to calculate the Epiphan framegrabber's frequency during that interval.
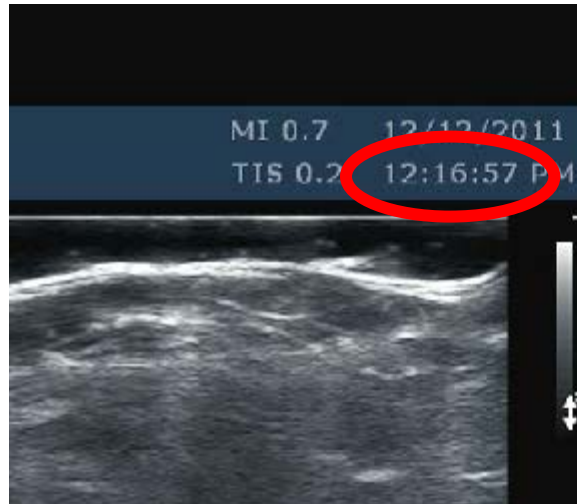
Figure 18: Timestamp (hour, minute, second) on ultrasound image

In this manner, each second of Vicon data was spline-fit using a third order polynomial and downsampled corresponding to the ultrasound time interval to the determined sampling frequency of the video recorder (6-17Hz). An illustration of this concept can be seen in Figure 19 in which the Vicon data (top) between the red arrows would be downsampled to match the number of ultrasound images (bottom) in that same window.
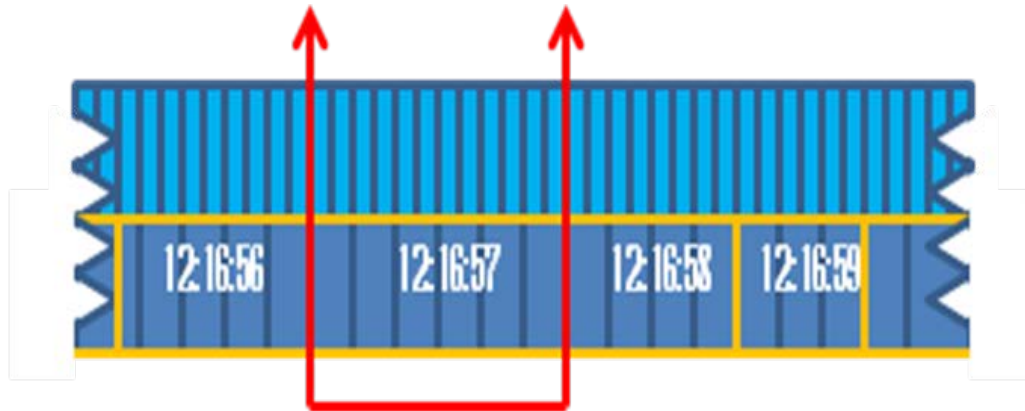
Figure 19: Linear envelopes of Vicon (top) and ultrasound (bottom) data

Vicon data during scanning portions of the trial, steps 3 and 5 of the six basic probe movements, was used for analysis. These portions were selected by identifying the end of the sync, the movement of the probe from the spine to the medial border, and the removal of the probe from subject's body after scanning the medial border, based on the position of the probe in the global coordinate system. As Vicon has higher spatial and temporal resolutions than the reconstructed data, which may be influenced by dynamic sampling frequency changes, Vicon position data of the probe was used to exclude portions of the trial when the probe was not in contact with the participant. An example of such regions can be seen in Figure 20.
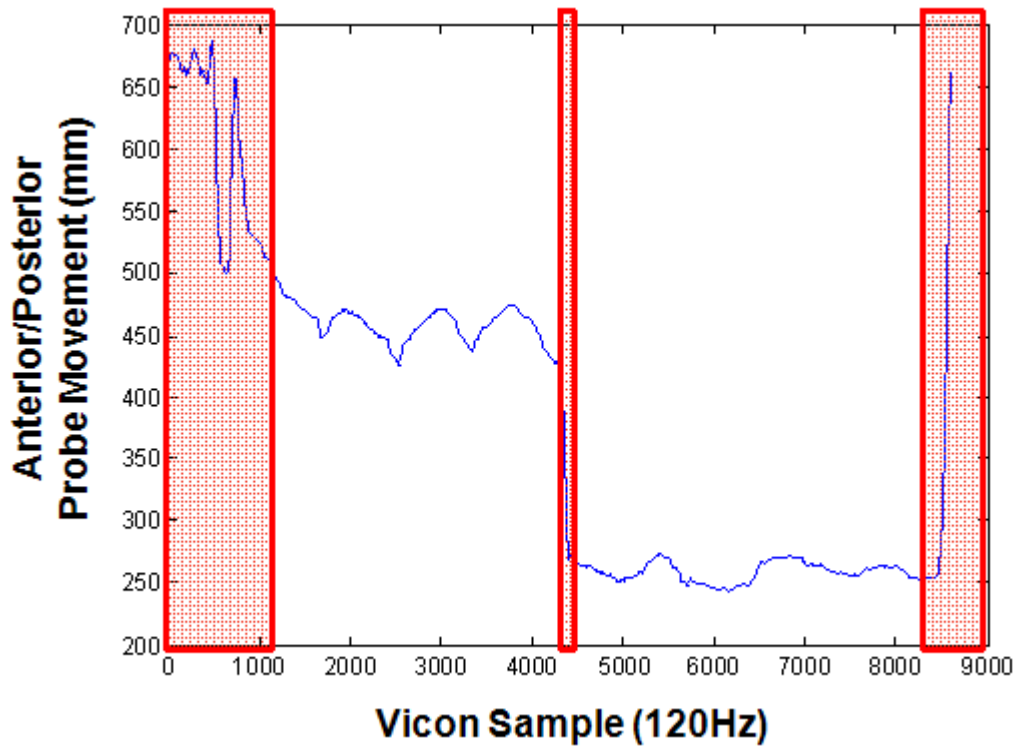
Figure 20: Portions of Vicon data when the probe was not contacting the subject

2.2.5.3 Reconstructing the Three-Dimensional Scapular Border

A series of transformations were applied to the point identified in each ultrasound image as the scapular border to determine the location of this point in three-dimensional space (Figure 21).
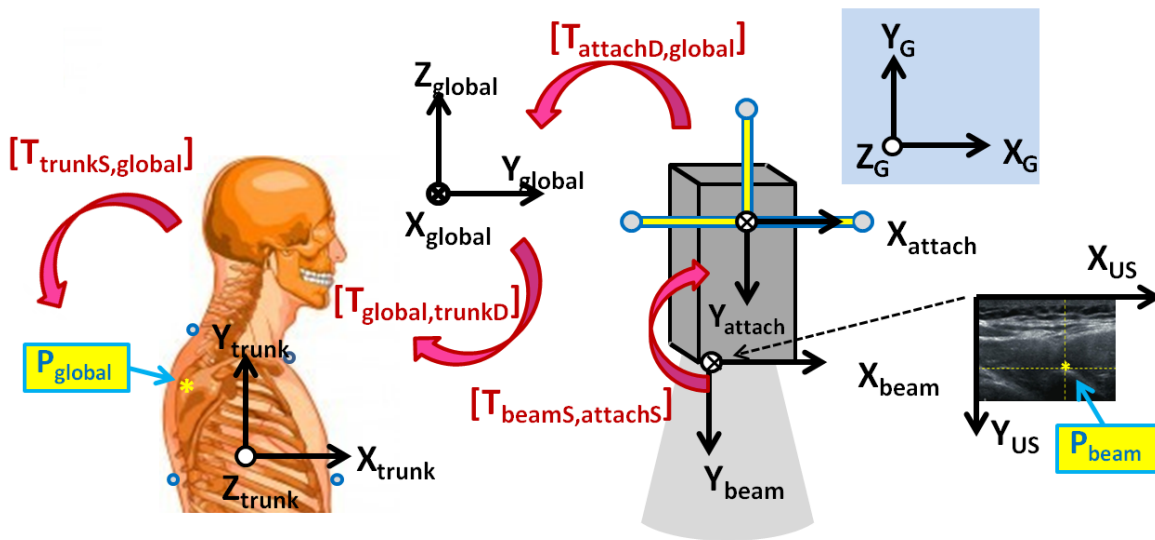
Figure 21: Coordinate Systems and Transformations for Rigid Bodies

The series of transformations can be seen below. In this equation, 'S' denotes data collected statically and 'D' denotes data collected at the time point of the trial that corresponds to the ultrasound image being processed.

$$P_{global} = \left[T_{trunkS,global}\right]\left[T_{global,trunkD}\right]\left[T_{attachD,global}\right]\left[T_{beamS,attachS}\right] * P_{beam}$$

In the aforementioned equation, P_{beam} is the location of the point in the ultrasound image. The z-component of this point is zero as the point is within the plane of the beam. A static calibration is performed to determine the rotation between the local coordinate system of the beam and the custom orthogonal attachment of the probe. During this calibration, four Vicon markers are attached in line with the beam of the probes, as seen circled in red in Figure 22, and a static trial is collected. This relation is determined using the following equation in which T_{beam} and T_{attach} are the local coordinate systems of the beam of the probe and the custom orthogonal attachment where $T_{beam,attach}$ is the transpose of the matrix:

$$T_{beam,attach} = (T_{attach})^T * T_{beam}$$

The beam coordinate system has the origin in the top left corner of the image. The x-axis points to the right, the y-axis points down and the z-axis points into the page. The z-component is zero for all P_{beam} as the points are within the plane of the image. The attachment consists of four arms to create redundancy in the case of drop-out of any one marker. The local coordinate system for the custom orthogonal attachment is centered at the midpoint between the markers on the left and right sides of the probe. The x-axis extends from the origin to the left marker, the z-axis points down, and the y-axis points forward toward the front of the probe.
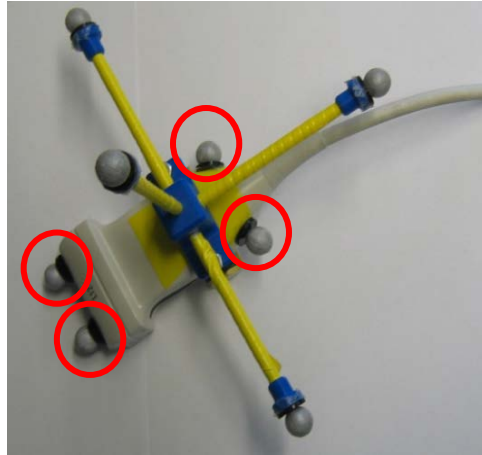
Figure 22: Location of Vicon Markers for Static Calibration of the Beam and Custom Orthogonal Attachment

Once a relation has been determined between the beam and custom orthogonal attachments, the position of attachment during the trial can be incorporated. Just like the location of the scapular border in the ultrasound image changes with each frame, so too does the position of the ultrasound probe in space. Applying the location of the attachment at the time corresponding to the time when the ultrasound image was collected, $T_{attachD,global}$, makes it possible to represent the point in the global coordinate system.

As trunk movement will affect scapular position, to account for any trunk movement that may have occurred, we input the position of the trunk at the time the image was collected, $T_{global,trunkD}$. This helps minimize any distortions that could be caused by the participant shifting the position of his/her torso during testing. Applying this transformation gave us the location of the point in the trunk coordinate system. In order to determine scapular rotation with respect to the trunk, it was necessary to have the scapular border in the global coordinate system, not the trunk local coordinate system. A final transformation was used which uses the average trunk

37

position for the entire trial to calculate $T_{trunkS,global}$. The trunk local coordinate system was determined according to the International Society of Biomechanics' recommendation with the y-axis as a vertical line extending upwards from the midpoint between T8 and the xyphoid to the midpoint between C7 and the sternum. The z-axis points to the right as the cross-product of the vector from T8 to the xyphoid and the vector from T8 to the sternum. Finally, the x-axis extends forward from the origin which is located at the sternum.

Once the three-dimensional location of the scapular border is determined for each of the ultrasound images collected during the trial, the points are pooled to create a three-dimensional reconstruction of the scapular border (Figure 23).
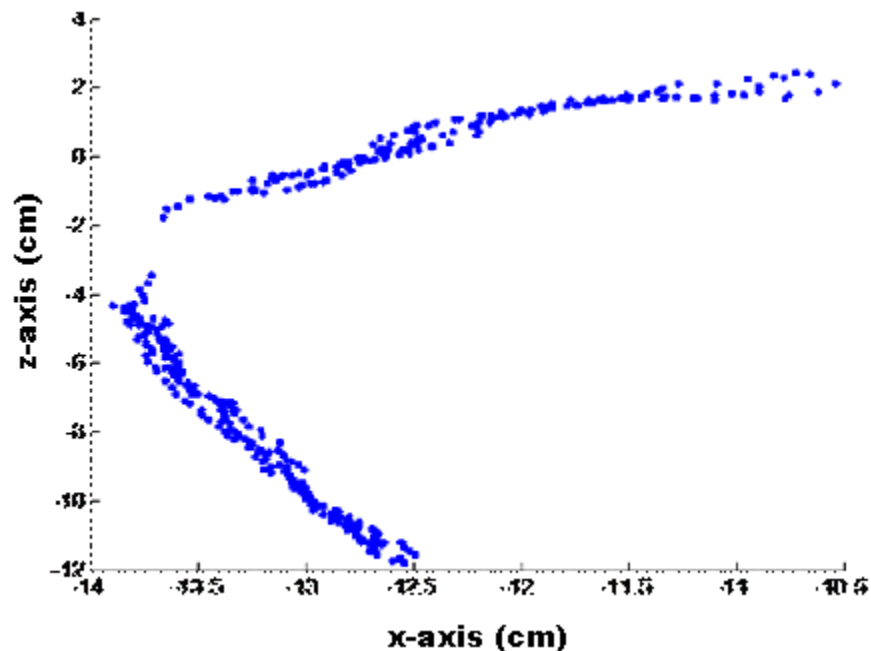
Figure 23: Reconstruction of three-dimensional scapular border, global coordinate system (posterior view of frontal plane)

2.2.5.4 Determining Scapular Position

The International Society of Biomechanics recommends using the three landmarks to determine the scapula local coordinate system: acromial angle (origin) root of the spine, and inferior angle. The z-axis extends from the root of the spine to the acromial angle. The x-axis extends anteriorly and is perpendicular to the plane formed by the three landmarks. The y-axis then points upwards as the cross-product of the x and z axes. This coordinate system was used to determine scapular position based on the landmarks digitized with the stylus. These three landmarks are not distinctly identified in the reconstructed scapular border, however similar principles to define our coordinate system relying on the plane the points lied in and a vector along the spine of the scapula (Figure 24).
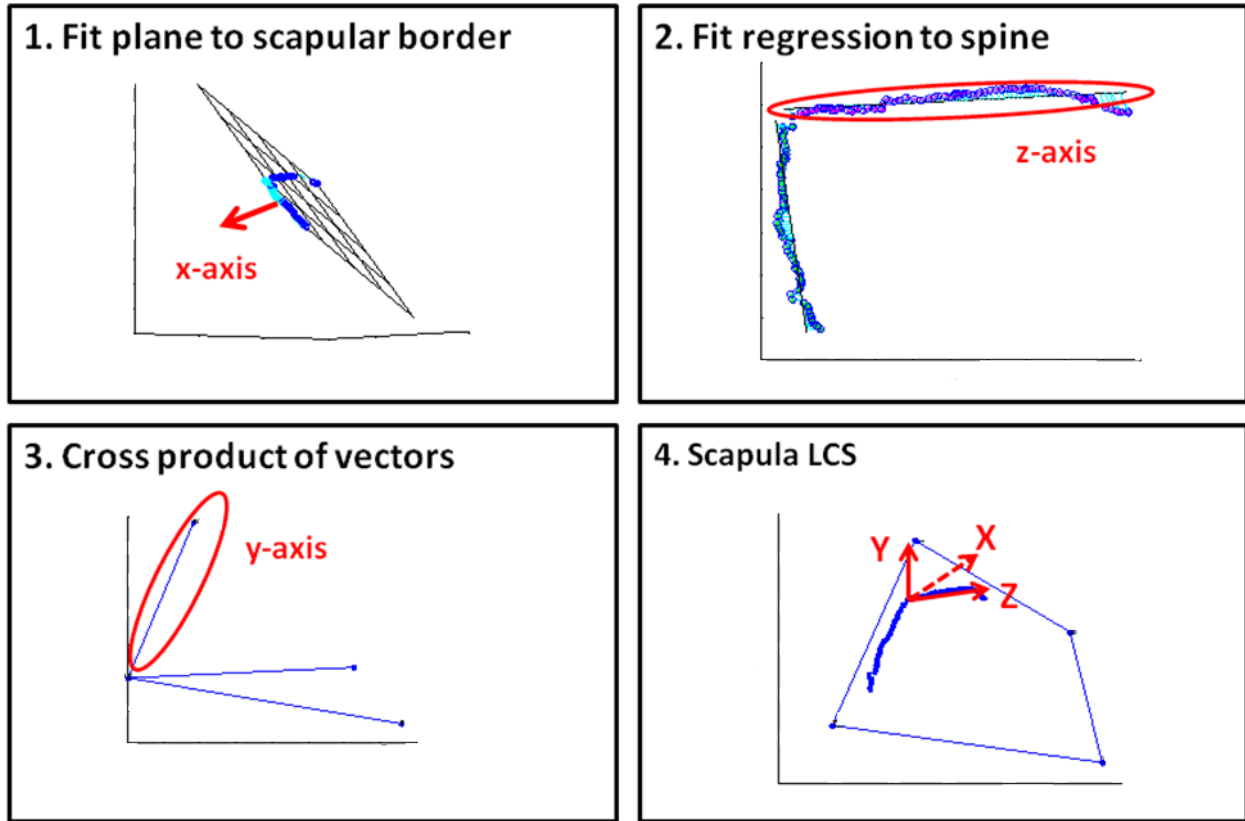
Figure 24: Local coordinate system of reconstructed scapular border

The scapular position was determined with respect to the trunk, where *T* is the transpose of the matrix:

$$T_{trunk,scap} = (T_{global,trunk})^T * T_{global,scap}$$

To determine rotations, we followed the International Society of Biomechanics' recommendation for Euler angle sequence.[94] A YXZ rotation sequence was used for matrix decomposition to determine scapular rotation. The first rotation was about the y-axis is internal/external rotation (α), the second was about the x-axis is upward/downward rotation (β),

40

and the third was about the z-axis is anterior/posterior tilting (γ) Scapular rotations were determined as follows where c is the cosine and s is the sine:

$$Ryx'z" = [R(y, \alpha)][R(x, \beta)][R(z, \gamma)]$$

$$Ryx'z" = \begin{bmatrix} cyc\alpha + sys\beta sa & cys\beta sa - cas\gamma & c\beta sa \\ c\beta s\gamma & cyc\beta & -s\beta \\ casys\beta - cysa & cycas\beta + sysa & c\beta ca \end{bmatrix}$$

$$\alpha = atan2\left(\frac{Ryx'z"(1,3)}{Ryx'z"(3,3)}\right) \qquad \beta = asin(-Ryx'z"(2,3)) \qquad \gamma = atan2\left(\frac{Ryx'z"(2,1)}{Ryx'z"(2,2)}\right)$$

Scapular rotations can be visualized as follows in Figure 25. With this coordinate system, positive rotations included internal rotation, downward rotation, and posterior tilting.
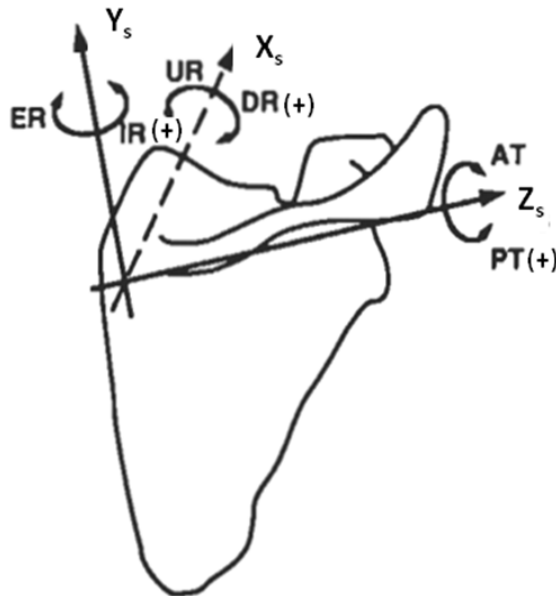
Figure 25: Scapula Coordinate System and Rotations: Internal / External Rotation IR/ER), Upward/ Downward Rotation (UR/DR), Anterior / Posterior Tilting (AT/PT),

2.2.5.5 Determining Humeral Elevation and Trunk position

The humeral coordinate system was determined using the following markers: acromion, lateral epicondyle, and medial epicondyle. The y-axis was formed by the line extending upward from the midpoint between the medial and lateral epicondyles to the acromion. The x-axis was the line formed perpendicular to the plane created by the lateral and medial epicondyles and the acromion, pointing forward. The z-axis was determined as the cross-product of the x and y-axes. The angle of humeral elevation was determined with respect to the trunk where T is the transpose of the matrix:

$$T_{trunk,Humerus} = (T_{global,trunk})^T * T_{global,Humerus}$$

A YXY rotation sequence was used for matrix decomposition to determine humeral elevation. The sequence of rotations was elevation in the glenohumeral plane, negative glenohumeral elevation, and glenohumeral axial rotation (Figure 26).
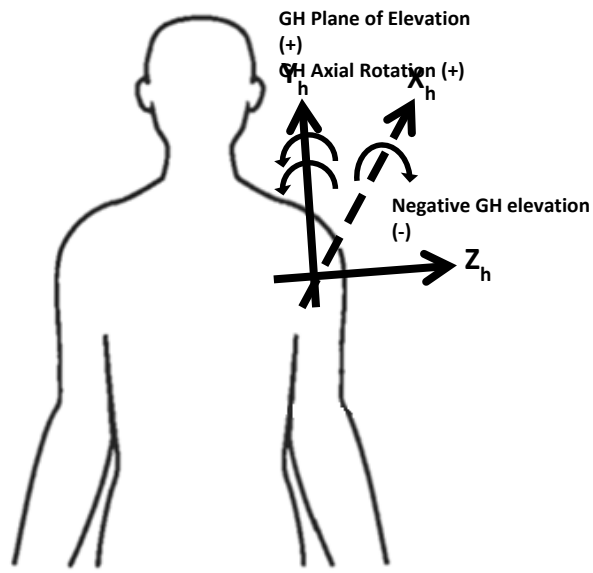
Figure 26: Humeral Local Coordinate System and Rotations

The trunk coordinate system can be seen in Figure 27. Trunk position was determined using a ZXY matrix decomposition of the trunk local coordinate system. The first rotation was flexion/extension, followed by lateral rotation, and axial rotation.
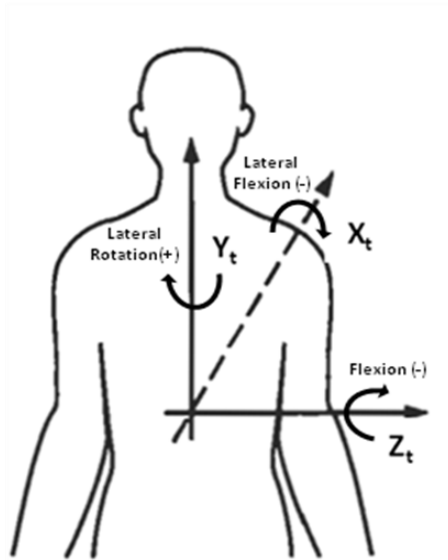
Figure 27: Trunk Local Coordinate System and Rotations

2.2.6   Statistical Analysis

In order to evaluate the three-dimensional ultrasound system calibration, the root mean square error between the known and measured dimensions of a scanned phantom was calculated. To evaluate the inter-rater and intra-rater reliability of manual point detection, intraclass correlations were calculated, ICC(2,1). The intraclass correlation coefficient (ICC) measures agreement between groups and ranges from 0 to 1. The ICC was interpreted using the categories of agreement suggested by Landis and Koch in which ≤ 0.4 is unacceptable, 0.41-0.60 is moderate, 0.61-0.80 is substantial, and ≥ 0.81 is almost perfect.[96]

ICCs were also used to evaluate the consistency in measured scapular rotations across repeated trials. The ICC(3,1) was calculated for each rotation (YX'Z'') of the scapula in each of

the testing positions (rest and elevation in the sagittal, frontal, and scapular planes). In addition to determining how reliable our measure was, we also wanted to determine the minimum detectable change (MDC) that could be measured. To calculate MDC, we first calculated the standard error of measurement (SEM). SEM was determined using the following equation:

$$SEM = SD_{pooled} * \sqrt{(1 - ICC)}$$

The SEM is representative of the square root of the absolute error variance and provides a range in which an individual's true score is expected to fall. 68.2% of the time a subject's score will fall within ± 1 standard deviation of his/her true score. SEM was then used to calculate the MDC at the 90% confidence level where:

$$MDC_{90} = SEM * \sqrt{2} * 1.64$$

MDC_{90} is important as it is a threshold of the amount of change required to be 90% confident that any differences we may find between groups in the future is a true change that exceeds the magnitude of measurement error.

To compare the measured scapular rotations resulting from the freehand three-dimensional ultrasound and the digitized landmarks, ICCs were used as well as Bland Altman plots to check for agreement. Bland Altman plots are a graphical method used to compare two measurement techniques. The difference between the two measurements is plotted on the y-axis, while the mean of the two measurements is displayed on the x-axis. Horizontal lines are added to the plot at the mean difference as well as the mean difference ± 1.96 * standard deviation of the differences which are defined as the limits of agreement. This method allows for identification of systematic bias and outliers.

To compare trunk and arm position between repeated trials, a repeated measures ANOVA was completed for both measures with a within subjects factor of testing position (rest

and elevation in the sagittal, frontal, and scapular planes). All statistical analyses were completed with IBM SPSS Statistics Software, version 20 (Armonk, NY: IBM Corp.) with the significance level set apriori at 0.05.

2.3   RESULTS

Twenty-two healthy able-bodied individuals (16 male, 6 female; age=50.5±11.6 years, height=1.72±0.13m, body mass=74.22±15.02kg) participated in this reliability study, approved by the local Institutional Review Board. Consent of each subject was obtained prior to the study. The results of the phantom scanning show a RMSE of 0.097 cm. For manual identification of the scapular border in ultrasound images, we found an inter-rater reliability ranged from 0.975 to 0.985 for the three videos and the intra-rater reliability ranged from 0.99 to 0.995 for rater 1 and from 0.978 to 0.993 for rater 2. The reliability of the three repeated scans completed for each subject can be seen in Table 1. Reliability ranged from substantial to almost perfect. In terms of scanning positions, the highest reliability was found for the rest position with all measures exceeding 0.90. Additionally, the first scapular rotation (internal/external rotation) had the highest reliability with all measures also exceeding 0.90. The lowest reliability was found for the second rotation of scapular upward/downward rotation.

Table 1: ICC for Repeated Freehand Three-Dimensional Ultrasound Scans

Scanning Position	Scapular Rotation (n=22)		
	Internal / External Rotation	Upward / Downward Rotation	Anterior / Posterior Tilting
Rest	0.946	0.889	0.922
Sagittal Plane 120°	0.926	0.687	0.872
Frontal Plane 120°	0.941	0.620	0.937
Scapular Plane 120°	0.929	0.798	0.896

The SEM was less than 2° for all trials and can be seen below in Table 2. SEM was less than 0.5° for internal/external rotation and anterior/posterior tilting for all testing positions. SEM was highest for upward/downward rotation, specifically in the sagittal and frontal planes.

Table 2: SEM for Repeated Freehand Three-Dimensional Ultrasound Scans

Scanning Position	Scapular Rotation (n=22)		
	Internal / External Rotation	Upward / Downward Rotation	Anterior / Posterior Tilting
Rest	0.16°	0.47°	0.19°
Sagittal Plane 120°	0.34°	1.14°	0.37°
Frontal Plane 120°	0.25°	1.33°	0.21°
Scapular Plane 120°	0.27°	0.65°	0.32°

As MDC is related to reliability and SEM, it is not surprising that the smallest MDC was also found when the arm was in the rest position and for the first scapular rotation (Table 3). For testing in the elevated positions, the MDC for internal/external rotation and upward/downward tilting were considerably smaller than the MDC for upward/downward rotation.

Table 3: MDC for Repeated Freehand Three-Dimensional Ultrasound Scans

Scanning Position	Scapular Rotation (n=22)		
	Internal / External Rotation	Upward / Downward Rotation	Anterior / Posterior Tilting
Rest	0.37°	1.08°	0.44°
Sagittal Plane 120°	0.79°	2.66°	0.86°
Frontal Plane 120°	0.57°	3.08°	0.49°
Scapular Plane 120°	0.62°	1.52°	0.74°

Summary plots of the consistency across trials in scapular position can be found in Figure 28. Each column represents a rotation (internal/external, upward/downward, and anterior/posterior tilting respectively) while each row represents a testing position (rest and elevation in the sagittal, frontal, and scapular planes). We found no significant differences across trials for arm or trunk position.
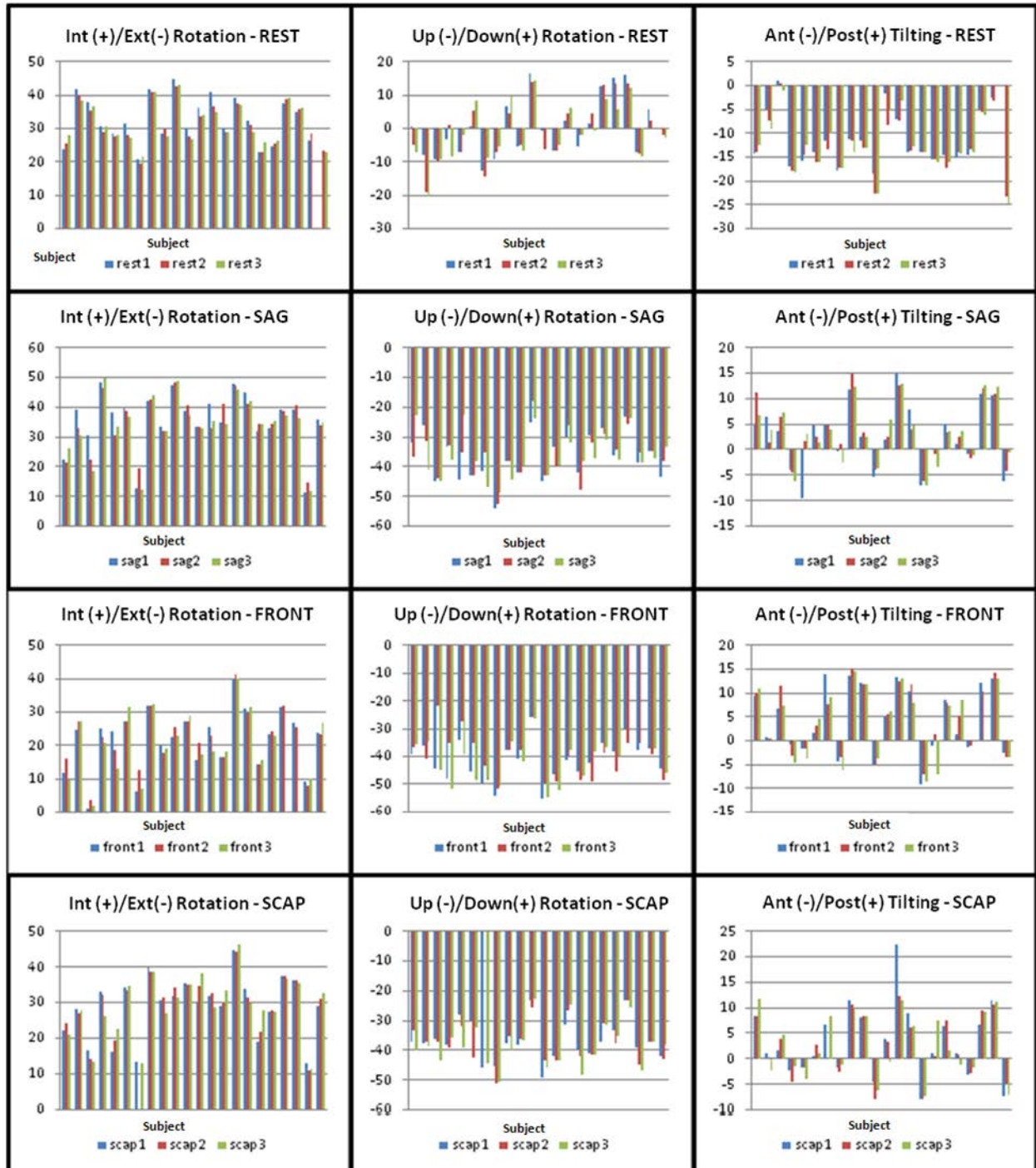
Figure 28: Scapular Rotations across Repeated Trials in All Testing Positions

An example of the reconstructed scapular border for one subject in each testing position can be seen below in Figure 29. From left to right the columns of the figure correspond to the scapula imaged at rest and elevated in the sagittal, frontal, and scapular planes. The top row is a view of the frontal plane from posterior to anterior while the bottom row is a view of the transverse plane from superior to inferior.
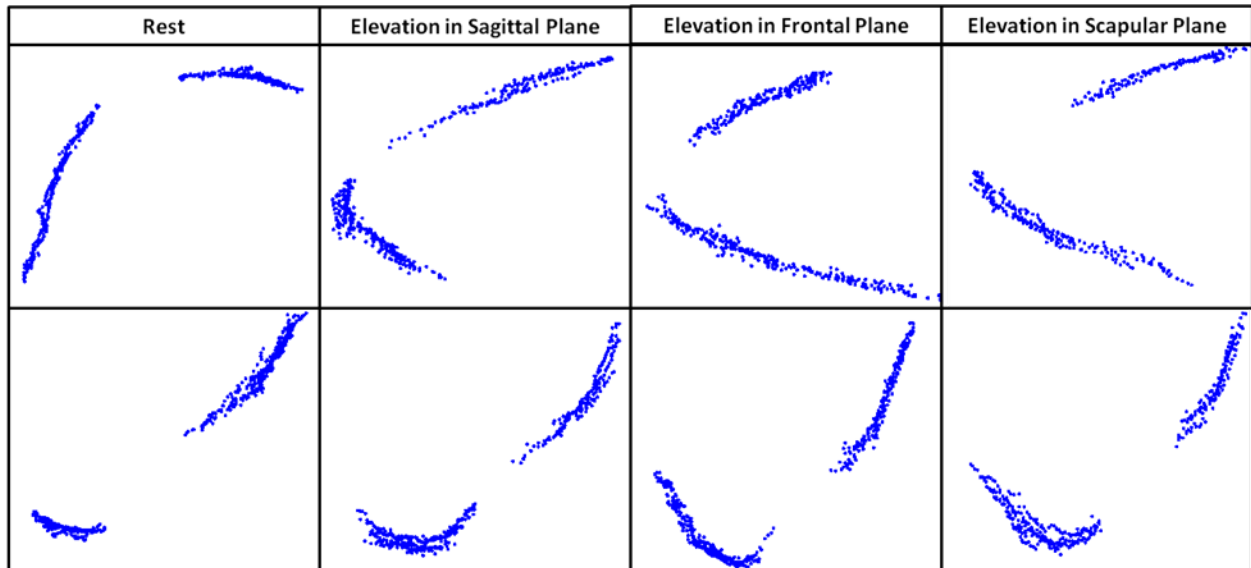
Figure 29: Example of reconstructed scapula in all testing positions (sagittal plane top, transverse plane bottom)

An example of a subject who had good agreement between digitization and ultrasound methods can be seen below in Figure 30. Shown in the figure are three views of the reconstruction (pink) and digitization (green) of the subject's scapula at rest.

50
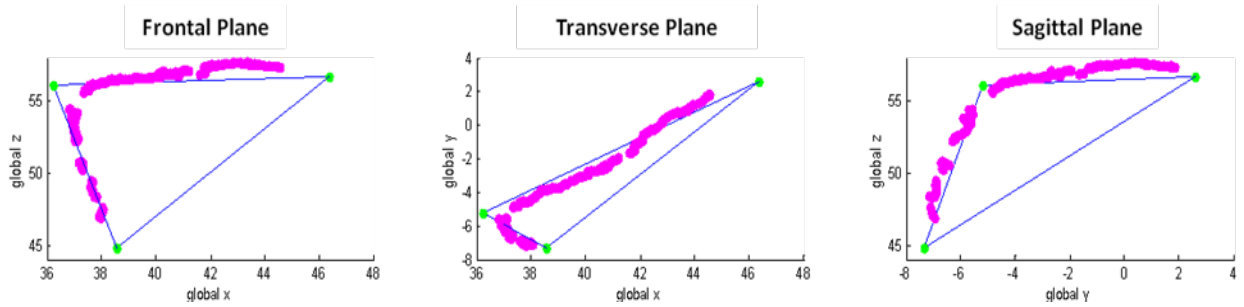
Figure 30: Digitization and Ultrasound Reconstruction of Scapula at rest with views of the frontal plane, transverse plane, and sagittal plane

Agreement between freehand three-dimensional ultrasound scanning and landmark digitization was not as strong as between trials for the freehand scanning (Table 4). Four arm position-scapular rotation pairings showed unacceptable reliability while others showed at least substantial reliability. The highest reliability between the two methods was found with the arm in the rest position.

Table 4: ICC for Freehand Three-Dimensional Ultrasound and Landmark Digitization

Scanning Position	Scapular Rotation (n=22)		
	Internal / External Rotation	Upward / Downward Rotation	Anterior / Posterior Tilting
Rest	0.826	0.739	0.762
Sagittal Plane 120°	0.835	0.400	0.759
Frontal Plane 120°	0.535	0.312	0.793
Scapular Plane 120°	0.608	0.428	0.337

51

Bland Altman plots can be seen below for each testing position (Figure 31-Figure 33). The difference between the two measurements is plotted on the y-axis, while the mean of the two measurements is displayed on the x-axis. Horizontal lines are added to the plot at the mean difference as well as the mean difference ± 1.96 * standard deviation of the differences which are defined as the limits of agreement. In general, good agreement would be denoted by an even spread of points within the limits of agreement, a mean difference close to zero. Points outside of the limits of agreement could indicate outliers. An uneven spread or trend from left to right could indicate a proportional bias where measurements don't agree equally through the range of measurements. A mean difference that is not close to zero would indicate one measurement is consistently higher than the other.
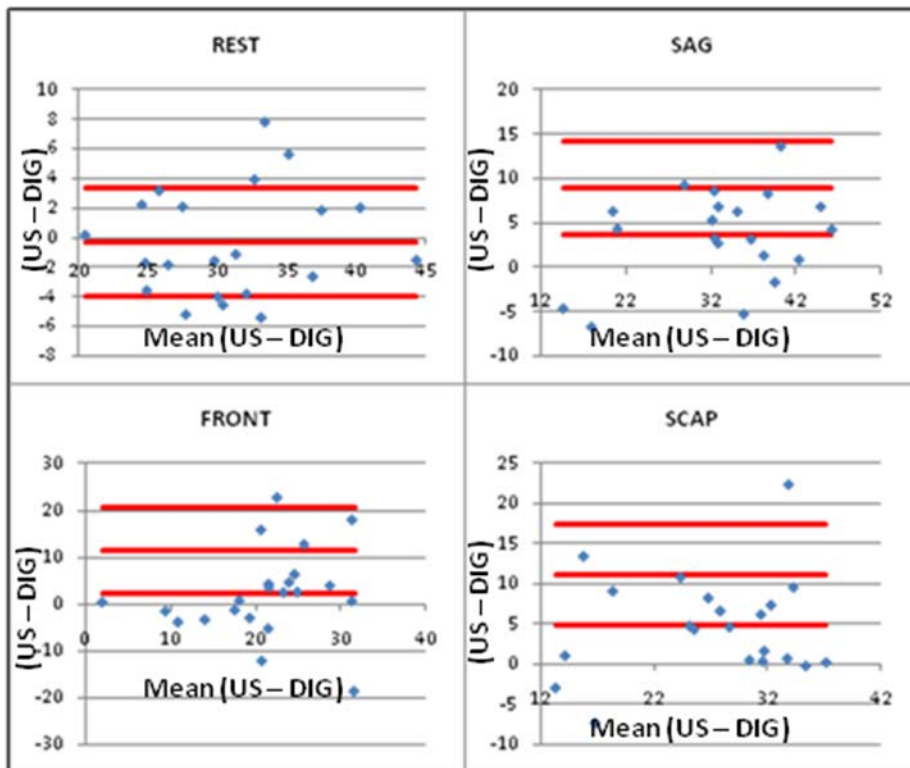
Figure 31: Bland Altman Plot for Internal/External Rotation between Freehand and Landmark Digitization Methods
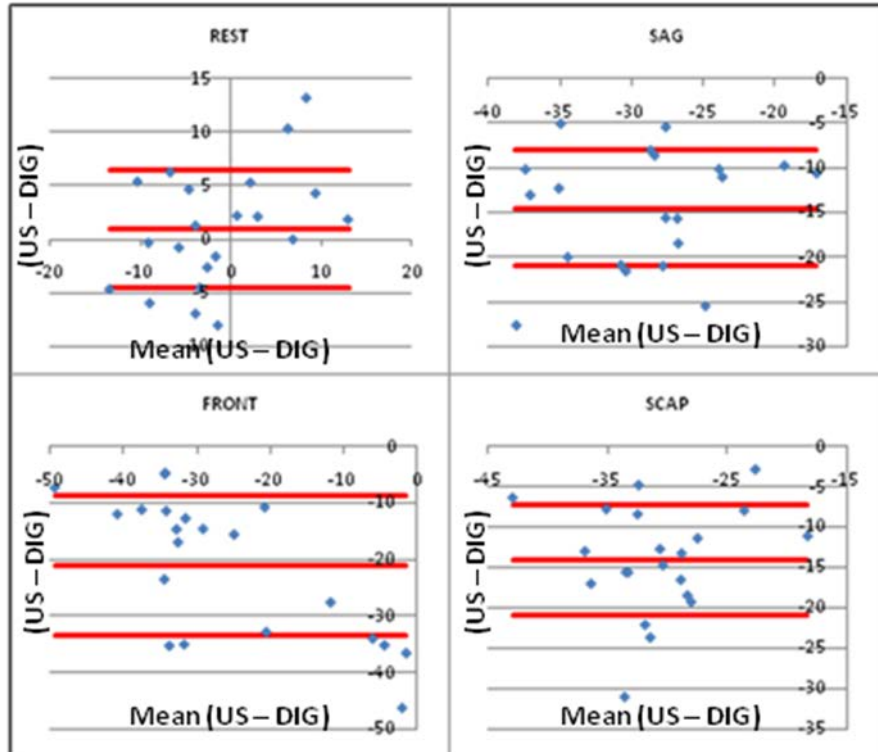
Figure 32: Bland Altman Plot for Upward/Downward Rotation between Freehand and Landmark Digitization Methods
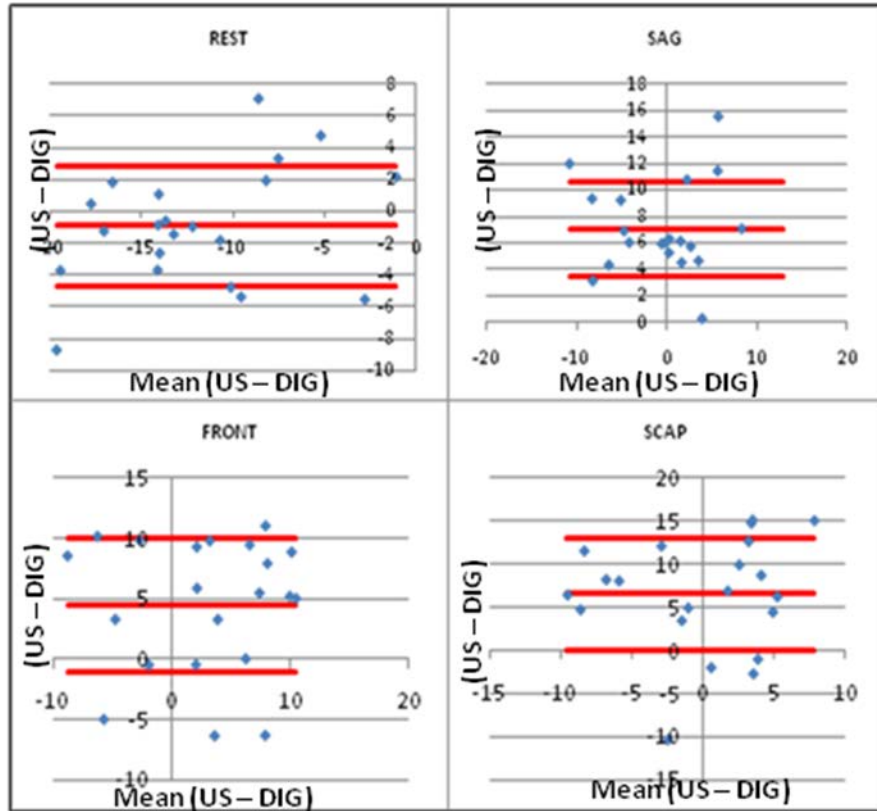
Figure 33: Bland Altman Plot for Anterior/Posterior Tilting between Freehand and Landmark Digitization Methods

Systematic error was found in all testing positions. Overall we found no trends in proportional error or error related to the measurement of the error. The one exception to this was for upward/downward rotation in the rest and frontal plane elevation positions. We suspected a trend that was confirmed by a significant linear relation (p=0.043 and <0.001 respectively), which can be seen in Figure 34.
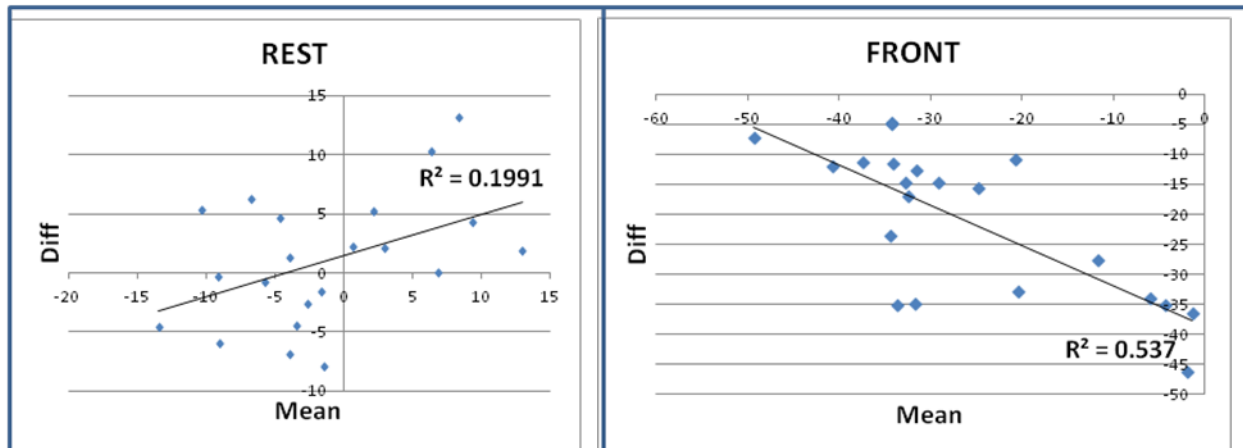
Figure 34: Proportional Bias in Bland Altman Plot for Upward/Downward Rotation at Rest and Elevated in the frontal plane.

The average internal/external rotation, upward/downward rotation, and anterior/posterior tilting across subjects for each testing position for both freehand ultrasound and digitization can be found in Table 5. Significant differences between the two methods can be seen in bold and underlined. No significant differences were found between the two methods at rest. We found in the elevated testing positions digitization resulted in less upward rotation and less posterior tipping. In the sagittal and frontal planes we found digitization resulted in significantly less internal rotation.

Table 5: Average Scapular Rotations across Subjects for Freehand Scanning and Digitization in All Testing Positions

Scanning Position	Internal (+) / External (-) Rotation (mean ± SD)			Upward (-) / Downward (+) Rotation (mean± SD)			Anterior (-) / Posterior Tilting (+) (mean±SD)		
	US	DIG	p-value	US	DIG	p-value	US	DIG	p-value
Rest	31.6±6.4	31.0±5.9	0.403	-0.5±8.5	-1.8±6.3	0.402	-12.4±5.9	11.4±4.8°	0.29
Sagittal Plane 120°	34.9±9.5	31.4±8.2	**0.006**	-36.4±6.9	-22.7±7.2	**<0.001**	3.1±5.°	-4.9±6.°	**<0.001**
Frontal Plane 120°	21.8±8.9	20.6±7.9	0.512	-40.8±6.6	-27.5±8.7	**<0.001**	4.3±7.1	-0.6±6.6	**<0.001**
Scapular Plane 120°	29.0±8.5	25.0±7.5	**0.015**	-37.6±6.6	-23.7±5.8	**<0.001**	2.9±6.3	-3.0±6.0	**0.001**

We found no significant differences in arm position for subjects between the freehand scanning and digitization trials. It is important to note that the average arm elevation angle, measured based on Vicon markers with respect to the trunk, for subjects in the elevated trials did not reach 120° but instead was closer to 90°. Average arm elevation angles for each testing position can be found below in Table 6.

Table 6: Average Arm Elevation Angle across Testing Positions

Testing Position	Arm Elevation Angle
Rest	18.3±6.0°
Sagittal Plane	89.4±14.2°
Frontal Plane	90.2±11.1°
Scapular Plane	82.9±13.0°

We found differences in trunk position between freehand scanning trials and digitization trials. There was greater trunk extension for the digitization trial than ultrasound scans in the rest (p=0.008) and sagittal plane elevation trials (p=0.011). Additionally there was greater lateral rotation for the digitization trial at rest (p=0.008) and frontal plane elevation (p=0.007).

2.4   DISCUSSION

The objective of this study was to evaluate the reliability of the freehand three-dimensional system, manual identification of the scapular border, and the scapular rotations determined based on ultrasound scanning. Further, this study also sought to compare rotations calculated based on ultrasound scanning to those calculated based on landmark digitization. We found a very low RMSE when comparing known to measured dimensions of a scanned phantom. Based on this, we are confident that the errors associated with our reconstruction of points from ultrasound space to the global coordinate system are less than 0.1cm. Additionally, we found the reliability

of the manual point detection technique to be greater than 0.9. This provides us with confidence that little error resulted from inconsistent identification of the scapular border.

Very high intra-rater reliability was found for all testing positions and all scapular rotations across trials. The greatest reliability was found in the resting position. This is not surprising as in it was possible that elbow flexion and wrist flexion could vary across trials in the elevated testing positions, thus affecting scapular position. Additionally, the rest position required no effort on the part of the participant to maintain. Internal/external rotation showed the highest reliability across trials, followed by anterior/poster tilting. Ludewig et al investigated reliability of their method, landmark digitization for humeral elevation in the scapular plane, to determine scapular rotations and found ICCs of 0.93 for internal/external rotation, 0.82 for upward/downward rotation, and 0.78 for anterior/posterior tilting.[72] We had ICCs that were equal to or exceeded the reliability of their study. Bourne et al also completed a reliability study on their methods which used bone pins for determining scapular position during elevation in the sagittal and frontal planes.[87] They found ICCs that exceeded 0.85 for internal/external rotation, 0.97 for upward/downward rotation, and 0.97 for anterior/posterior tilting. Comparatively, our reliability exceeds that of Bourne for internal/external rotation. Reliability for other rotations is not as strong as Bourne, however still shows substantial to excellent reliability. This finding is significant when acknowledging that while bone pins reliable they are also highly invasive.

Many other studies do not report SEM for scapular rotation measurements. Ludewig et al reported SEM for the scapular plane of less than 3° for internal/external rotation and upward/downward rotation and less than 2° for anterior/posterior tilting.[72] Our SEM was less than 2° for all rotations in all testing positions. Bourne et al did not report SEM but did report RMSE ranging from 1.2° to 4°.

Minimum detectable change for scapular movement has not been reported by previous studies. As MDC is a function of SEM, we can compare it to the study by Ludewig et al. With their reported range of SEM form from 2-3°, the resulting MDC_{90} would be 4.6-7.0°. Comparatively our MDC_{90} is lower at less than 1° for internal/external rotation and anterior/posterior and approximately 3° or less for upward downward rotation in all positions. The MDC_{90} is the smallest difference we can detect with 90% certainty that we are above the threshold of error. In other words, if we found an increase in internal rotation greater than 1° after some type of intervention we would be 90% confident that the change was a true change and not a result of measurement error or variability between trials. It is important to note that the MDC is not the same as a clinically meaningful difference. To determine a clinically meaningful difference between groups or with an intervention, we would need to associate the change with external criteria, such as a difference in clinical exam scores.

At rest we found 32° of internal rotation which is in good agreement with other studies that found internal rotation ranging from 30-33°.[49, 72, 78, 97] For elevation in the sagittal, frontal and scapular planes we found internal rotations ranging from 22 to 35°. This is in contrast to the other two studies that reported elevation to 90° which both found external rotation.[54, 87] However, both of these studies also found external rotation at rest which is in contrast to other literature. [49, 72, 78, 97] As presented in Table 7, there is a disagreement between studies as to whether the scapula is internally or externally rotated across testing positions. In general, while our results may not agree in magnitude with other studies using bone pins, we found increased external rotation with humeral elevation, which is what we would have expected.

Table 7: Internal/External Rotation with Humeral Elevation Reported By Other Studies

Testing Plane	Study Authors	Method	Humeral Elevation (°)	Mean (°)	Stdev (°)
		Scapular Rotations – (+) Internal / (-) External			
Rest	Ludewig[72]	Digitized Landmarks	0	33	9
	Culham[49]		0	30.2	
	Johnson[78]	Digitized Landmarks	0	30	
	McClure[54] *(derived from plot)*	Electromagnetic sensor	Min	-37	
	Lukasiewicz[23] *(derived from plot)*	Digitized Landmarks	Rest	47	
	Current Study	**Freehand 3D Ultrasound**	**18.3±6.0**	**31.6**	**6.4**
Sagittal	McClure[54] *(derived from plot)*	Electromagnetic sensor	60	- 41.5	
	McClure[54] *(derived from plot)*	Electromagnetic sensor	90	- 43	
	Bourne[87]	Bone pins	90	-18	6
	Current Study	**Freehand 3D Ultrasound**	**89.4±14.2**	**34.9**	**9.5**
	Johnson[78]	Digitized Landmarks	120	6	
	Meskers[92]	Digitized landmarks	0-150	0	
	Van der Helm[98]	Digitized Landmarks	0-180	-25	
Frontal	Bourne[87]	Bone pins	90	-27	11
	Current Study	**Freehand 3D Ultrasound**	**90.2±11**	**21.8**	**8.9**
	Van der Helm[98]	Digitized Landmarks	0-180	-25	
	Meskers[92]	Digitized Landmarks	0-150	3	
	McClure[88]	Bone pins	16-153	-26	11
Scapular	McClure[54] *(derived from plot)*	Electromagnetic sensor	60	-37	
	Ludewig[72]	Digitized Landmarks	90	28	
	McClure[54]	Electromagnetic sensor	90	-37	
	Lukasiewicz[23] *(derived from plot)*	Digitized Landmarks	90	41	
	Current Study	**Freehand 3D Ultrasound**	**82.9±13**	**29.0**	**8.5**
	Kondo[66]	3D Double Radiograph	0-max	6	
	Ludewig[72]	Digitized Landmarks	140	20	6
	McClure[88]	Bone pins	11-147	-24	12.8
	Lukasiewicz[23] *(derived from plot)*	Digitized Landmarks	Max	4.5	

At rest we found approximately 1° of upward rotation which is in accordance with other studies that report 2-3° of upward rotation at rest.[72, 97] As can be seen in Table 8, our study had comparatively less upward rotation in the sagittal (36°) and frontal (40°) planes compared to other studies that evaluate humeral elevation at 90° (42-49°, 49°).[54, 87] In the scapular plane we found slightly higher upward rotation (37°) than other studies (21-35°).[54, 87] A summary of upward rotations found in other studies, organized by testing plane and humeral elevation, can be found in Table 8.

Table 8: Upward/Downward Rotation with Humeral Elevation Reported By Other Studies

Testing Plane	Study Authors	Method	Humeral Elevation (°)	Mean (°)	Stdev (°)
Scapular Rotations: (-) Downward / (+) Upward					
Rest	Ludewig[72]	Digitized Landmarks	0	2	6
	Culham[49]		0	10	1.3
	Laumann		0	3	3
	McClure[54] *(derived from plot)*	Electromagnetic sensor	Min	17	
	Lukasiewicz[23] *(derived from plot)*	Digitized Landmarks	Rest	26	
	Current Study	**Freehand 3D Ultrasound**	**18.3±6.0**	**0.5**	**8.5**
Sagittal	McClure[54] *(derived from plot)*	Electromagnetic sensor	60	26	
	McClure[54] *(derived from plot)*	Electromagnetic sensor	90	42	
	Bourne[87]	Bone pins	90	49	7
	Current Study	**Freehand 3D Ultrasound**	**89.4±14.2**	**36.4**	**6.9**
	Meskers[92]	Digitized landmarks	0-150	58	
	Inman[99]	2D radiographs	30-150	50	
	Van der Helm[98]	Digitized landmarks	0-180	60	Van der Helm[98]
Frontal	Bourne[87]	Bone pins	90	49	7
	Current Study	**Freehand 3D Ultrasound**	**90.2±11**	**40.8**	**6.6**
	Meskers[92]	Digitized landmarks	0-150	60	
	Inman[99]	2D radiographs	30-150	40	
	McClure[88]	Bone pins	16-153	46	7
	Van der Helm[98]	Digitized landmarks	0-180	60	
Scapular	McClure[54] *(derived from plot)*	Electromagnetic sensor	60	22	
	McClure[54] *(derived from plot)*	Electromagnetic sensor	90	35	
	Ludewig[72]	Digitized Landmarks	90	21	5
	Current Study	**Freehand 3D Ultrasound**	**82.9±13**	**37.6**	**6.6**
	McQuade[74]	Digitized Landmarks	0-135	22	
	Ludewig[72]	Digitized Landmarks	140	36	4
	McClure[88]	Bone pins	11-147	50	4.8
	Poppen[64]	2D radiographs	0-150	54	
	Doody[70]	2D goniometry	5-176	59	
	Lukasiewicz[23]	Digitized Landmarks	Max	40	

Table 8 (continued).

Kondo[66]	3D Double Radiograph	0-Max	32	

Our study found 12° of anterior tipping at rest. Other studies report a range from 40° anterior tipping at rest to 30° posterior tipping at rest so it is difficult to make comparisons across studies. In the elevated testing positions we found 3-4° of posterior tilting. This is in agreement with Bourne et al who reported 5° of posterior tilting with elevation to 90° in the sagittal plane. There are a limited number of other studies that report tiling with the humerus elevated to 90°. In general, all studies show a trend of the scapula moving to a more posterior tilted position with elevation which is in agreement with our results (Table 9).

Table 9: Anterior/Posterior Tilting Humeral Elevation Reported By Other Studies

Testing Plane	Study Authors	Method	Humeral Elevation (°)	Mean (°)	Stdev (°)
	Scapular Rotations – (+) Posterior/ (-) Anterior Tilting				
Rest	Ludewig[72]	Digitized Landmarks	0	-8	4
	Culham[49]		0	30.2	
	McClure[54]	Electromagnetic sensor	Min	-39	
	Lukasiewicz[23] *(derived from plot)*	Digitized Landmarks	Rest	12	
	Current Study	Freehand 3D Ultrasound	18.3±6.0	-12.4	5.9
Sagittal	McClure[54]	Electromagnetic sensor	60	2	
	Current Study	**Freehand 3D Ultrasound**	**89.4±14.2**	**3.1**	**5.0**
	McClure[54]	Electromagnetic sensor	90	-4	
	Bourne[87]	Bone pins	90	5	2
	Meskers[92]	Digitized landmarks	0-150	24	
Frontal	Bourne[87]	Bone pins	90	44	11
	Current Study	**Freehand 3D Ultrasound**	**90.2±11**	**4.3**	**7.1**
	Meskers[92]	Digitized Landmarks	0-150	13	
	McClure[88]	Bone pins	16-153	31	11
	Van der Helm[98]	Digitized Landmarks	0-180	30	
Scapular	**Current Study**	**Freehand 3D Ultrasound**	**82.9±13**	**2.9**	**6.3**
	Ludewig[72]	Digitized Landmarks	90	-2	3
	Lukasiewicz[23] *(derived from plot)*	Digitized Landmarks	90	22	
	McQuade[74]	Digitized Landmarks	0-135	31	
	Ludewig[72]	Digitized Landmarks	140	7	5
	McClure[88]	Bone pins	11-147	30	13
	Poppen[64]	2D radiographs	0-150	40	
	Van der Helm[98]	Digitized landmarks	0-180	30	
	Kondo[66]	3D Double Radiograph	0-max	9	
	Lukasiewicz[23]	Digitized Landmarks	Max	34.6	9.7

Overall, this study and others have found a high amount of variability in scapular rotations across subjects. For humeral elevation above 90° other studies have reported a range of standard deviations of 6-11° for internal/external rotation, 4-7° for upward/downward rotation and 2-13° for anterior/posterior tilting. With this in mind, the variability we saw between subjects in our study is expected and not likely a result of our measurement technique. For our study, subjects ranged in age from 30 to 73 years with an average age of 50. We had 9 females participate in our study and 13 males. Ludewig et al had more females (n=14) and fewer males (n=11) and participants were younger with an age range of 18-40 years.[72] McClure et al and Bourne et al used a much smaller sample for their studies (n=3 women and n=5 men).[87-88] Their subjects were much younger in age than our sample (27-37 years). Culham et al examined only women in their study.[49] Lukasiewicz et al also had a younger sample with an age range from 25-54 years for 20 healthy controls. McClure et al had the largest sample of the comparative studies (n=45) and most similar age profile (43.6±12.4 years).

Differences between ultrasound and digitization were found for all elevated testing positions. Difficulty palpating was noted for the elevated positions with muscle contraction making it more difficult to palpate the acromial angle and root of the spine. While other studies have reported good results with digitization, we hypothesize that palpation may have been a source of error in our digitization.[72] Digitization produced less upward rotation, posterior tipping and internal rotation, which is less consistent with previous studies than our freehand ultrasound measures. Contraction of the deltoid during elevation decreased the ability to contact the acromial angle. It is possible that this could have contributed to a decrease in upward rotation and internal rotation if digitized as more posterior and inferior. The trapezius also contracted during elevation and digitization of the root of the spine may have been more misguided as a

result. Digitization of this anatomical landmark more superiorly or anteriorly would have also decreased upward or internal rotation. Other digitization studies also used active contraction at the desired position of humeral elevation and may have encountered the same obstacles. However, raters performing the digitization in these studies may have been more experienced with palpation of bony landmarks. While all subjects in this study were a normal weight based on BMI, it is possible that the presence of adipose tissue may have also led to errors in digitization. As we did not evaluate the reliability of digitization in this study, we are unable to conclude if palpation techniques are the source of errors between methods.

2.4.1   Limitations

The results of this study are based on a relatively small (n=22) sample of healthy able-bodied individuals. To apply these methods to future studies it is also important to evaluate the reliability with other populations of interest. Body composition has an effect on the quality of ultrasound imaging as significant adipose tissue or muscle mass can affect impedance. All participants in this study had a BMI of less than 25 and were not overweight and imaging may have been easier because of this. This study was also limited by the palpation skills of the individual completing the landmark digitization. In many instances difficulty was noted with palpating landmarks with the arm in elevated positions.

As previously indicated, there are variations associated with the sampling frequency of the frame grabber used to collect ultrasound data in this study. To compensate for this variable rate, we resampled our data based on an approximate rate determined by the timestamp on ultrasound images. Inherently, this introduces additional error into our calculations as the

approximation cannot make up for the asynchrony in the time domain. While high reliability was still found between trials, future studies should avoid use of devices with dynamic sampling.

An additional limitation is the cost of the motion tracking used in this study. We used 10 Vicon cameras run with a Vicon Giganet. This system was used as we had already acquired it for other studies in our lab. Other systems such as the Optitrak are available that could significantly reduce the costs of the overall system.

2.5   CONCLUSION

Freehand three-dimensional ultrasound shows promise as a tool for evaluating scapular kinematics. We were able to apply this method to a variety of different testing positions and achieve high intra-rater reliability in all positions. Additionally, our SEM was less than 2° for all measurements and less than 0.5° for most. We did not find excellent agreement between our method and landmark digitization, however we hypothesize this may be because landmark digitization was not a good standard for comparisons and affected by inaccuracies resulting from difficulty palpating. Future studies should incorporate a more consistent gold standard or a case and control group to evaluate validity. Our results agree with the pattern of movement found in other studies with the scapula moving towards a more externally rotated, upwardly rotated, and posterior tilted position. As body composition affects the ultrasound image, it is important to be aware of the limitations imposed on this method by the presence of large amounts of adipose tissue or muscle mass.

3.0   COMPARING SCAPULAR KINEMATICS BETWEEN MANUAL
WHEELCHAIR USERS AND ABLE-BODIED CONTROLS

3.1   INTRODUCTION

The prevalence of shoulder pain among wheelchair users is higher than the general population with 31-73% experiencing shoulder pain.[100] Pain can result from subacromial impingement syndrome, rotator cuff tears, bursitis, and tendinitis.[7,43] Shoulder pain and pathology are generally not the result of isolated episodes and have been linked in many cases to changes in scapular movement. The scapula is part of three joint interfaces and serves as the base for humeral movement. Altered scapular kinematics have been found to be associated with rotator cuff pathology[19, 21-22], impingement[3, 23-24, 26, 28, 52-54], shoulder instability[24, 29-31], and adhesive capsulitis.[25, 32-33, 55]   Among wheelchair users, surgical interventions are often not successful in addressing pain.[6, 16-17] Previous studies have shown that early intervention is associated with faster recovery.[48] As such, emphasis on preventative measures to decrease the prevalence of shoulder pain in this population is integral. In order to make such interventions possible, it is necessary to characterize abnormal scapular movement. No previous studies have been done that investigate scapular kinematics of wheelchair users as compared to healthy controls. As wheelchair users are susceptible to overuse injuries due to the higher forces and repetitive nature of daily activities, it could be worthwhile to compare this population to a control

group with reduced demands on the upper extremity. Further, other studies have not examined how scapular position at rest or subject characteristics (age, height, weight, BMI, trunk position, and shoulder tendon and bone health) relate to scapular movement with arm elevation.

The overall goal of this study was to use freehand three-dimensional ultrasound to compare scapular movement between able-bodied controls and manual wheelchair users. We hypothesized that due to overuse injuries, manual wheelchair users would present with pathology and similar to able-bodied groups with subacromial impingement would have decreased external rotation, upward rotation and posterior tilting both at rest and in elevated positions as compared to controls. A secondary goal of this study was to determine what subject characteristics could be used to predict scapular kinematics. We evaluated the relationship between scapular position and subject age, BMI, clinical exam scores, reported shoulder pain, and resting trunk and scapular positions. Additionally, among wheelchair users we also investigated if scapular position was related to years of wheelchair use and reported pain during activities of daily living. We hypothesized that decreased external rotation, upward rotation and posterior tilting would be associated with: increased age, increased body mass index, higher clinical exam scores (indicates greater pathology), greater shoulder pain, increased years of wheelchair use, increased pain during daily activities, and increased trunk flexion, and a scapular position at rest which was more internally rotated, downward rotated, and anteriorly tilted.

Our previous study (Chapter 2.0) found that freehand three-dimensional ultrasound was an effective tool to measure scapular kinematics in static positions with high reliability and lower SEM across multiple trials. As this study only included controls, we also wanted to evaluate the reliability of this method for determining scapular position among wheelchair users. As such, we also evaluated the reliability between trials and SEM. To minimize subject burden, only 2 trials

were completed on wheelchair users, compared to the 3 for controls). We compared these to measures from the controls and also looked for learning effects (improvements over time on behalf of the ultrasonographer) for all subjects.

3.2   METHODS

3.2.1   Participants

Manual wheelchair users and controls were enrolled in this study. Controls were gender and age matched within ±5 years to wheelchair users. Three wheelchair users had wheelchairs equipped with power assist wheels. Among wheelchair users diagnoses/injuries included bilateral below knee amputation (n=1), guillian barre syndrome (n=1), extensive leg fractures resulting in nerve damage (n=1), multiple sclerosis (n=3), traumatic brain injury (n=1), paraplegia (n=9), tetraplegia (n=6). This study was approved by the local Institutional Review Board. Consent of each subject was obtained prior to the study. Subjects were eligible to participate in this study if they were over the age of 18, spoke English, and able to raise their arm above their head. To be eligible for the study manual wheelchair users also had to use a wheelchair as their primary means of mobility (>80% of mobility). Subjects were excluded from this study if they had a history of fractures or dislocations in the shoulder from which they had not fully recovered, had upper extremity impairment, weakness or spasticity that prevented smooth movement, or if they could not complete reach tasks while seated with support straps around the trunk. Testing of

wheelchair users occurred both at the National Veteran's Wheelchair Games (NWVG) (n=16) and the Human Engineering Research Labs (HERL) (n=22).

3.2.2 Questionnaires

Subjects were asked to complete basic intake forms and pain questionnaires. The basic intake form asked about subject age, ethnicity, height, weight, dominant handedness and if any shoulder pain was experienced in the last 7 days. If the participant was a wheelchair user, we also asked questions on type of injury or diagnosis and date of injury or diagnosis. A short questionnaire regarding history of shoulder pain and upper extremity surgical history was also administered. The Wheelchair Users Shoulder Pain Index (WUSPI), which asks about pain during daily activities, was administered to wheelchair users. The WUSPI consists of 15 items and each item is scored using a continuous 10-cm visual scale.[101]

3.2.3 Clinical Evaluation

The clinical examination was administered to all participants and consisted of physical and ultrasound exams of the upper extremity to determine if the subject had shoulder pathology. The dominant shoulder was the only shoulder examined as we anticipated finding more pathology on the dominant side. The physical exam has been previously described and consisted of palpation over the bicipital groove/biceps tendon, acromioclavicular (AC) joint, and acromioclavicular joint as well as the Neer test, Hawkin's-Kennedy test, painful arc, Jobe's test, resisted external rotation, and O'Brien's test for the labrum and AC joint. For each item the sign/symptom of pain is scored as either absent (0), equivocally present (1), definitely present

71

(2).[102] The sum of all scores is the Physical Exam of Shoulder Scale (PESS). The PESS ranges from 0 (sign or symptom of pain is definitely absent for all items) to 22 (sign or symptom of pain is definitely present for all items). The ultrasound exam has (USPRS) also been previously described and included static evaluation of bony surfaces and tendons of the rotator cuff as well as dynamic evaluation of impingement. [102] The USPRS ranges from 0 (normal tendon fibrillar patterns, smooth cortical surface, and no evidence of impingement) to 20 (fuller thickness tendon tears, marked cortical irregularity, and marked impingement). A full description of the PESS and USPRS scoring can be found in Appendix E.

3.2.4   Testing Procedure

The same testing setup used for the reliability study was used for this study (2.2.3). Controls followed the same testing protocol listed in the reliability study (2.2.4). Manual wheelchair users (MWUs) completed a similar protocol however trials were only completed twice, rather than three times, in each testing position.

3.2.5   Data Analysis

Freehand three-dimensional ultrasound data was processed in the same manner as the reliability study (2.2.5). Average scapular rotations across trials were determined for each subject. The WUSPI score for each item was determined and summed for a total score. The corrected score was used which divided the total score by the total number of items completed and multiplied by 15, the total number of items.[101, 103] Similarly, the sum of scores for each item on the USPRS and PESS were tallied.

3.2.6   Statistical Analysis

Demographic variables were compared across groups using paired comparisons or Chi Square (age, gender, ethnicity, height, weight, and BMI). To evaluate differences in scapular rotations between controls and wheelchair users we performed an ANOVA for each of the scapular rotations (internal/external rotation, upward/downward rotation, and anterior/posterior tilt) with a between group factor of group (control or wheelchair user), and a within group factor of testing position (rest and arm elevation in the frontal, sagittal, and scapular planes). We evaluated resting position of the scapula and trunk and presence of pain/pathology as covariates. Trunk and arm position were compared across groups. To determine if any subject characteristics should be added as covariates, we dichotomized the following variables to determine if there was a relation to scapular rotation: PESS to pain and no pain (0, >0), USPRS to above and below the median score (<=5, >5), years since injury (<=10 years, >10 years), age to above and below the mean (<=50 years, >50 years), and BMI to overweight or not overweight (>=25 kg/m^2, <25 kg/m^2) .

To evaluate the reliability of applying this method to determining movement among manual wheelchair users, ICCs were used to evaluate the consistency in measured scapular rotations across repeated trials. As was done with the controls in Study 1 (2.0), the ICC was calculated for each rotation (YX'Z'') of the scapula in each of the testing positions (rest and elevation in the sagittal, frontal, and scapular planes). This calculation was used to determine the SEM for each rotation and position for this group.

To characterize any differences in SEM between groups, we elected to compare the number of reconstructed points in the scapular border for subjects. The number of reconstructed

points in the scapular border provides insight to the quality of ultrasound imaging and density of the point cloud that our scapular positions were determined from. We hypothesized that fewer points in the reconstructed border would lead to greater variation between trials. As testing occurred in two different locations, NVWG and HERL, we also wanted to determine if there were differences between testing locations so we compared the number of reconstructed points for subjects between testing sites.

To investigate the relationship between pathology and scapular position in the combined group of controls and wheelchair users, a multiple regression was performed to predict each of the scapular rotations based on USPRS score, PESS score, age, BMI, trunk flexion, and resting scapular position. As some of the data collected was unique to wheelchair users (WUSPI score, years of wheelchair use), a multiple regression was also performed on just this subset of data with these predictors added in addition to those aforementioned. Predictor variables for both models were tested for correlation and collinearity. All statistical analyses were completed with IBM SPSS Statistics Software, version 20 (Armonk, NY: IBM Corp.) with the significance level set apriori at 0.05. To correct for multiple comparisons the Holm test was used which orders unadjusted p-values and then accepts or rejects the tests with decreasing rigidity, based on the number of tests already done.

3.3   RESULTS

3.3.1   Differences in Scapular Kinematics between Able-Bodied Controls and Manual Wheelchair Users

Twenty-two able-bodied individuals (13 male, 9 female; age = 50.5±11.6 years, height = 1.72±0.13m, body mass = 74.22±15.02kg, body mass index = 24.22±2.87 m/kg^2) and 22 manual wheelchair users (13 male, 9 female; age = 50.6±12.2 years, height = 1.73±0.13m, body mass = 73.3±13.8kg, body mass index = 24.56±4.85 m/kg^2, years of wheelchair use = 16.3±9.4 years) participated in this study. We found no between group differences for age (p=0.958), gender (p=1), ethnicity (p=0.621), height (p=1), weight (p=0.75) or BMI (p=0.668). We anticipated differences between groups for clinical exam scores however none were found for PESS (p=0.86) or USPRS (0.154). When comparing dichotomized scores for the clinical exam we found a significant difference between groups for USPRS X^2(1)=5.867, p=0.015. Fourteen wheelchair users had a USPRS greater than 5 compared to only 6 controls. A summary of median and inquartile ranges by group for clinical exam and WUSPI scores can be found in Table 10. We found trunk extension was significantly greater for AB than MWU at rest and with the arm elevated in the scapular plane. There were no differences in arm position across groups in any of the testing positions.

Table 10: Median and Interquartile Ranges for PESS, USPRS, WUSPI

Group	Score	Median	IQR
AB	PESS	2	0.5-3.0
	USPRS	3.5	1.0-5.8
MWU	PESS	2	0-4.0
	USPRS	6.5	4.0-8.0
	WUSPI	2.5	0-17.4

Summary plots comparing the two groups can be found in Figure 35. Each column represents a rotation (internal/external, upward/downward, and anterior/posterior tilting respectively) while each row represents the difference between a testing position and rest (ie elevation in the sagittal plane – rest).
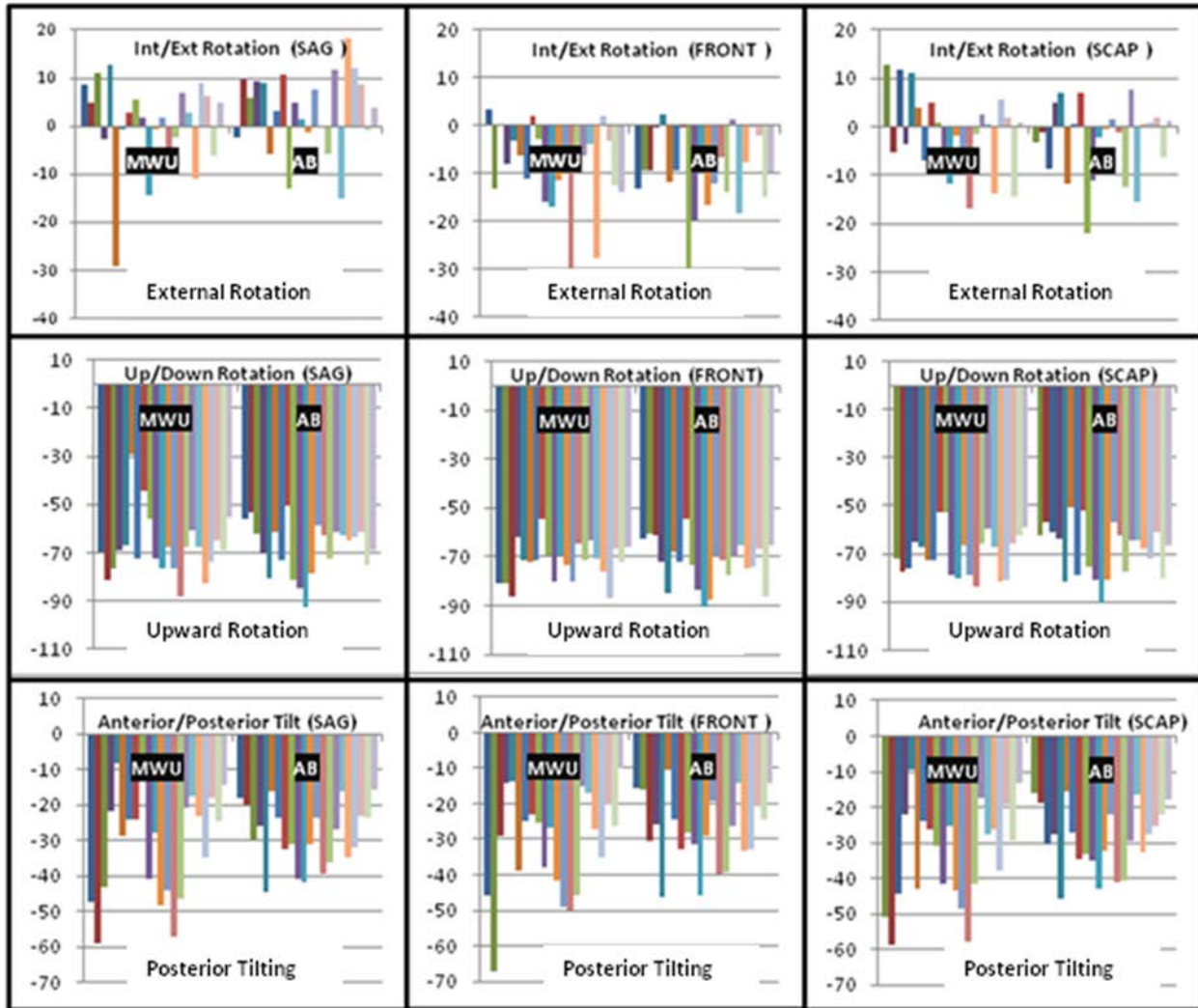
Figure 35: Comparing Scapular Rotations in All Testing Positions between MWU and AB (Testing Position – Rest)

A two-way mixed ANOVA with a between subjects factor of group, a within subjects factor of testing position, and covariates as described above yielded no significant differences for any of the scapular rotations. A description of average group values and standard deviations for each scapular rotation can be found below in Table 11. Mauchly's test indicated the assumption of sphericity had been violated for all three scapular rotations to the Huynh-Feldt estimates of sphericity were used to correct the degrees of freedom. Internal/external rotation was not significantly different between groups $F_{(1,41)}=0.117$, $p=0.734$. Upward/downward rotation was not significantly different between groups $F_{(1,41)}=0.382$, $p=0.540$. Anterior/posterior tilting position was not significantly different between groups $F_{(1,41)}=0.382$, $p=0.540$. There was not a significant interaction between testing position and group for any of the scapular rotations.

Table 11: Mean ± Standard Deviation Scapular Rotation for MWU and AB for All Testing Positions

Scanning Position	Scapular Rotation					
	Internal / External Rotation		Upward / Downward Rotation		Anterior / Posterior Tilting	
	MWU	AB	MWU	AB	MWU	AB
Rest	32.3±1.4°	31.6±1.3°	-5.3±2.0°	-0.5±2.5°	-14.0±1.3°	-12.4±1.2°
Sagittal Plane 120°	34.1±2.5°	34.9±3.6°	-37.0±3.6°	-36.4±3.6°	1.1±2.8°	3.1±1.8°
Frontal Plane 120°	23.1±2.5°	21.8±1.8°	-40.0±4.8°	+40.8±3.6°	1.2±3.5°	4.3±1.4°
Scapular Plane 120°	30.8±1.9°	28.8±2.0°	-37.7±3.3°	-37.0±3.7°	-1.4±1.8°	2.8±1.8°

A summary of the SEM for MWUs across trials can be seen in Table 12. SEM was higher for all rotation/testing position pairings for MWUs as compared to able-bodied controls (2.3).

Table 12: SEM for Scapular Rotations among MWUs across Trials

Scanning Position	Scapular Rotation					
	Internal / External Rotation		Upward / Downward Rotation		Anterior / Posterior Tilting	
	MWU	AB	MWU	AB	MWU	AB
Rest	0.24°	0.16°	0.69°	0.47°	2.87°	0.19°
Sagittal Plane 120°	1.63°	0.34°	1.72°	1.14°	6.27°	0.37°
Frontal Plane 120°	3.08°	0.25°	2.91°	1.33°	1.15°	0.21°
Scapular Plane 120°	2.10°	0.27°	1.60°	0.65°	1.43°	0.32°

To further investigate these differences in error between the two groups, we tallied the number of reconstructed points in the scapular border for each subject in each testing position. Comparisons between groups revealed significantly more reconstructed points among controls in all testing positions (<0.001) (Figure 36).
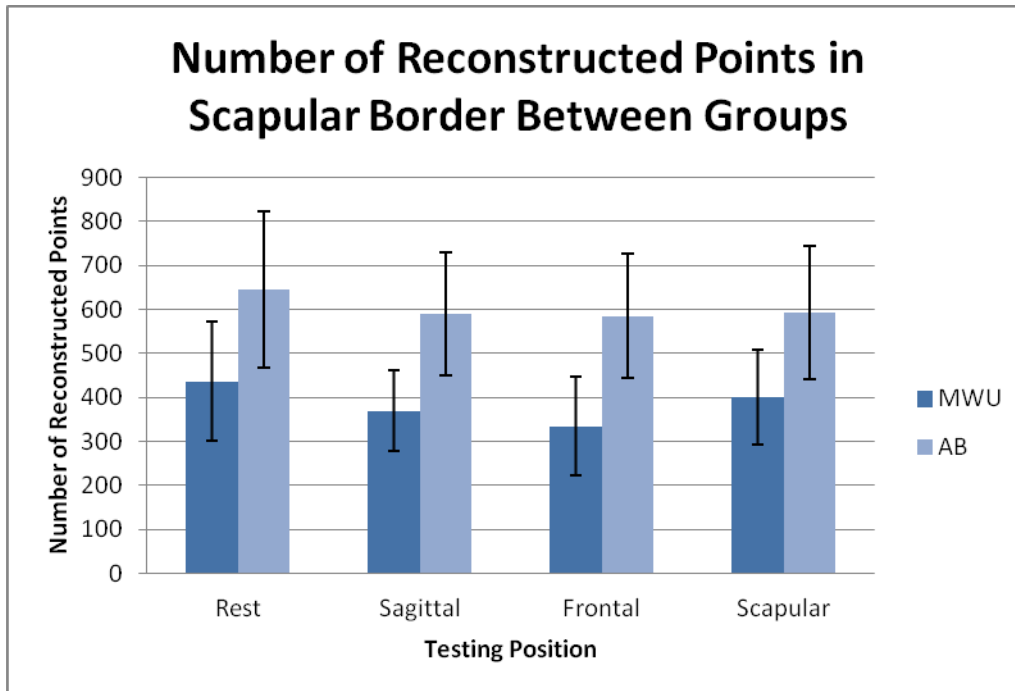
Figure 36: Mean Number of Reconstructed Points in the Scapular Border for Controls and Wheelchair Users (n=22 MWU, n=22AB)

We found that the scapular borders of those tested at HERL consisted of significantly more reconstructed points (p<0.001) (Figure 37).
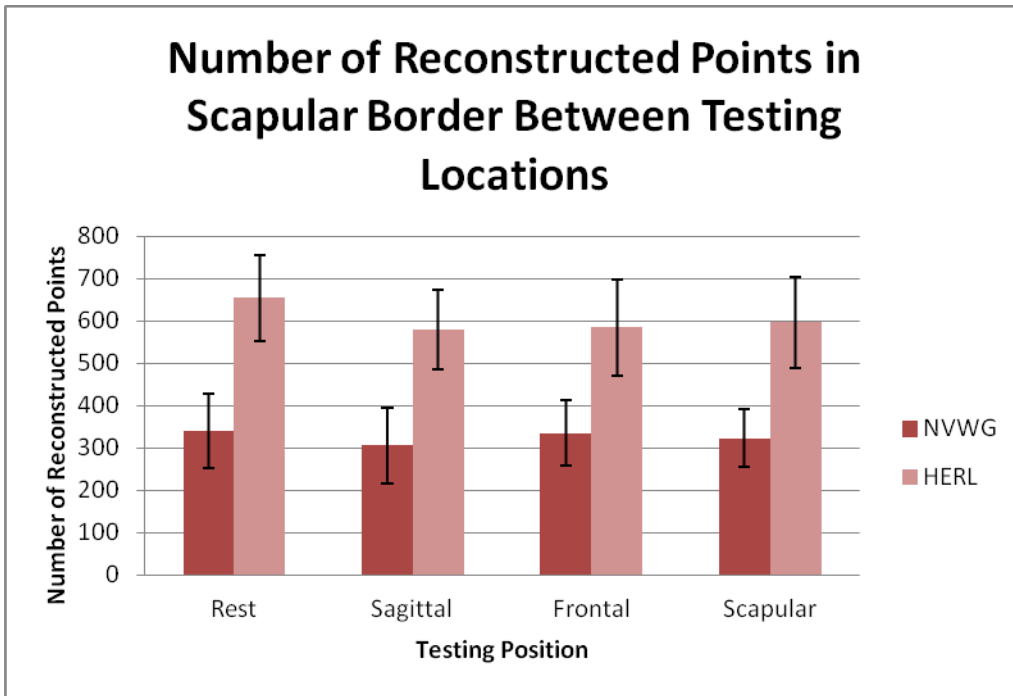
Figure 37: Number of Reconstructed Points in the Scapular Border Between Testing Locations (NVWG & HERL) (n=16 NVWG, n=28 HERL)

As differences were found between testing locations, we also compared controls to only the wheelchair users tested at HERL. We found no significant differences between groups and in this instance wheelchair users had scapular borders with significantly more points than controls (Figure 38).
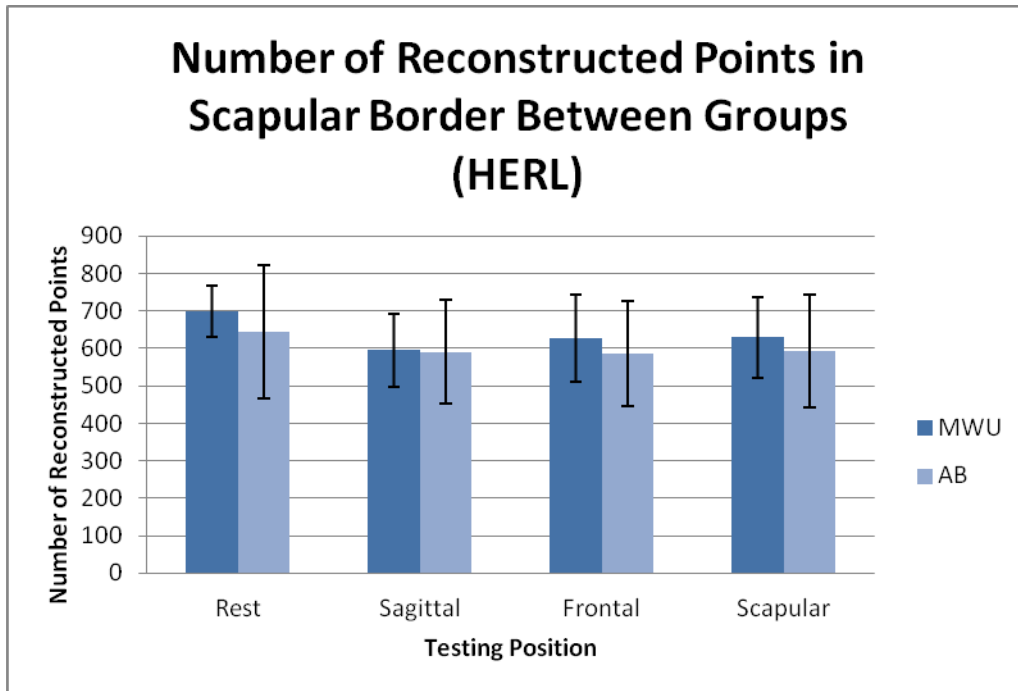
Figure 38: Number of Reconstructed Points in the Scapular Border for Controls and Wheelchair Users Tested at HERL (n=6 MWU, n=22 AB)

We also evaluated how the number of reconstructed points varied with chronological time of study testing. Linear regressions yielded a significant relation between time and number of reconstructed points in all testing positions: rest ($R^2=0.530$, $p<0.001$), sagittal ($R^2=0.588$, $p<0.001$), frontal ($R^2=0.596$, $p<0.001$), and scapular ($R^2=0.575$, $p<0.001$). A plot of reconstructed points for each subject (time ordered) can be seen below in Figure 39.
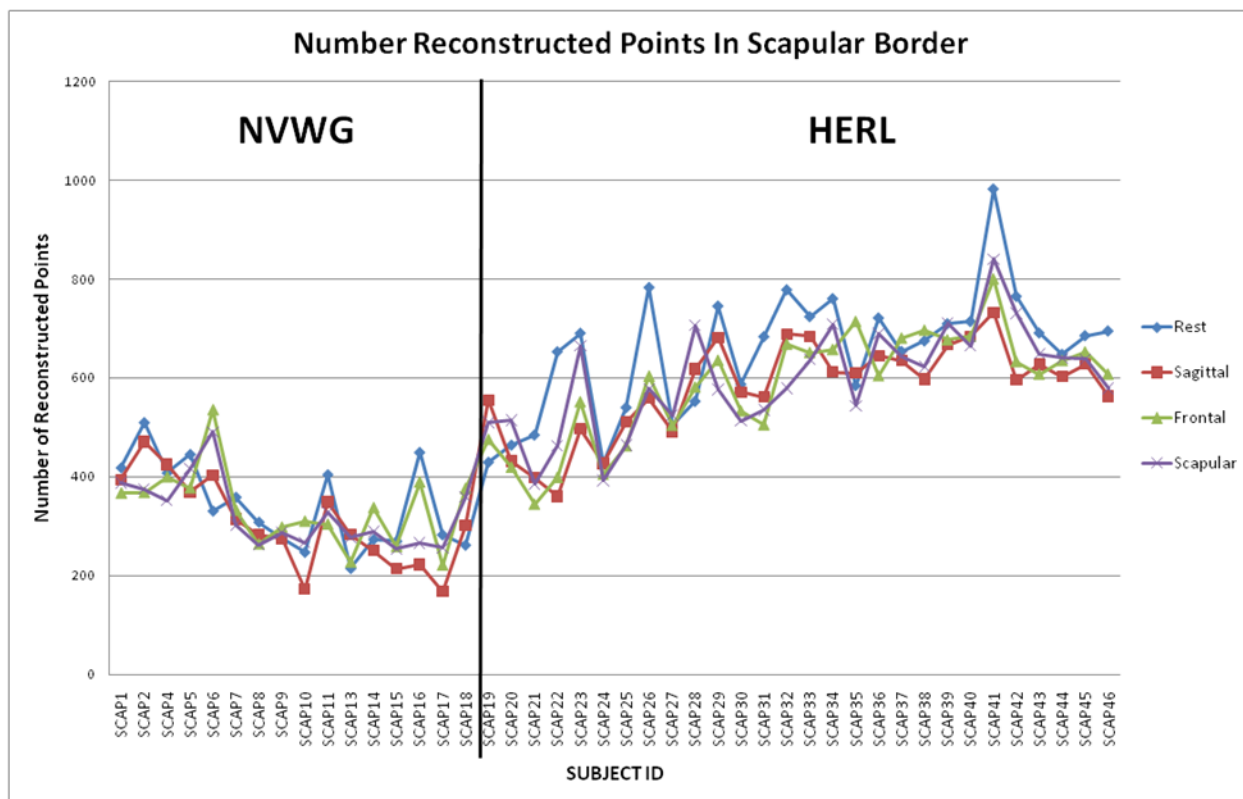
Figure 39: Number of Reconstructed Points in the Scapular Border Over Time (n=16 NVWG, n=28 HERL)

To represent these differences in a more visual manner, we have provided plots of the reconstructed scapula border for a wheelchair user tested at the NWVG, a wheelchair user tested at HERL, and an able-bodied control tested at HERL (Figure 40). Each subject is displayed in a column while the rows represent different testing positions (top to bottom: rest and elevation in the sagittal, frontal, and scapular planes). It is possible to see a clear visual difference in the density of the reconstructed border between subjects tested at HERL and the subject tested at the NVWG.
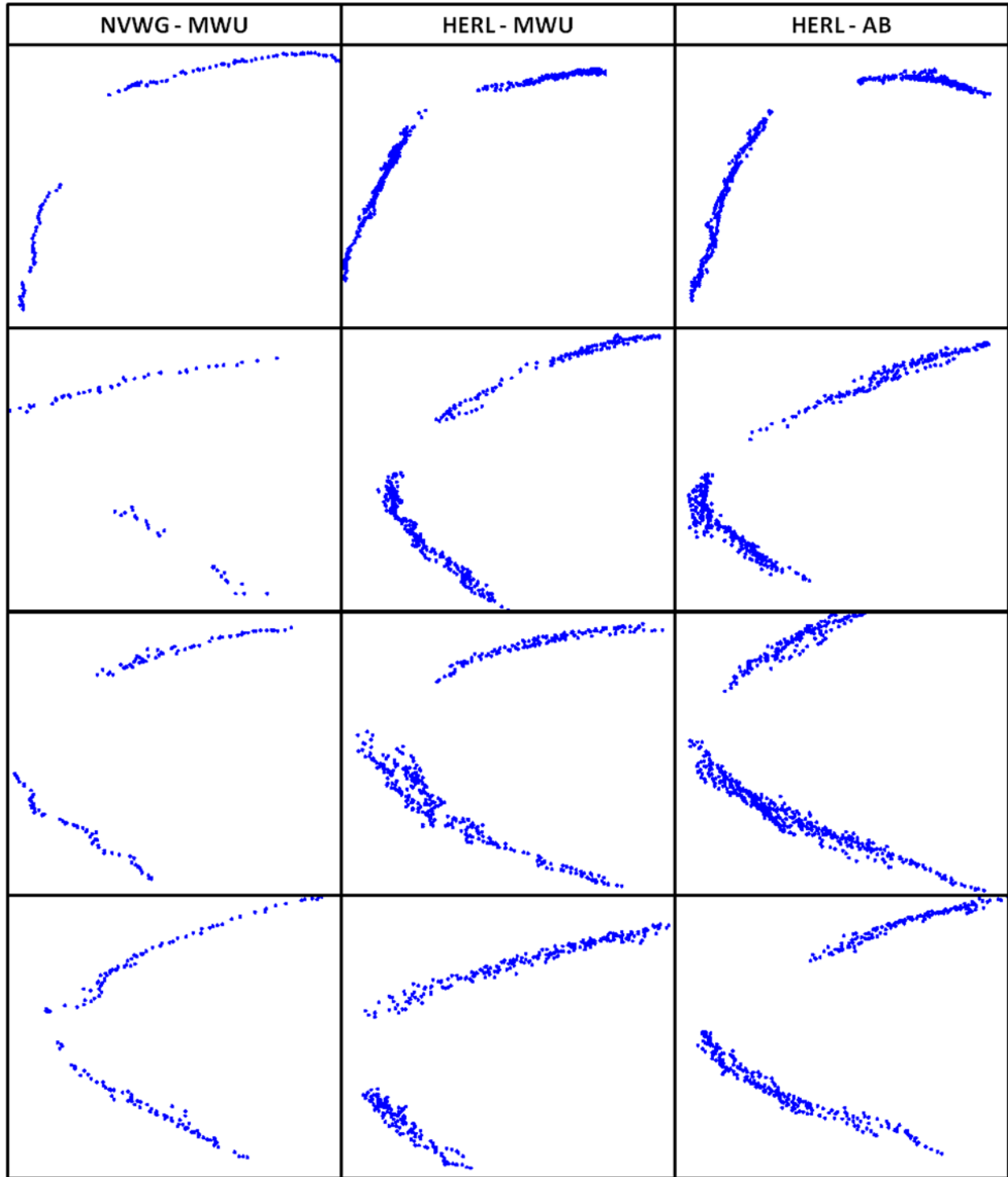
Figure 40: Examples of Reconstructed Scapular Borders for a Wheelchair User Tested at NVWG, a Wheelchair User Tested at HERL, and an Able-Bodied Control Tested at HERL (Rows from Top to Bottom are Rest and Elevation in the Sagittal, Frontal, and Scapular Testing Planes)

3.3.2 Predicting Scapular Kinematics based on Subject Characteristics

Multiple regression analyses were used to evaluate the relationship between scapular kinematics and subject characteristics (age, years since injury, BMI, PESS, USPRS, WUSPI, trunk position at rest, and scapular position at rest). In investigating relationships between regression predictor variables we found greater BMI was correlated greater anterior tilting at rest (r=0.348, p=0.021) and higher USPRS scores were correlated to increased age (r=0.543, p<0.001). Increased trunk extension at rest was correlated with higher USPRS scores (r=0.137, p=0.036), downward rotation at rest (r=0.377, p=0.012), and anterior tilting at rest (r=0.371, p=0.013). Among wheelchair users, WUSPI and PESS scores were correlated (r=0.574, p=0.005) and greater years of wheelchair use was correlated with downward rotation at rest (r=0.477, p=0.025).

At rest we found no correlation between internal/external rotation and any of the predictor variables. Downward rotation in this testing position was correlated with decreased trunk flexion at rest (r=0.377,p=0.012). Posterior tilting was predicted by trunk flexion at rest (β=-0.314, p=0.032) and BMI (β=-0.286, p=0.05) in a multiple regression model (R^2=0.142, F(2,41)=5.635,p=0.007).

In the sagittal plane testing position, we found internal rotation was predicted by internal rotation at rest (β=0.574, p<0.001), trunk extension at rest (β=0.377,p=0.001), posterior tilting at rest (β=-0.347,p=0.002) and USPRS score (β=-0.211, 0.049) in a multiple regression model (R^2=0.649, F(4,38)=18.345,p<0.001). Downward rotation in this position was correlated to downward rotation at rest (r=0.718,p<0.001). Posterior tilting was predicted by posterior tilting at rest (β=0.6, p<0.001) and internal rotation at rest (β=-0.365,p<0.002) in a multiple regression model (R^2=0.369, F(2,40)=20.134,p<0.001).

In the frontal plane testing position we found internal rotation was predicted by internal rotation and trunk extension at rest (β=0.428, p=0.001), internal rotation at rest (β=0.369,p=0.002), and posterior tilting at rest (β=-0.273, p=0.026) in a multiple regression model (R^2=0.518, F(3,40)=14.343,p<0.001). Downward rotation in this position was correlated to downward rotation at rest (r=0.316,p=0.037). Posterior tilting was predicted by posterior tilting at rest (β=0.524, p<0.001), and internal rotation at rest (β=-0.394,p<0.002) in a multiple regression model (R^2=0.424, F(2,41)=15.608,p<0.001).

In the scapular plane testing position we found internal rotation was predicted by internal rotation and trunk extension at rest (β=0.355, p=0.004), internal rotation at rest (β=0.48,p<0.001), and posterior tilting at rest (β=-0.289, p=0.015) in a multiple regression model (R^2=0.556, F(3,40)=16.713,p<0.001). Downward rotation in this position was correlated to downward rotation at rest (r=0.49,p=0.001). Posterior tilting was predicted by posterior tilting at rest (β=0.48, p<0.001), internal rotation at rest (β=-0.275,p<0.019) and BMI (β=-0.028,p<0.023) in a multiple regression model (R^2=0.497, F(3,40)=13.151,p<0.001).

A summary the relation between scapular rotations in all testing planes and predictor variables can be found below in Table 13.

Table 13: Relation between Scapular Rotations and Predictor Variables (+ indicates positive relation, - indicates negative relation)

Testing Plane	Scapular Rotation	Predictor					
		Trunk Flexion @ Rest	Internal Rotation @ Rest	Downward Rotation @ Rest	Posterior Tilting @ Rest	BMI	USPRS
Rest	Internal Rotation						
	Downward Rotation	-					
	Posterior Tilting	+				+	
Sagittal	Internal Rotation	+	+		-		-
	Downward Rotation			+			
	Posterior Tilting		-		+		
Frontal	Internal Rotation	+	+		-		
	Downward Rotation			+			
	Posterior Tilting		-		+		
Scapular	Internal Rotation	+	+		-	-	
	Downward Rotation			+			
	Posterior Tilting		-		+		

While not significantly different after applying the correction for multiple comparisons, we found a trend towards more posterior tilting for males in the frontal and scapular plane testing positions (p=0.042-0.0580. We also found trends towards more upward rotation and posterior tilting among those under 50 years of age in the rest testing position (p=0.039).

In addition to the regression analysis, we also used paired comparisons to determine if the following dichotomized variables were associated with differences in scapular position: PESS (0, >0), USPRS (<=5, >5), years since injury (<=10 years, >10 years), age (<=50 years, >50 years), and BMI (<25 kg/m^2, >=25 kg/m^2) . We found significantly less upward rotation with PESS >0 in all testing positions (p=0.009-0.034) (Figure 41).
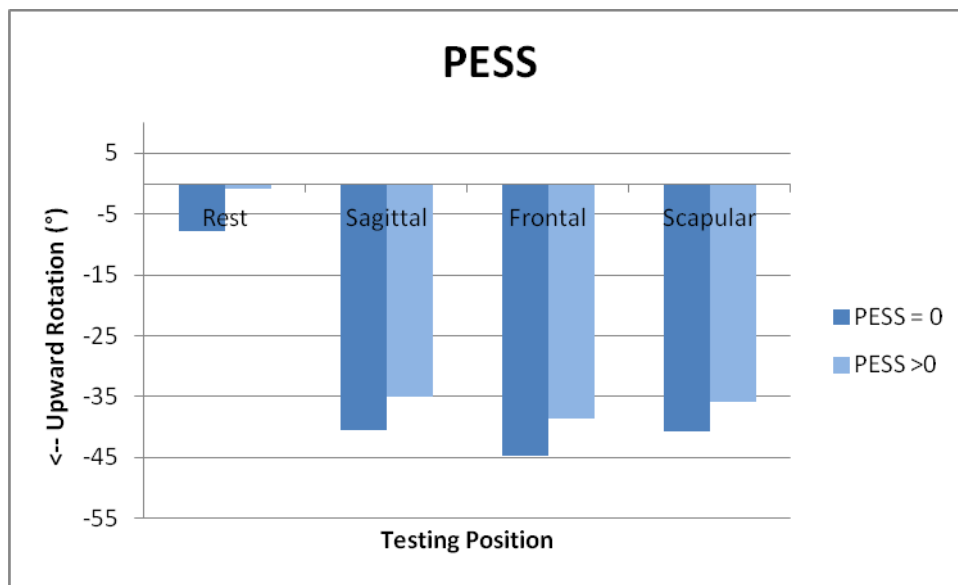
Figure 41: Relationship between Dichotomized PESS and Upward/Downward Rotation (n=44)

We also found significantly less upward rotation in the frontal and scapular plane testing positions with USPRS >5 (p=0.009-0.025) (Figure 42).
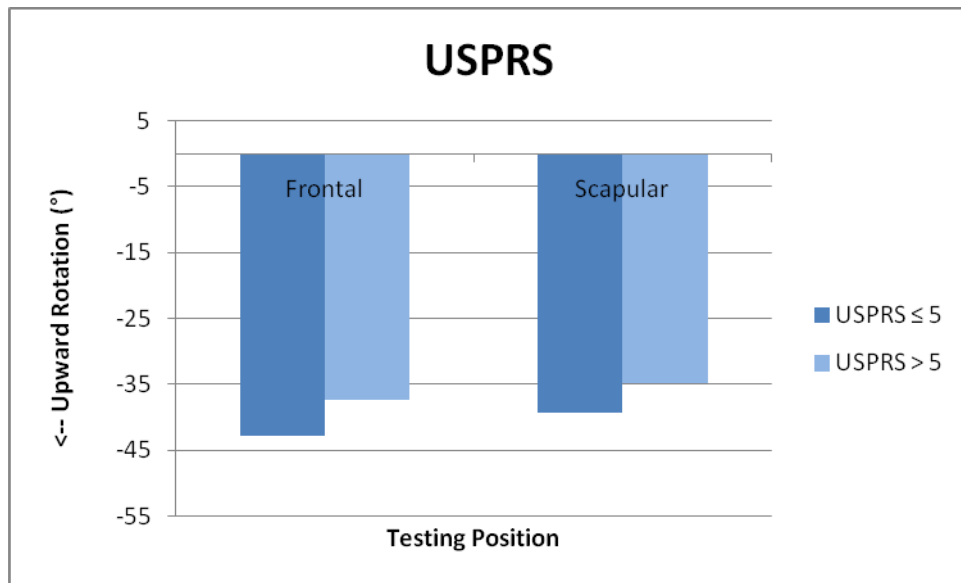
Figure 42: Relationship between Dichotomized USPRS and Upward/Downward Rotation (n=44)

Additionally, we found significantly more internal rotation among those using a wheelchair for great than 10 years in all testing positions (p=0.004-0.021) (Figure 43).
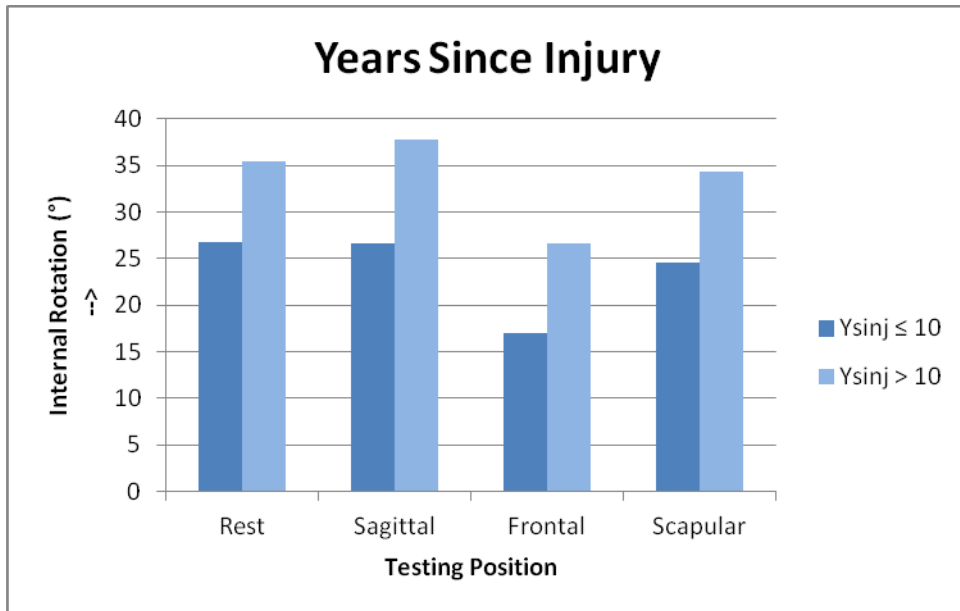
Figure 43: Relationship between Dichotomized Years since Injury and Internal/External Rotation (n=22)

Significantly more posterior tilting was present in all testing positions among those with a BMI less than 25 kg/m^2 (p=0.001-0.015) (Figure 44).
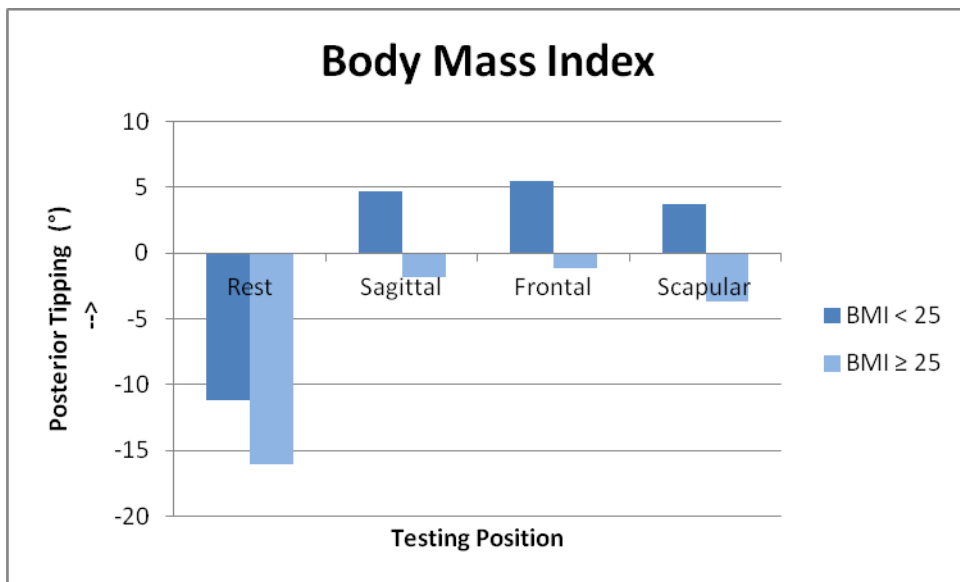
Figure 44: Relationship between Dichotomized Body Mass Index and Anterior/Posterior Tipping (n=44)

3.4   DISCUSSION

We found no differences in scapular movement between manual wheelchair users and controls. This lack of difference may be supported by the lack of difference between groups in clinical scores. We anticipated wheelchair users would present with increased shoulder pathology, due to the repetitive nature of wheelchair propulsion and high demand on the shoulder joint in transfers and other activities of daily living. Previous studies have found differences between individuals with and without shoulder impingement. The physical exam was designed to test for shoulder impingement but we found no differences between groups. It is possible that this lack of difference is a result of the population of wheelchair users recruited for this study. Sixteen wheelchair users were recruited at the NVWG and likely represent more active users than the general population. It is possible that the shoulder pain and pathology we expected to see among these users would inhibit participation in sports. Further, impingement is likely to elicit pain with overhead activities. As our protocol involved such activities is also possible that individuals with this type of shoulder pathology would not have enrolled in the study. This is further supported by how few individuals self-reported experiencing shoulder pain in the 7 days preceding testing (n=5). Additionally, the average WUSPI score was 10.5±15.0 with only 8 participants with a score above the mean and 9 participants reporting no pain. A study comparing WUSPI scores among individuals with paraplegia and tetraplegia found comparably higher scores (17.3±24.5 and 29.4±36.6 respectively).[10] Another study found an average WUSPI score of 17.7±21.3.[104] Comparatively, our study had much lower levels of shoulder pain reported. We believe that the lack of significant differences in clinical scores is not indicative of a paucity of pathology among manual wheelchair users but rather the result of a selection bias.

Previous literature presents mixed results on differences found between individuals with and without impingement (Table 14). Overall, no studies have shown differences between groups for internal/external rotation. Disagreement exists across studies for whether upward rotation and posterior tipping increase or decrease or whether there is a difference at all. In this context, it may not be surprising that we did not find consistent differences between groups. Other studies have also suggested that differences in scapular kinematics are more clear when introducing loading, however in this study all tests were completed in an unloaded condition.[3]

Table 14: Differences in Scapular Movement among Individuals with Impingement Syndrome (X indicates no difference)

Testing Plane	Study Authors	Subjects	Methods	Arm Elev	Internal/ External Rotation	Upward/ Down Rotation	Anterior/ Posterior Tipping
Resting	McClure[54]	45 Impingement 45 healthy	Electromagnetic Position Sensor	90°	X	X	X
Sagittal	McClure[54]	45 Impingement 45 healthy	Electromagnetic Position Sensor	90°	X	Increased Upward Rotation	X
	Hebert[52]	41 Impingement signs (29 confirmed impingement) 41 Contralateral shoulders	Electromagnetic Position Sensor	70, 90, 110°	X	X	x
Frontal	Endo[26]	27 with unilateral impingement 27 Contralateral shoulders	Anteropost-erior Radiograph	45, 90°	X	Decreased Upward Rotation	Decreased Posterior Tilting
	Hebert[52]	41 Impingement signs (29 confirmed impingement) 41 Contralat shoulders	Electromagnetic Position Sensor	70, 90, 110°	X	X	x
Scapular	McClure[54]	45 Impingement 45 healthy	Electromagnetic Position Sensor	90°	X	X	Increased Posterior Tilting
	Lukasiewicz[23]	17 Impingement 20 Healthy	Digitized Landmark	30° increment	X	Increased Upward Rotation	Decreased Posterior Tilting (8-9°)
	Ludewig[3]	26 Symptomatic 26 Asymptomatic	Digitized Landmark	30-60, 61-90 and 91-120°	X	Decreased Upward Rotation	Increased Posterior Tilting (91-120° humeral elevation)
	Graichen[62]	20 Impingement 14 Asymptomatic 20 Contralateral shoulders	MRI with 3D reconstruction		X	X (subsample of 5 showed greater upward rotation)	X

Our SEM was higher among wheelchair users than was reported for able-bodied individuals in the first study (2.3). Comparisons of the number of reconstructed points in the scapular border between the two groups of subjects showed significantly higher number of points for controls. As each point contributes to the data set used to determine the scapular coordinate system (by fitting a plane to all of the data and a linear regression to the spine of the scapula), fewer points indicates that each point has a larger individual contribution to the overall fitting. As such, any outliers would have been more likely to influence the scapular rotation calculations if fewer points were present. We found similar differences when comparing the data collected at HERL to data collected at the NVWG; significantly fewer points were aggregated in scapular borders of subjects tested at the NVWG. To determine whether differences between groups (able-bodied vs wheelchair users) were caused by differences in physiological characteristics between groups that complicated scanning or they resulted from different testing locations, we compared between groups for data among individuals tested at HERL. We found no significant differences between groups and in fact, the scapular border of the MWUs were more densely populated with points. An over-time analysis showed the number of points in the reconstructed scapular border increasing over time. In all, we are led to believe that the increased SEM among wheelchair users is not a result of higher error associated with scanning this population, but rather a learning curve associated with the ultrasonographer performing the technique over time.

The results of the multiple regression analyses for scapular rotations at rest revealed that individuals with higher BMI showed decreased posterior tilting. No studies have been done in the past that evaluate the relation between BMI and scapular positioning. Individuals in this study with greater trunk flexion had greater upward rotation and less posterior tilting at rest. Our results align with Finley et al who found greater upward rotation and decreased posterior tilting

94

of the scapula when the arm was at rest among subjects who sat upright compared to those who slouched.[105] These slouched postures mimic the seating position of wheelchair users, characterized to include thoracic kyphosis and rounded shoulders. [104, 106] Previous studies have also related this posture to muscle imbalance and shoulder pain.[104, 106] Across all elevated testing positions (sagittal, frontal, and scapular) increased internal rotation was predicted by increased internal rotation and trunk flexion at rest. In the same manner, less upward rotation and posterior tilting in elevated testing positions were predicted by less upward rotation and posterior tilting, respectively, at rest. In the sagittal and frontal plane testing positions we found more posterior tilting was predicted by greater internal rotation at rest. These relationships indicate that scapular position when the arm is elevated is predicted in large by resting posture and in this study other factors such as age, BMI, PESS, USPRS, WUSPI or years since injury did not add to the prediction.

As previously mentioned, contrary to our hypotheses, pain and pathology were not significant predictors of scapular position in the majority of multiple regression analyses. USPRS score was significantly correlated to the difference in posterior tilting between elevated and rest positions for the sagittal and scapular planes (r=-0.343,p=0.023 and r=0.349,p=0.020). This suggests that increased pathology was related to less posterior tilting with humeral elevation, which is in agreement with other studies.[3, 54] While it was not a significant predictor in all multiple regression models, BMI was significantly correlated to increased anterior tilting in all testing positions (r:0.348-0.483, p:0.001-0.021). Again, this suggests an increase in weight adversely affects scapular tilting. Further investigation revealed that when analyzing as separate groups, this relationship was only significant for manual wheelchair users. This may suggest that body geometry and weight distribution may affect posterior tilting. Among wheelchair users,

those using a wheelchair for more than 10 years demonstrated greater internal rotation in all testing positions. This is in accordance with characteristic seating posture of wheelchair that includes rounded shoulders. [104, 106] This increase in internal rotation can be detrimental as it may put the head of the humerus closer to the anterior aspect of the acromion.[107]

3.4.1 Limitations

This study had a relatively small sample size (n=22) compared to other studies comparing scapular kinematics between individuals with and without shoulder pathology. This study is also limited by the order in which individuals were tested. Due to the timing of the opportunity to collect a large amount of data at the NVWG, 73% of our wheelchair users in this study had been recruited before any able bodied controls were tested as part of the study.

The study intended to test individuals at 120° of humeral elevation however results show on average only 90° of elevation was achieved. This is likely due to inaccurate goniometer measurements that resulted in underestimating 120° of humeral elevation. Other studies have shown differences between groups are better elucidated at higher arm elevation angles and we may have missed uncovering potential differences between groups.[3] Further, we anticipated a clear distinction between groups with manual wheelchair users exhibiting greater pathology. If we had groups with more significant differences in shoulder pathology we may have found these differences.

This study showed there was a learning curve associated with effectively performing freehand three-dimensional ultrasound to determine scapular rotations. This indicates that ample time should be provided prior to testing on a range of body types to allow the ultrasonographer to become proficient. The most difficulty was found with increased adipose tissue or muscle above

the scapula; new raters should specifically seek out experience in scanning individuals with both of these body types. Number of reconstructed points in the scapula border could be used as an outcome measure to assess readiness of a new rater to commence scanning. We would suggest that a minimum of 600 reconstructed points is achieved to demonstrate competence. Regarding the learning curve, future studies should also incorporate further reliability testing prior to evaluating any between group differences.

3.5   CONCLUSION

While no between group differences were found, this study is the first that we know of to compare scapular kinematics between wheelchair users and controls. This is also the first study that combines subjects from different population pools (able-bodied and wheelchair users) and attempts to use resting trunk and scapula postures to predict scapular kinematics when the arm is elevated. This study found a relation between BMI, PESS, USPRS and years of wheelchair use with scapular kinematics, variables that have not been previously evaluated simultaneously. We found an improvement over time in scanning techniques to visualize the scapular border. Future studies should ensure that adequate training time is provided if these methods are to be used by other raters in the future.

4.0 FREEHAND THREE-DIMENSIONAL ULTRASOUND TO EVALUATE SCAPULAR POSITION DURING DYNAMIC MOVEMENT

4.1 INTRODUCTION

Studying dynamic movement of the scapula is a challenging task as the scapula has six degrees of freedom and glides underneath overlying tissue. Direct visualization of the bone is ideal but often limited by cost, availability, and exposure to radiation. Bone pins provide accurate representation of movement but their invasiveness limits sample sizes to less than 10 in previous studies.[76, 87-88, 93] As with evaluation of static postures, skin based marker systems have also been applied to dynamic scapular movement. In both instances, there is error associated with these systems associated with skin motion artifact. Karduna et al investigated how skin based electromagnetic trackers placed on the acromion and spine of the scapula compared to rotations determined with bone pins.[76] Root mean square error between methods ranged from 3.2° to 11.4°. Correction factors were applied, though based only on the 8 subjects in the study, and errors were still above 4°. We believe that rather than developing methods which attempt to compensate for skin motion artifacts, freehand three-dimensional ultrasound could instead be applied which allows for direct visualization of bone. Freehand three-dimensional ultrasound has been used for imaging organ volumes, echocardiography, and image guided surgery but to our knowledge has never been applied to dynamic joint movement.

The overall goal of this study was to apply freehand three-dimensional ultrasound methods, previously used to look at scapular position in static postures, to dynamic scapular movement. One of the goals of this study was to compare to the scapular rotations of individuals between static trials and dynamic trials. Additionally, we desired to evaluate intermediate angles of functional elevation during dynamic movement (30°, 45°, 60°, and 75°) and hypothesized we would see incremental increases in external rotation, upward rotation, and posterior tipping throughout the movement. A secondary goal was to evaluate the effect of loading on scapular movement. For this we had subjects hold a 3-5 lb hand weight and compared movement between dynamic trials. We also wanted to compare dynamic scapular movement between controls and manual wheelchair users. We anticipated the overuse injuries common among wheelchair users, due to the nature of wheelchair propulsion and demands of activities of daily living, would elucidate differences between this population and able-bodied controls with comparably lower daily demands on the shoulder.

4.1.1 Participants

This study consisted of a subset of age-matched participants from Study 2 (Chapter 3.0). Based on the preliminary nature of this study, we eliminated subjects which had any abnormalities noted during testing (inconsistent hand placement, spasms during testing, arm not against guide pole during arm elevation). Nine age-matched wheelchair users and 9 controls were evaluated in this study.

4.1.2 Testing Procedure

Dynamic trials were completed after the static trials in the scapular plane. For these trials, participants raised and lowered their arm to the stop marker twenty times. To control the speed of movement, subjects were cued with a pacing video that gave them a 5 second count to raise their arm and a 5-second count to lower their arm. Participants were given time to practice moving smoothly to this count. Subject's held their arm in the raised position for 2 seconds before lowering and then were given a 10 second rest period after each time they lowered their arm to prevent fatigue. This trial took 7.5 minutes to complete. During this trial, rather than moving the ultrasound probe continually along the scapular border the probe was held still during each raise-lower pairing. As 20 repetitions occurred, 20 aspects of the scapular border were imaged. An additional dynamic trial was completed in the scapular plane while the subject held either a 3, 4, or 5lb hand weight as determined by subject weight (< 133 lbs, 134 – 155 lbs, and > 155 lbs respectively). This loaded condition was only done during the dynamic trial as fatigue was a concern.

4.1.3 Data Analysis

Dynamic trials were processed in the same manner as the reliability study (2.2.5). The one difference in processing was there was no manual identification of when the ultrasound probe was in contact with the scapula as the probe was moving throughout the trial. An example of what a fully reconstructed trial looked like can be seen below in Figure 45.
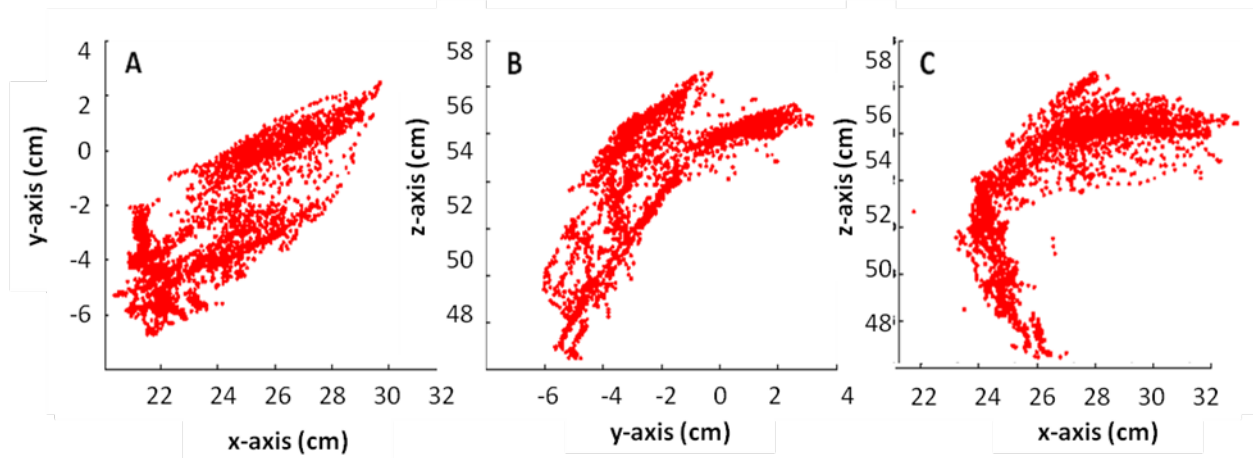
Figure 45: Reconstructed Scapular Border for Entire Dynamic Trial with Views of the Transverse Plane (A), Sagittal Plane (B) and Frontal Plane (C)

Evident in these images are two clear regions where the scapula was at rest and elevated. These regions appear more distinctly as more data was collected in each with rest held for 10s and elevated held for 2s.

Once all of the data was reconstructed, the next step was to determine the angle of humeral elevation throughout the trial. A custom Matlab program was written to manually identify the regions of arm raising and lowering based on Vicon data (Appendix D). These key periods of movement were defined as the time following rest and the time before the subject reached maximum elevation. Maximum elevation and the following rest period for the second abduction movement can be seen below in Figure 46.
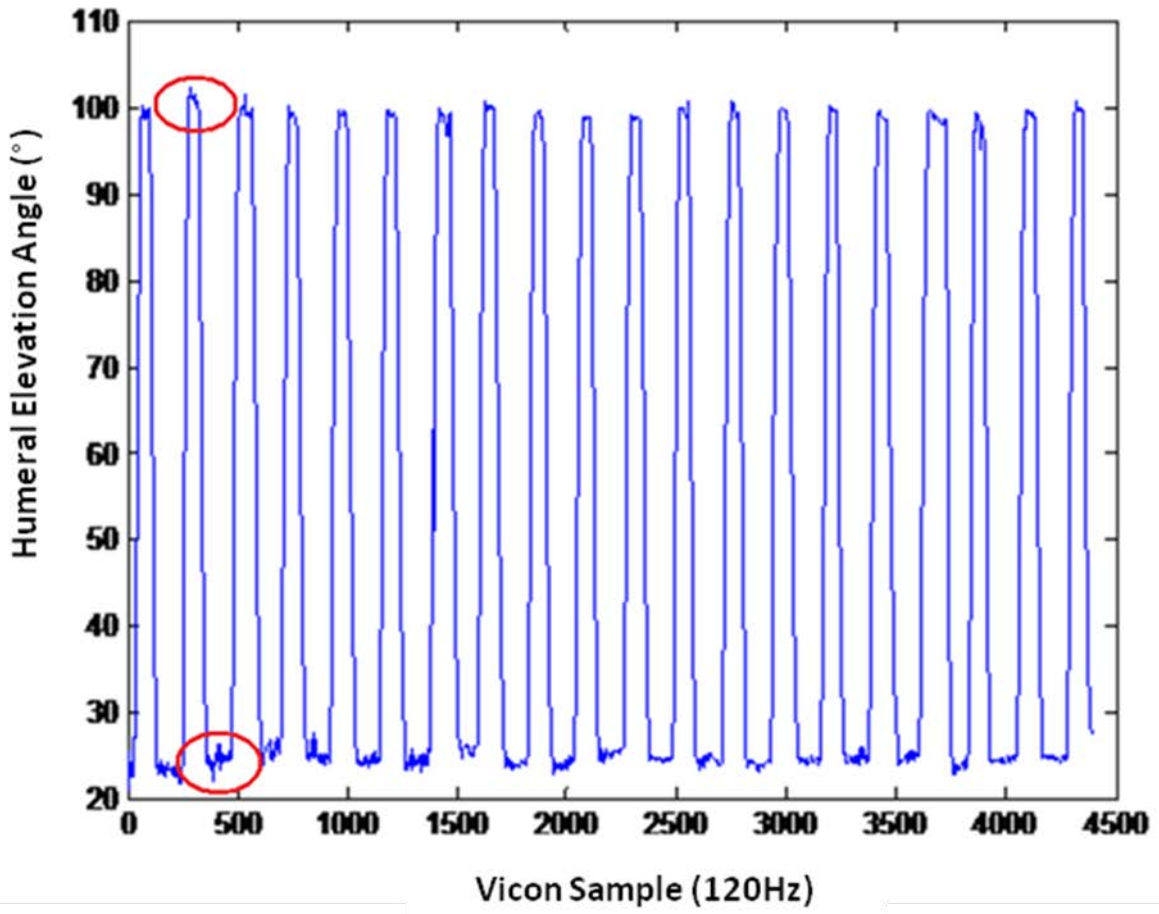
Figure 46: Identifying Humeral Elevation/Depression during the Trial

To evaluate our scanning methods used in the dynamic trial with respect to the static trial, we first determined the amount of humeral elevation each subject had during the static trial in the scapular plane. As subjects held their arm in the elevated position for 2s during each abduction-adduction movement, we believed that there would be enough data points to sample based on humeral angle. As there was some variation in humeral angle between abduction-adduction movements we elected to sample the dynamic data at the angle of elevation from the static trial $\pm$ 1° (ie if during the static trial the subject held their arm at 89° we pulled all reconstructed points from the dynamic data which corresponded to 88°, 89° or 90° humeral elevation).

For evaluating intermediate angles of humeral elevation we had initially planned to extract reconstructed points that corresponded with humeral elevation angles of interest in the same way we analyzed the data when comparing to static trials. However, due to a limited sampling frequency, paired with the frequency of arm movement, we did not always have ultrasound data to pair with all time points of interest. Additionally, this was confounded by the fact that there were portions of the abduction movement in which we were not able to clearly identify the scapula in ultrasound images. Because of these factors, we applied time normalization and spline fitting to extrapolate our data. This process is illustrated in Figure 47. Step 1 is identifying the upward movement of humerus. The humeral elevation angle and reconstructed ultrasound data are then each time normalized to 100% and third order polynomial was used to spline fit each data set. Step 4 was to determine at what percentage of that time period the arm was at the angles of interest (30°, 45°, 60° and 75°). We then pulled the corresponding reconstructed ultrasound point for each angle of interest.
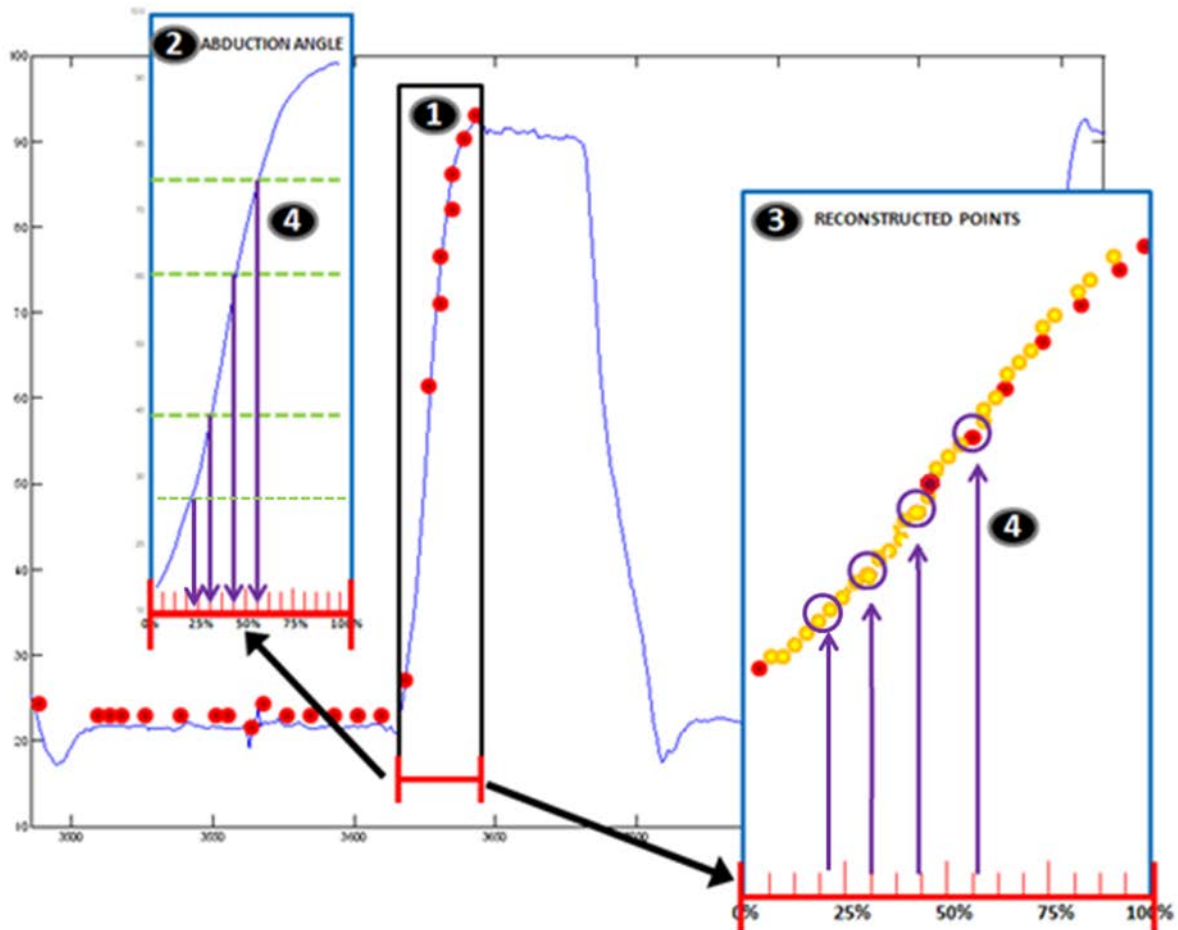
Figure 47: Time Normalization and Spline Fitting of Humeral Elevation Angle and Reconstructed Ultrasound Data

An example of a reconstructed trial can be seen below in Figure 48. This plot shows a view of the frontal plane of the reconstructed scapular border from posterior to anterior for the intermediate angles of 30° (black), 45° (red), 60° (blue), and 75° (green) elevation.
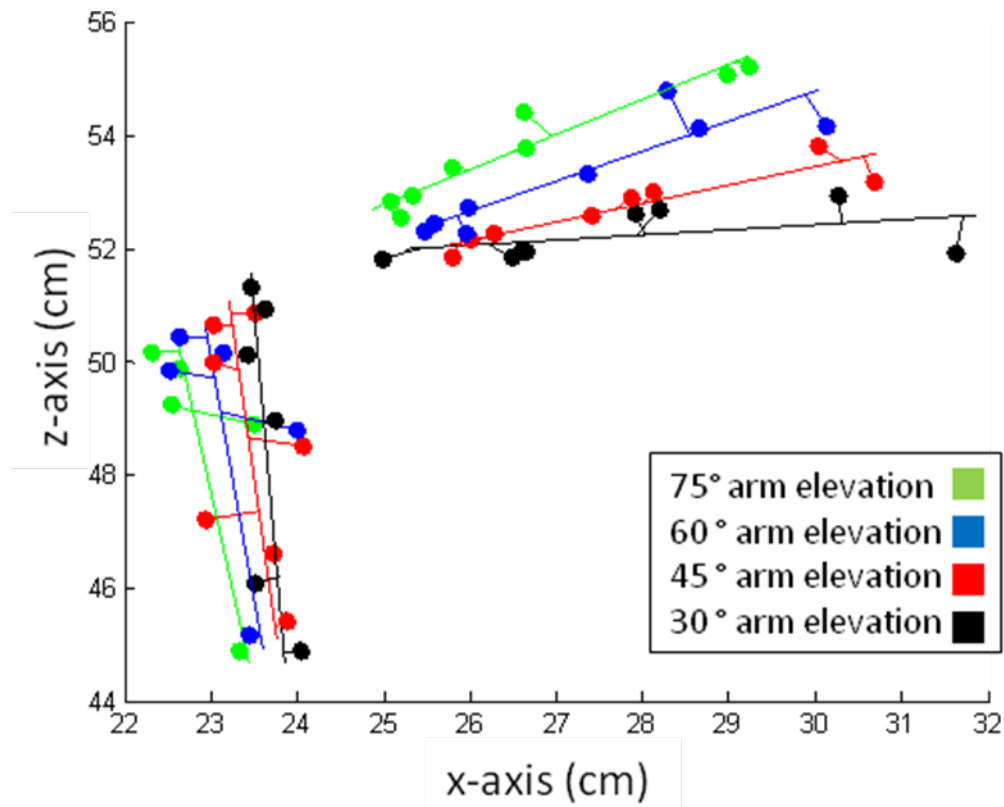
Figure 48: Reconstructed Dynamic Trial

Following point reconstruction, we fit a local coordinate system to the aggregate of the reconstructed points for each arm elevation in the same manner as with the static trials (2.2.5.4). Average scapular rotations across trials were determined for each subject.

4.1.4 Statistical Analysis

We compared our dynamically reconstructed scapula border to the statically derived data set for the rest and elevated scapular positions through correlation and paired comparisons. We also checked for any differences in trunk position between these two sets of trials. The remainder of

our analysis for dynamic trials mirrored the analysis completed for static trials. To evaluate differences in scapular rotations between controls and wheelchair users we performed a three-way repeated measures ANOVA for each of the scapular rotations (internal/external rotation, upward/downward rotation, and anterior/posterior tilt) with a between group factor of group (control or wheelchair user), and within group factors of arm elevation angle (30°, 45°, 60°, 75°) and loading (unloaded and holding hand weight). We performed repeated planned contrasts in which each elevation angle was compared to the preceding angle (45° to 30°, 60° to 45°, 75° to 60°) for elevation angle. Trunk and arm position were compared across groups for dynamic trials. All statistical analyses were completed with IBM SPSS Statistics Software, version 20 (Armonk, NY: IBM Corp.) with the significance level set apriori at 0.05. The Holm test was used to correct for multiple comparisons.

4.2   RESULTS

Prior to discussing the results, it is important to note that 20 points per reconstructed scapula at each extracted humeral angle (based on the 20 abduction-adduction repetitions) were not achieved for all subjects. This is because for some subjects, the scapula border wasn't visibly identified until later in arm elevation period (ie there was no data to interpolate from for 30°), the end of the elevation period was missing (ie there was data to extrapolate to for 75°), or visualization of the scapula during that abduction or adduction movement was not achieved. This concept is illustrated below in Figure 49, where the blue area contains no reconstructed points. The yellow line/circle in the blue area indicate a missing point that could be not extracted for 30° humeral elevation.To ensure an adequate number of points were present to accurately fit a local

106

coordinate to the scapula we set a minimum number of 5 reconstructed points for both the spine and medial border at each angle of arm elevation. Subjects with less than 5 points on each border were excluded. Additionally, some subjects reached a max elevation in dynamic trials which was less than that of static trials. We did not make comparisons between static and dynamic trials for these individuals.
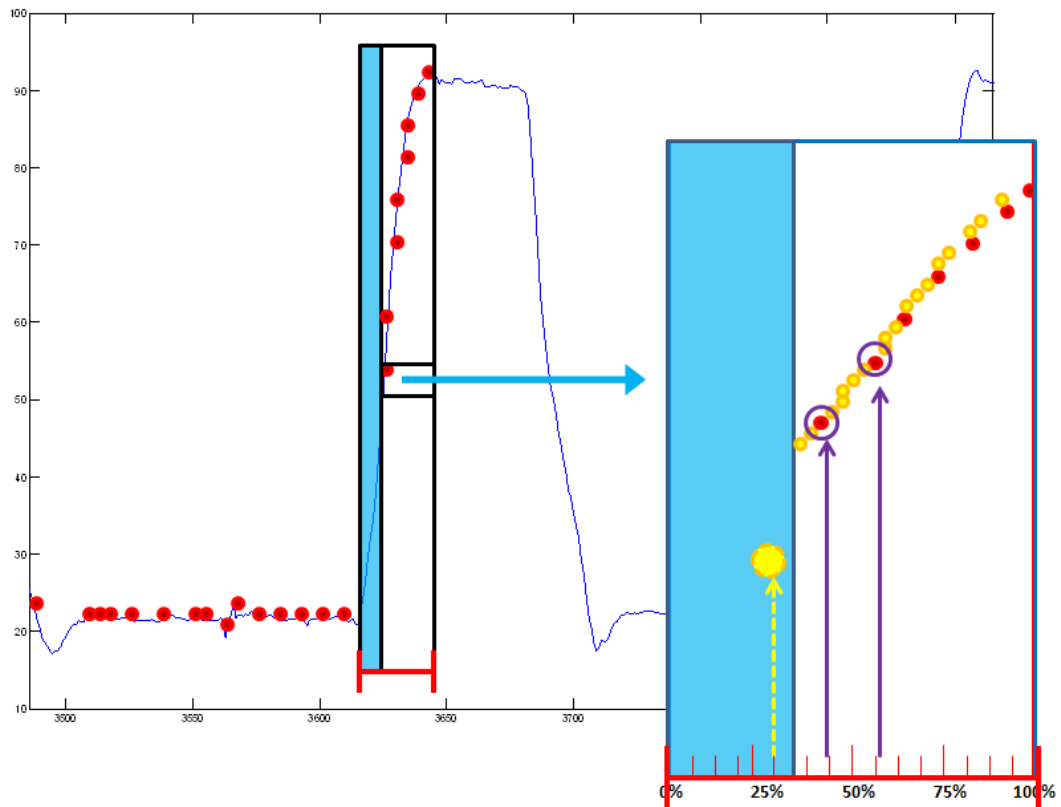
Figure 49: Missing Data in Dynamic Scapular Border Reconstruction

Nine wheelchair users (5 male, 4 female; age =51.2±8.5 years, height = 1.74±0.12m, body mass =69.6 12.9±kg, body mass index = 23.0±3.6 m/kg^2, years of wheelchair use = 16.6±10.2 years) and 9 able-bodied controls (5 male, 4 female; age =51.4 ± 9.8years, height =

1.72±0.14m, body mass = 72.8±16.5kg, body mass index = 24.2±2.4 m/kg^2) participated in this study. Among these individuals we found significant differences between static and dynamic trials for upward rotation and posterior tilting. There was significantly more upward rotation (p=0.004) and posterior tilt (p=0.038) in static trials. A summary of average rotations across participants in both trials can be found in Table 15 with significant differences bolded.

Table 15: Comparison of Scapular Rotations between Static and Dynamic Trials at Maximum Humeral Elevation Angle (Average ± Stdev)

	Internal (+) / External (-) Rotation	Upward (-) /Downward (+) Rotation	Anterior (-) / Posterior (+) Tilting
Static	31.7±9.7°	**-39.4±6.6°**	**0.38±8.3°**
Dynamic	29.4±8.4°	-29.5±10.4°	-3.51±10.8°

We found a significant correlation between the two types of trials for internal/external rotation (r=0.776, p=0.001) and anterior/posterior tilt (r=0.853, p<0.001). For a visual representation of this data we have plotted the difference between dynamic and static trails for all scapular rotations (dynamic - static) in Figure 50.
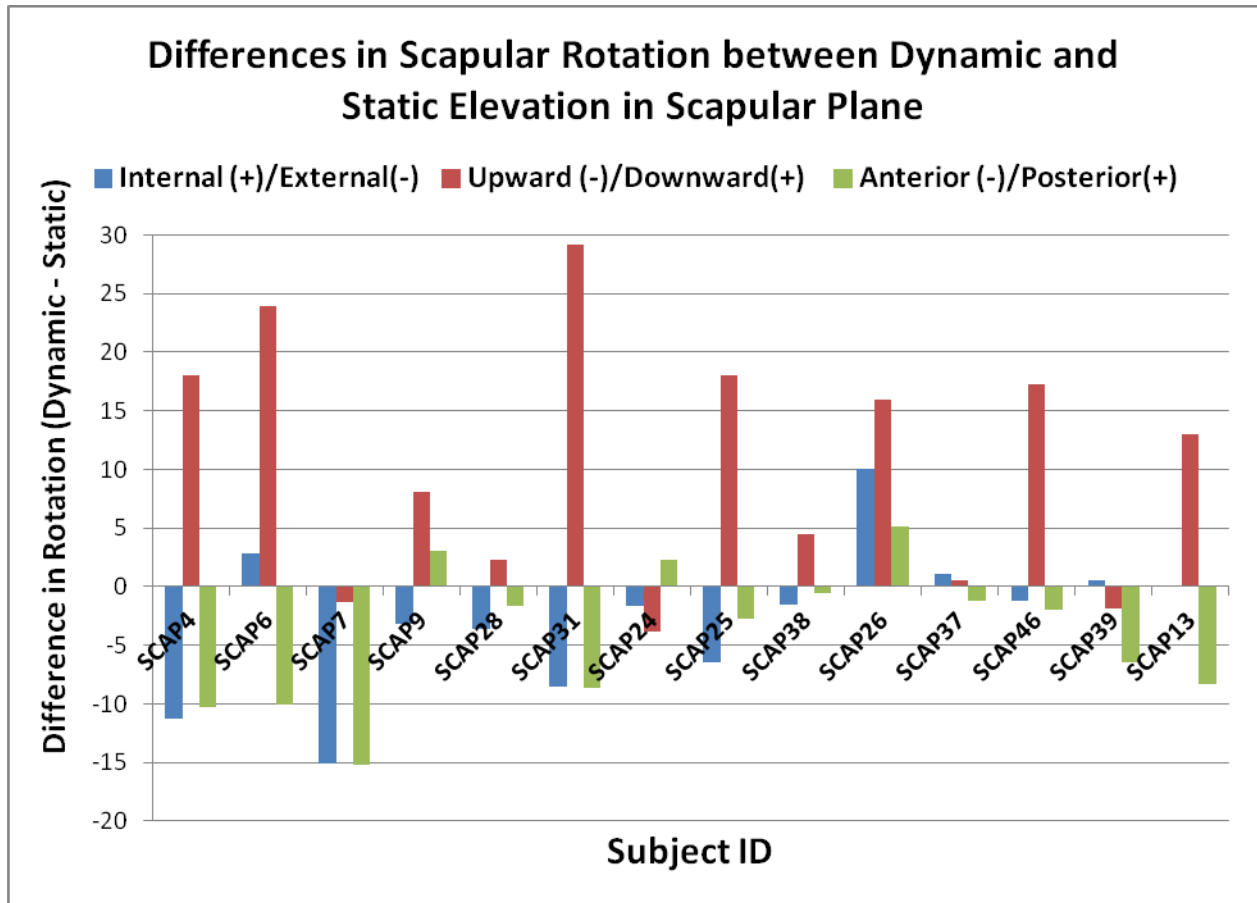
Figure 50: Difference in Scapular Rotations between Static and Dynamic Trials

For the dynamic trials, no significant differences were found in trunk position between loaded and unloaded trials (p=0.24:0.844). On average subjects had a trunk position of 4.4±1.2° of flexion, -0.13±0.63° of lateral rotation, and 2.0±0.91° of lateral flexion. The results of the three-way repeated measures ANOVA to evaluate the effects of loading, arm position and subject type will be discussed for each main effect, followed by interaction effects. For the first scapular rotation, internal/external rotation, we found angle of elevation to have a significant main effect F(3,45)=8.365, p=0.001. Planned contrasts revealed internal rotation increased from 45° to 60° (p=0.018) and from 60° to 75° (p=0.007). Angle of elevation was also a significant

109

main effect for upward/downward rotation (p=0.003, p<0.001, and p<0.001 respectively). There was a significant increase in upward rotation for all incremental increases in elevation from 30° to 75°(p=0.003, p<0.001, and p<0.001 respectively). Finally, angle of elevation was also a significant main effect for anterior/posterior tilting $F(3,45)=34.973$ p<0.001 with significant increases for all incremental increases in elevation from 30° to 75° (p<0.001, p=0.018, and p<0.001 respectively). A summary of the average scapular rotations across subjects for each angle of elevation can be seen in Table 16.

Table 16: Average Scapular Rotations across Subjects for Different Arm Elevation Angles (Unloaded)

Arm Elevation Angle	Scapular Rotation		
	Internal (+) / External (-) Rotation (mean ± SD)	Upward (-) / Downward (+) Rotation (mean±SD)	Anterior (-) / Posterior Tilting (+) (mean±SD)
30°	17.0±16.9	14.3±21.7	-6.2±10.1
45°	10.45±22.8	-5.7±11.9	-6.8±5.5
60°	33.4±8.14	-17.1±8.4	-5.4±7.3
75°	36.2±7.7	-21.6±5.5	-3.2±9.1

Additionally, the same information for the loaded condition can be seen in Table 17.

Table 17: Average Scapular Rotations across Subjects for Different Arm Elevation Angles (Loaded)

Arm Elevation Angle	Scapular Rotation		
	Internal (+) / External (-) Rotation (mean ± SD)	Upward (-) / Downward (+) Rotation (mean±SD)	Anterior (-) / Posterior Tilting (+) (mean±SD)
30°	12.09±23.5	14.3±21.6	-6.6±8.7
45°	31.3±9.7	-11.6±11.5	-7.7±4.9
60°	32.6±9.06	-16.5±13.1	-6.2±6.5
75°	34.8±10.0	-24.1±9.4	-4.3±7.0

To illustrate these increases in internal rotation, upward rotation, and posterior tilting with arm elevation revealed through the planned comparisons, we have plotted the difference in scapular rotations between 30° and 45° (green), 45° and 60° (red), as well as 45° and 60° (purple) below in Figure 51. The left column shows scapular rotations for the unloaded condition while the right column shows the loaded condition. From top to bottom the rows illustrate internal/external rotation, upward/downward rotation, and anterior/posterior tilting.
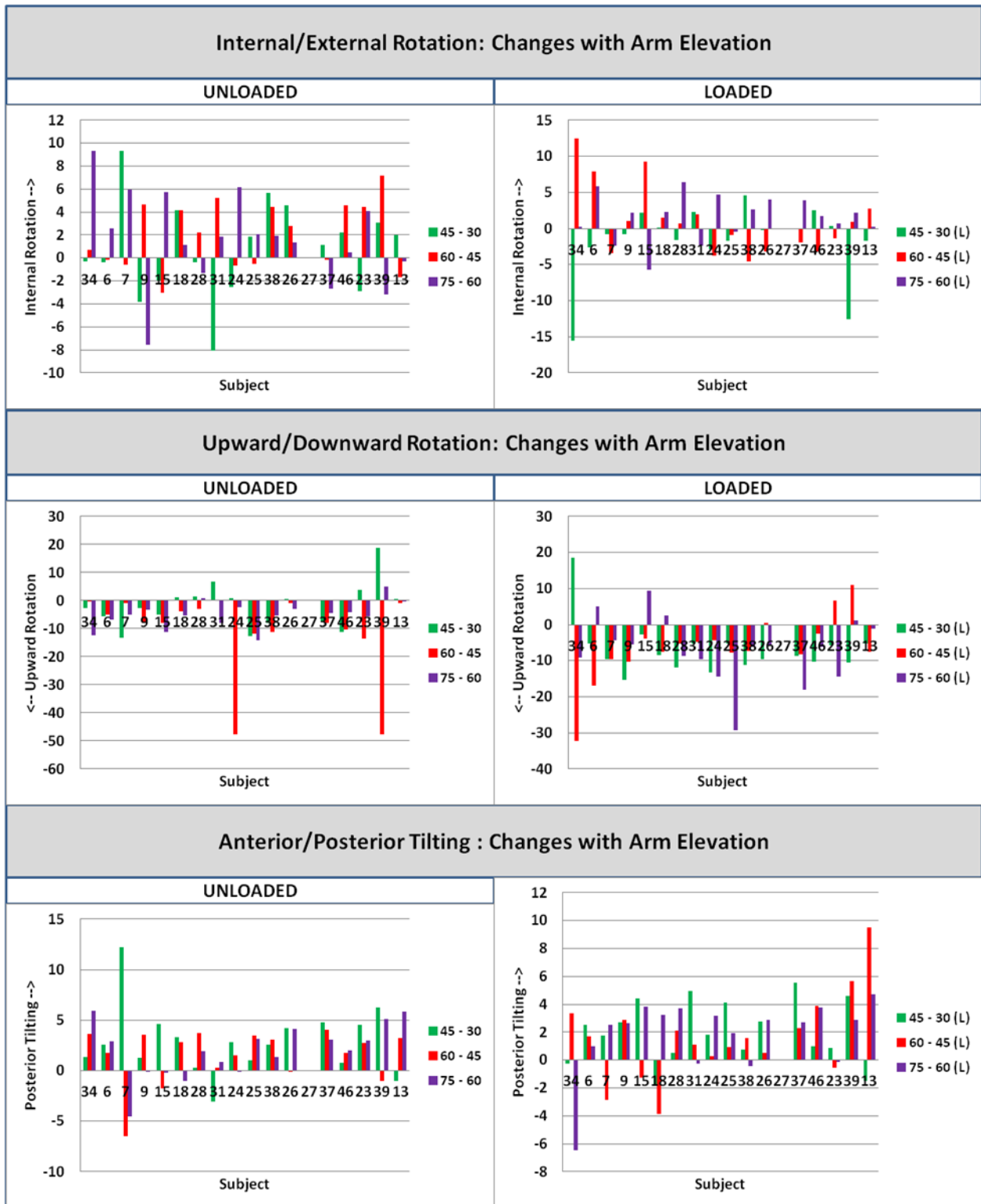
Figure 51: Changes in Scapular Rotation with Arm Elevation

There was not a significant main effect of loading on any of the scapular rotations. A summary of scapular rotations for each arm elevation angle for both loaded and unloaded conditions can be found below in Table 18.

Table 18: Scapular Rotations for Loaded and Unloaded Trials

Arm Elevation Angle	Scapular Rotation					
	Internal (+) / External (-) Rotation (mean ± SD)		Upward (-) / Downward (+) Rotation (mean±SD)		Anterior (-) / Posterior Tilting (+) (mean±SD)	
	No Loading	Loaded	No Loading	Loaded	No Loading	Loaded
30°	17.0±16.9	12.09±23.5	14.3±21.7	14.3±21.6	-6.2±10.1	-6.6±8.7
45°	10.45±22.8	31.3±9.7	-5.7±11.9	-11.6±11.5	-6.8±5.5	-7.7±4.9
60°	33.4±8.14	32.6±9.06	-17.1±8.4	-16.5±13.1	-5.4±7.3	-6.2±6.5
75°	36.2±7.7	34.8±10.0	-21.6±5.5	-24.1±9.4	-3.2±9.1	-4.3±7.0

While the high standard deviations in the table above show the large variance across subjects, this is further illustrated below in Figure 52. Each plot shows the difference in the scapular rotation between loaded and unloaded conditions for 30° (blue), 45° (red), 60° (green), and 75° (purple). The direction of difference between the two conditions varies by subject as well as angle of elevation.
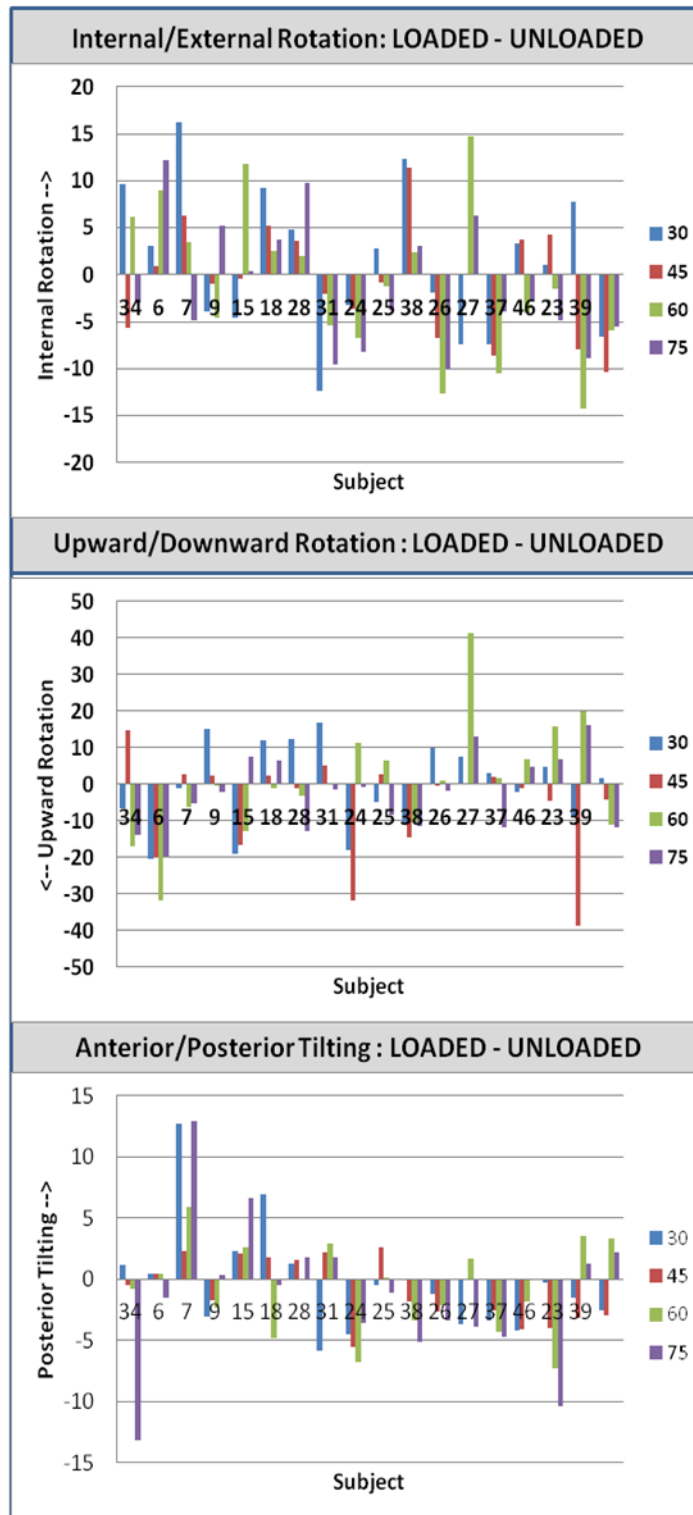
Figure 52: Differences in Scapular Rotations with Loading (Loaded-Unloaded)

114

An example is shown below for two subjects with clear visual differences between static and dynamic trials (Figure 53). Each row is a subject and each column is a different angle of elevation. In each plot, the lighter color is indicative of the unloaded condition and the darker color is the loaded condition.
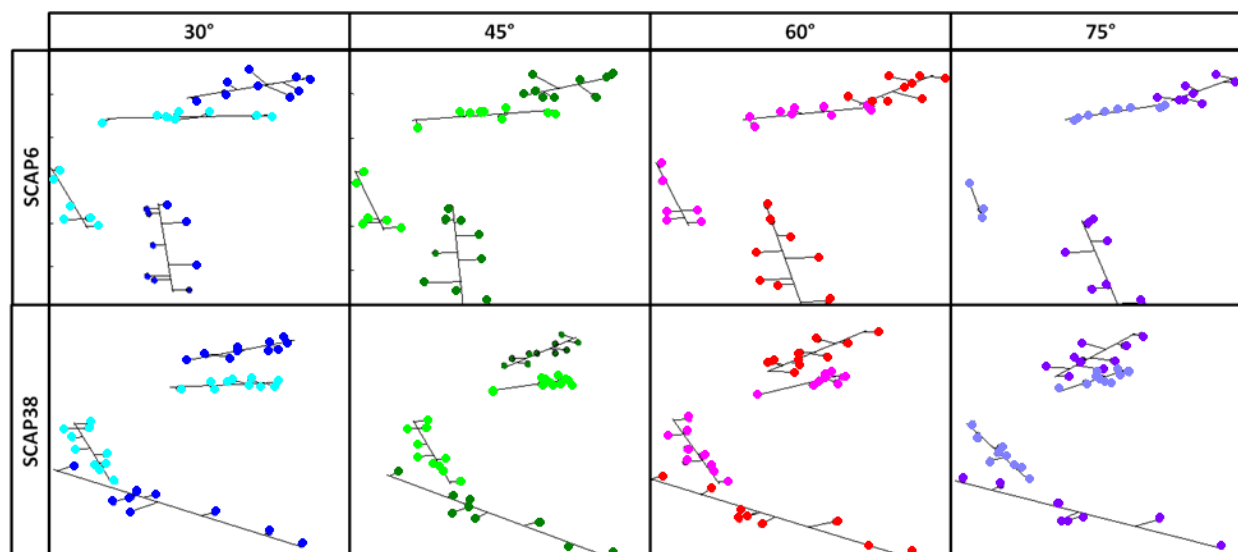
Figure 53: Reconstructed Scapulae for Loaded and Unloaded Conditions of Select Subjects (Sagittal Plane, Medial to Lateral)

These distinct visual differences are supported by consistent differences in scapular rotations with increasing arm angles of elevation. For the subject SCAP6 there is significantly greater internal rotation, upward rotation, and posterior tilting with increases in arm elevation angle (Figure 54). Subject SCAP38 remained in anterior tilt for all positions in both loading

115

conditions but showed the same trend toward increased internal rotation upward rotation and posterior tilting in the loaded condition for angles of arm elevation (Figure 55).
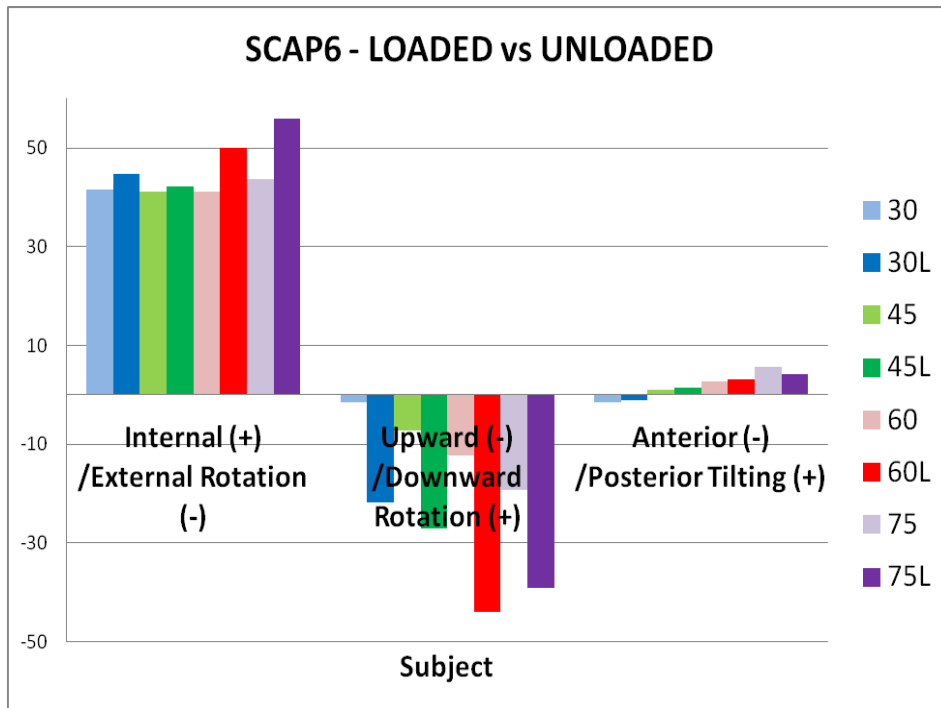
Figure 54: SCAP6 Scapular Rotations in Loaded and Unloaded Conditions
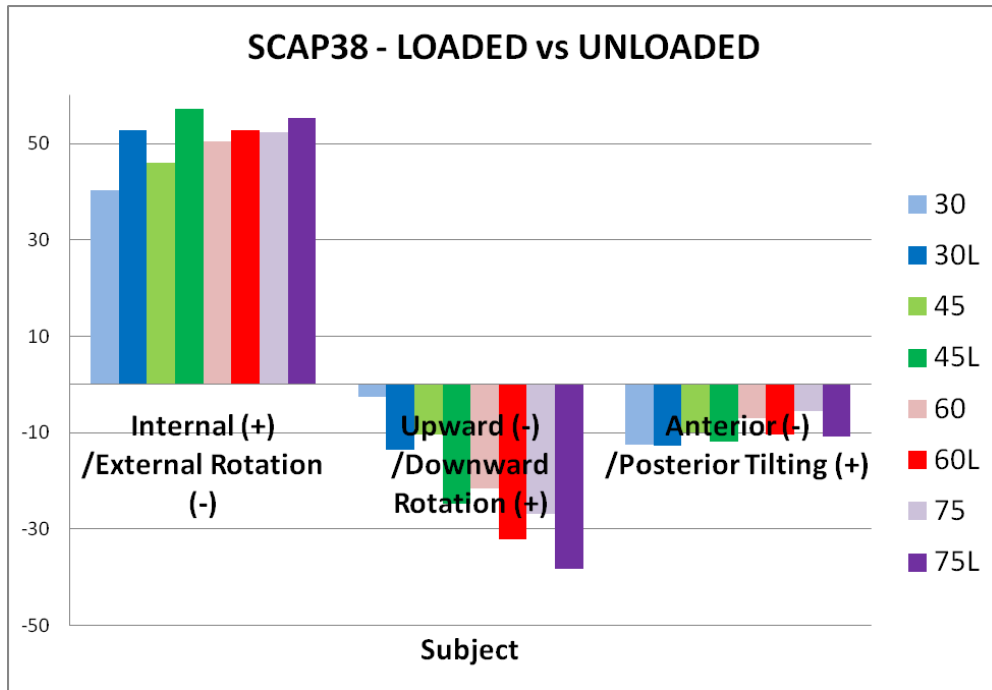
Figure 55: SCAP38 Scapular Rotations in Loaded and Unloaded Conditions

There was no main effect of group for any of the scapular rotations. The average rotations across subjects in each group can be seen in Table 19. While there was no significant effect of group, likely because of the large standard deviations and relatively small sample size, AB had greater average internal rotation and posterior tilting than MWU at all elevations.

117

Table 19: Scapular Rotations of MWU vs AB for All Elevation Angles (Unloaded)

Arm Elevation Angle	Scapular Rotation					
	Internal (+) / External (-) Rotation (mean ± SD)		Upward (-) / Downward (+) Rotation (mean±SD)		Anterior (-) / Posterior Tilting (+) (mean±SD)	
	MWU	AB	MWU	AB	MWU	AB
30°	29.2±9.0	35.1±7.2	-7.9±10.9	0.1±11.9	-10.0±9.9	-9.1±2.7
45°	29.2±7.8	35.0±7.1	-10.1±7.6	-0.8±14.4	-7.6±6.7	-5.8±4.1
60°	30.5±6.5	36.4±8.9	-13.4±6.3	-20.8±8.9	-6.4±9.6	-4.4±4.3
75°	32.4±7.2	39.9±6.7	-19.1±5.0	-24.0±5.1	-5.2±12.2	-1.2±4.4

The variation across subjects in both groups can be seen below in Figure 56. Participants in both groups are internally rotated during the entire 30°-75° range of motion and upwardly rotated for 60° and 75°. While all subjects were in anterior tilt at 30°, anterior/posterior tilting varied much more across subjects throughout the rest of range with some moving towards more posterior tilt and others moving towards more anterior tilt.

Figure 56: Scapular Rotations of MWU vs AB for All Elevation Angles (Unloaded)

The between group differences during the loaded condition can be seen below in Table 20.

Table 20: Scapular Rotations of MWU vs AB for All Elevation Angles (Loaded)

Arm Elevation Angle	Scapular Rotation					
	Internal (+) / External (-) Rotation (mean ± SD)		Upward (-) / Downward (+) Rotation (mean±SD)		Anterior (-) / Posterior Tilting (+) (mean±SD)	
	MWU	AB	MWU	AB	MWU	AB
30°	30.9±6.8	35.9±9.2	-6.6±12.2	-2.1±8.6	-8.5±6.4	-11.2±3.2
45°	28.8±8.4	34.0±10.8	-11.7±12.8	-11.6±10.8	-7.1±5.5	-8.5±4.4
60°	32.6±8.7	32.6±10.0	-22.6±10.5	-10.3±13.1	-5.6±8.5	-6.7±4.0
75°	33.4±9.2	36.2±11.1	-25.0±8.9	-23.2±10.3	-4.0±9.2	-4.6±4.4

Plots for the loaded condition can be found below in Figure 57. For anterior/posterior tilting, plots are very similar in direction to the unloaded condition but differ in magnitude.
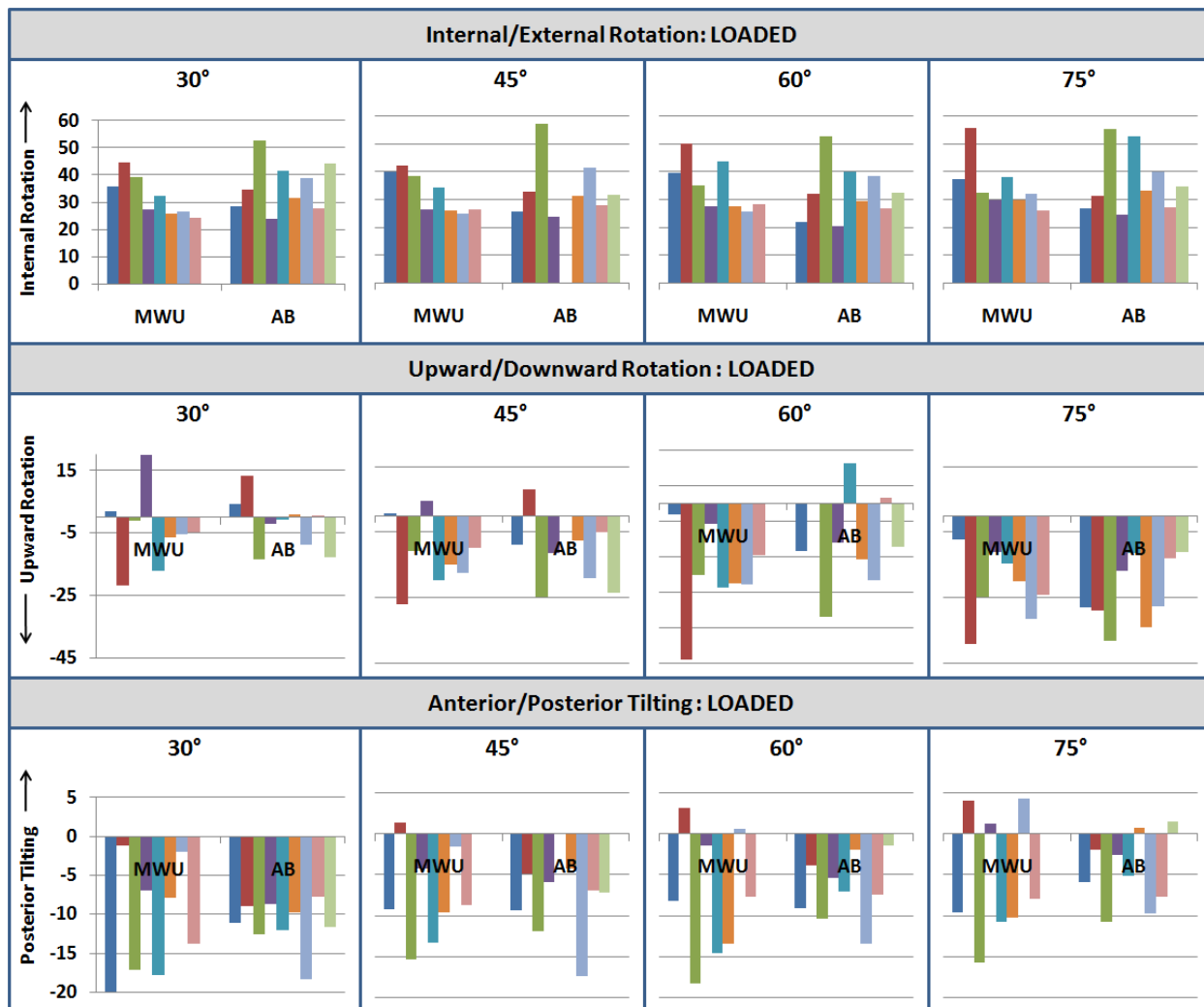
Figure 57: Scapular Rotations of MWU vs AB for All Elevation Angles (Loaded)

121

These differences may be explained in part by the significant interaction that was found between loading and group for anterior/posterior tilting $F(1,15)=7.229$, $p=0.017$. The interaction effect indicates the groups respond differently to loading. As can be seen below in Figure 58, posterior tilting decreased in the loaded condition for wheelchair users and increased for able-bodied controls.
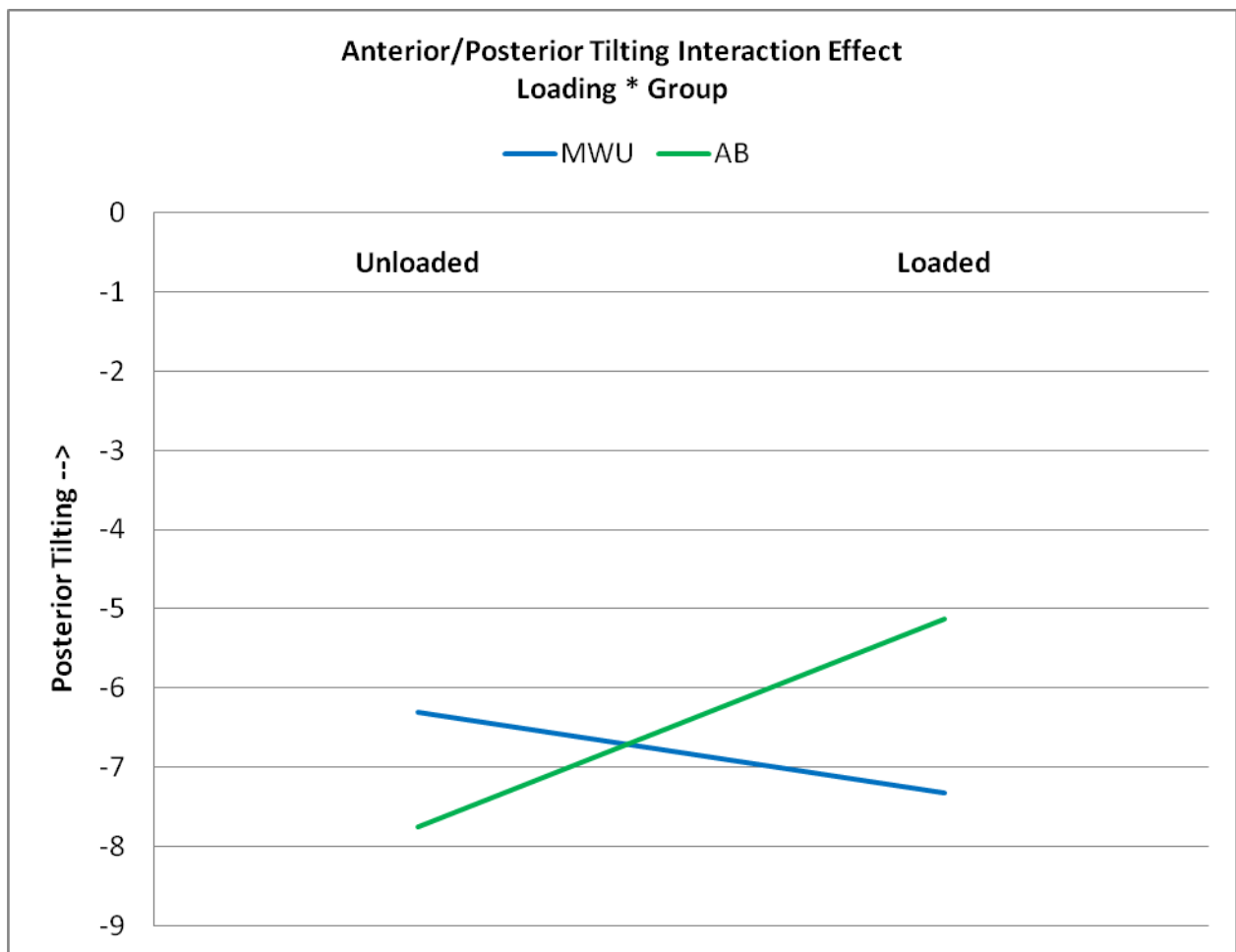
Figure 58: Anterior/Posterior Tilting Interaction Effect

Additional interaction effects were also found for internal/external rotation and upward/downward rotation. For internal/external rotation a three way interaction was found between elevation angle, loading and group $F(3,45) = 2.973$, p=0.042. Planned comparisons indicate the interaction occurred between 45° and 60° (p<0.001) and 60° and 75° (p=0.011). Plotted below in Figure 59 is the average internal rotation across subjects for each group at the three levels of arm elevation of interest. An interaction is indicated by a difference in slope or crossing of lines between loaded and unloaded conditions. It can be seen that the interaction is for the control group as the loaded and unloaded lines converge at 60° and then diverge towards 75°.
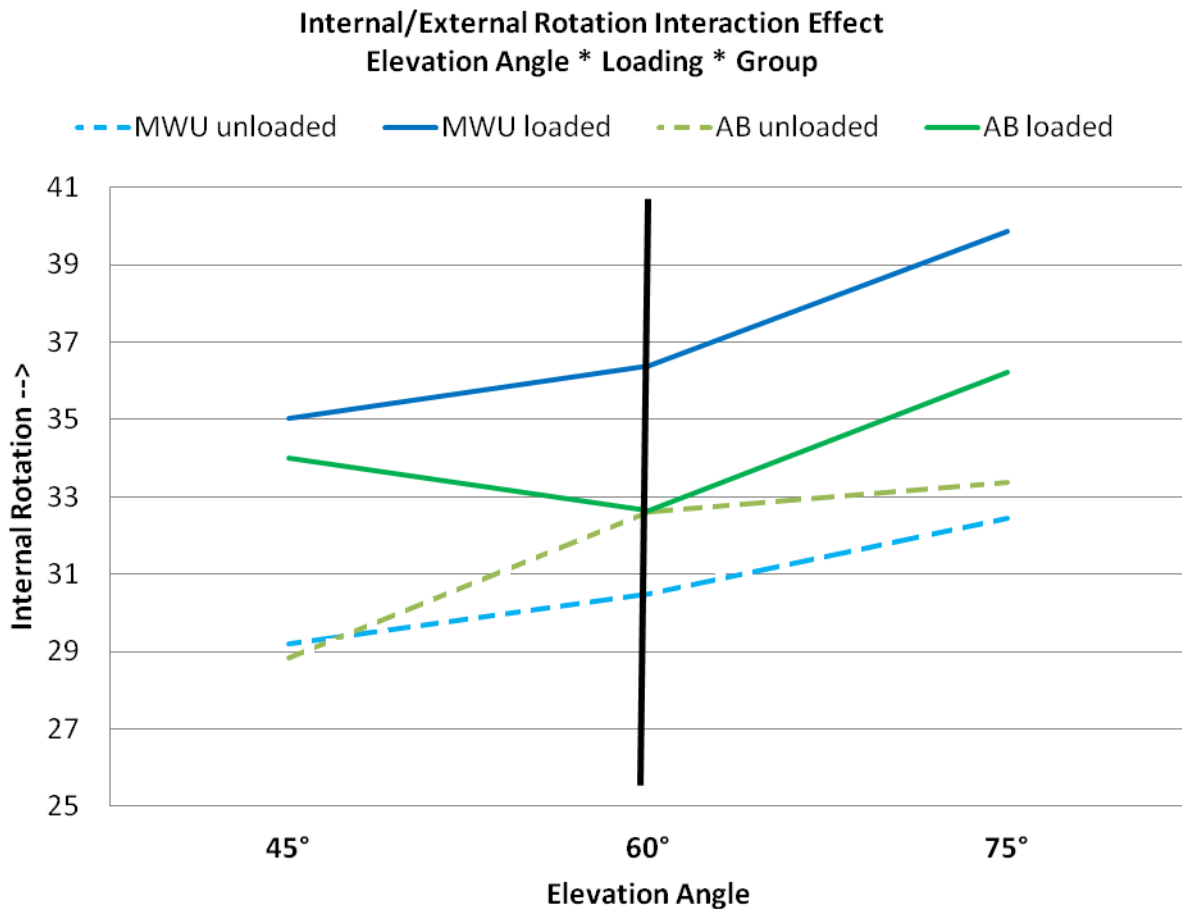
Figure 59: Internal/External Rotation Interaction Effect

For upward/downward rotation a three-way interaction was also found between elevation angle, loading and group $F(3,45) = 5.493$, p=0.010. This interaction was only significant between 45° and 60°. As seen below in Figure 60, there is no difference in upward rotation for controls at 45° while at 60° upward rotation increases for the unloaded condition and decreases for the loaded condition. For wheelchair users there is an increase in upward rotation for both conditions but a greater increase for the loaded condition.
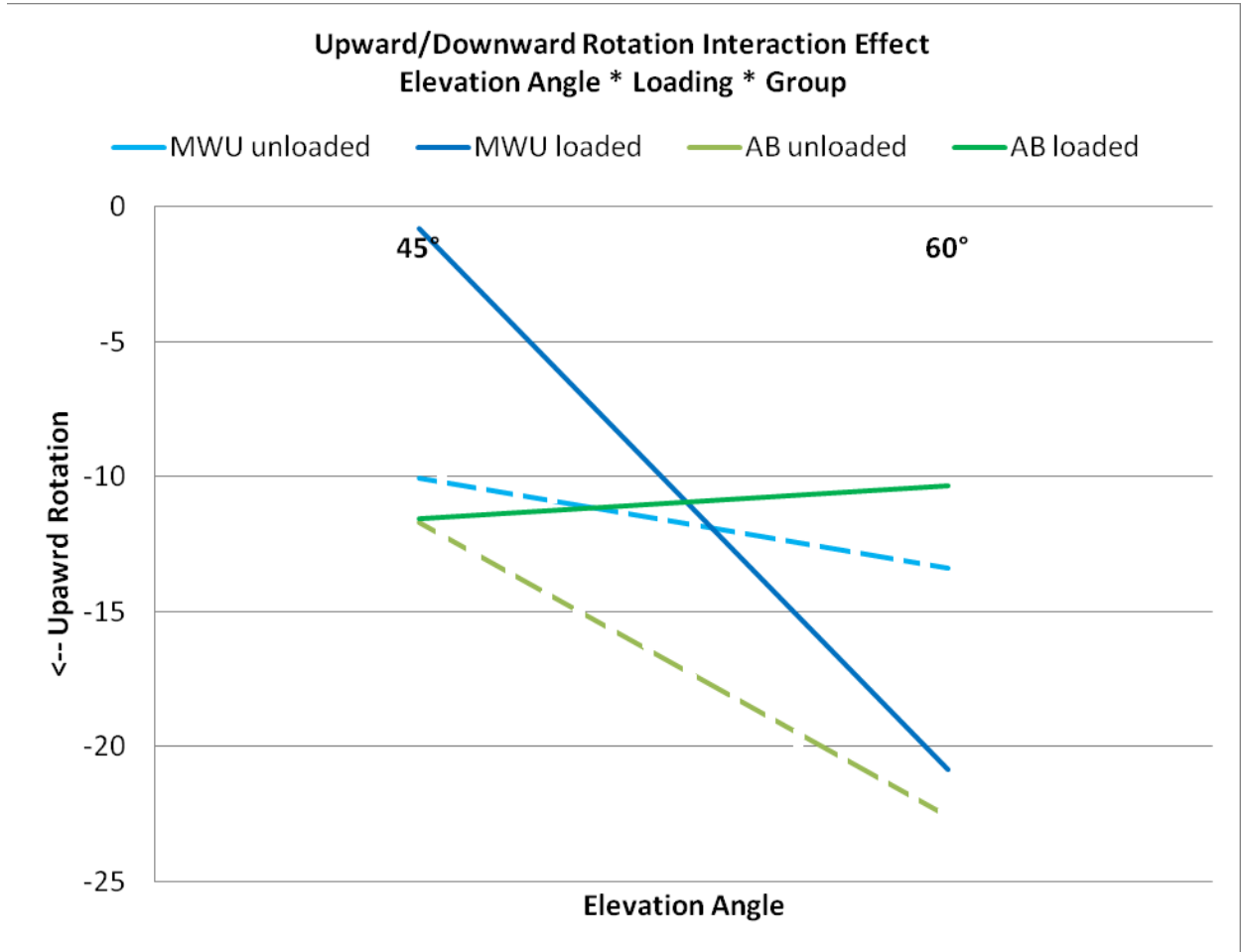
Figure 60: Upward/Downward Rotation Interaction Effect

4.3   DISCUSSION

Despite not being able to draw conclusions about the repeatability of our dynamic measures, we were able to create a reconstruction of the scapular border that showed a pattern of increased internal rotation, upward rotation and posterior tilting as arm elevation increased

during dynamic trials. For internal rotation there was not a significant increase from 30° to 45° and for posterior tilting there was not a significant difference from 45° to 60°. McClure et al also completed a study of scapular position using skin based electromagnetic tracking during dynamic arm movement in the scapular plane however, only a summary plot with means and standard deviations at 5° intervals is presented.[88] As the error bars overlap, it is hard to determine if there would have been consistent increases at the intermediate levels measured in this study. Bourne et al also measured dynamic scapular movement using bone pins but only in the frontal and sagittal planes.[87] Ludewig used skin based electromagnetic tracking during dynamic movement and examined three phases: 31-60°, 61-90° and 91-120°.[3] Summary plots for this study are only provided for averaged loaded trials however the pattern of movement with increases in upward rotation, posterior tipping, and internal rotation is in agreement with our study. As dynamic movement analysis in three-dimensional space of a complex structure using freehand ultrasound has never been completed before, the agreement of our results with the pattern of movement in previous studies shows proof of concept that this technology could be used for this application.

We found differences in scapular position between static and dynamic trials. Fayad et al also completed a study using skin based electromagnetic sensors to compare scapular position in static positions and with slow movement.[108] They found significant differences between static and dynamic trials so it is not surprising that we also found differences between the two types of trials. Our original intention with comparing static and dynamic trials was to provide validation of the dynamic methods however in retrospect it was not appropriate to expect the trials would be the same. Similar to subjects that did not reach the angle of humeral elevation from the static trial in the dynamic trial, we also found subjects who raised their arm higher in dynamic trials. It is possible that pulling data which does not correspond to the end range of the motion completed

126

produces different results. We also had subjects who varied more than 2-3° in max elevation between abduction-adduction repetitions and as a result, the scapular border was less densely populated with points. As was discussed in Chapter 3, fewer points may decrease reliability. Overall, we cannot draw any conclusions about the repeatability of measuring dynamic scapular kinematics by comparing static and dynamic trials. To achieve this outcome we would have to do a reliability study which consisted of subjects completing more than one dynamic trial. Time restrictions on testing for the current study did not allow for this as static reliability testing took a considerable amount of time with subjects provided with rest periods between each trial. Additionally, this study was part of a larger study that tested movement in three planes of elevation; if fewer planes were tested this would allow for more repetitions in each plane. Finally fatiguing the subjects was a significant concern.

Studies on the effects of loading on scapular movement are limited, and the main focus is generally to compare individuals with impingement to those without. Some studies only look at scapulohumeral rhythm[80, 109-110] while others rely on two dimensional radiography[111]. The aforementioned study by Ludewig et al used a 2.3kg and 4.6kg hand weights.[3] The reported average scapular rotation across loading conditions was 23° upward rotation (averaged across loading conditions) and 11° anterior tipping (averaged across loading conditions). No differences were found for internal rotation between loaded and unloaded positions. Myers et al did a study where subjects were loaded to 25% their maximum voluntary contraction at 30°, 60°, 90° and 120° arm elevation.[112] For 30° they found 2.34°±8.00° upward rotation, 29.85°±9.71° internal rotation and 7.61°± 4.51° anterior tipping. Comparatively, for the AB in this study we found 0.1°±11.9° upward rotation, 35.1°±7.2° internal rotation, and 9.1°±2.7° anterior tilting at 30° arm elevation. For 60° elevation, Myers et al found 11.67°±7.59° upward rotation, 33.65°±10.10°

internal rotation an 6.21°±5.36° anterior tipping. For this amount of humeral elevation we found 13.6°±5.1° upward rotation, 36.4°±8.9° internal rotation, and 4.4°±4.3° anterior tilting. While we did not find differences between loaded and unloaded conditions, the scapular rotations we found for loaded conditions at 30° and 60° of arm elevation were within the same range and show good agreement as the study by Myers et al. The study by Ludewig et al reported higher upward rotation and anterior tipping however the weights used in this study were considerably higher than ours (5-10lbs instead of 3-5 lbs) and did not vary based on the subject's weight.

Our study did not find any differences between groups. When comparing individuals with impingement syndrome to those without, Ludewig et al found decreased upward rotation (4.1°) and no difference in posterior titling at 60° elevation.[3] Myers et al found decreased upward rotation (~7°), decreased internal rotation (7°) and no difference in posterior tipping between throwing athletes and controls at 30° and 60° elevation. Ludewig et al found an interaction between load and group however theirs was for internal/external rotation, not anterior posterior tipping. As discussed in Chapter 3, it may be the case that we did not find between group differences because there was not considerable pathology among our wheelchair users as compared to our controls. It is possible that a sampling of individuals with increased shoulder pathology, as evidenced by scores on the clinical exams, would show differences. Further, our sample size was limited and in the midst of the high between subjects variability we presented in Chapter 3, a larger sample may be required to find between group differences.

While we did not find significant main effects of group or loading, we did find interactions between elevation angle, loading, and group. For anterior/posterior tilting there was no interaction with arm elevation angle, only loading and group. Wheelchair users decreased posterior tilting with loading while controls increased posterior tilting. Loading appeared to

cause a more consistent increase in internal rotation among manual wheelchair users while the response of controls varied with arm elevation angle. Loading affected the upward rotation of both groups differently depending on arm elevation angle. For wheelchair users there was less upward rotation at 45º and greater upward rotation at 60º with loading. In contrast, there was little difference between loading and unloading for controls at 45º while elevation to 60º resulted in decreased upward rotation with loading and increased upward rotation without loading. These interactions effects indicate a complex relationship between factors which should be explored further in the future with larger sample sizes.

4.3.1   Limitations

As discussed in the methods section, there are limitations to this study based on our sampling frequency, dynamic sampling of the frame grabber, and ability to capture quality ultrasound images. With a 5s period to raise the arm and an average of 90° of elevation in this period, the arm was moving at ~18°/s. Our ultrasound image collection capped at 10Hz. Further, our ultrasound images were collected at a dynamic frequency. These factors working in tandem required us to spine fit and time-normalize our data to determine one representative point for each angle of humeral elevation in each trial. This decreased the amount of data we had for each trial to at most twenty representative points. A system which is able to pull video at the native ultrasound data collection rate (60Hz) and has no inconsistencies in collection rate would not only increase the amount of data but also remove the need to downsample to just one representative point for each abduction-adduction movement. This increased amount of data and lack of need to downsample could also reduce the length of the dynamic trials. Dynamic trials were time consuming, requiring 7.5 minutes for each trial. Improving the system as

129

aforementioned could allow us to determine the actual number of abduction-adduction repetitions needed and reduce trial time. In addition to the small sample size employed as part of this study, we were also potentially limited in finding differences between groups by the max arm elevation angle subjects achieved. Other studies have found differences between 90° and 120° or between 120° and max elevation.[3, 112] As most of our subjects only reached 90°, further studies should incorporate direct feedback on arm elevation angle to ensure postures are achieved that are more likely to elucidate differences. A final limitation in this study was the extensive time required to analyze dynamic trials. With the manual techniques we employed raters had to individually analyze ~4,500 sequential images for each trial; this is a very lengthy and time consuming process. Future studies may want to investigation full three-dimensional reconstructions powered by algorithms to remove the need for time consuming manual identification of the scapula in images. Automatic detection of the scapular would remove the need to manually process individual ultrasound images. Additionally, a full three-dimensional reconstruction of the surface of the scapula could provide an even more thorough understanding of scapular movement than the spine and medial border can provide.

4.4   CONCLUSIONS

This study demonstrates the feasibility of applying freehand three-dimensional ultrasound to evaluate dynamic scapular movement, essentially create a tool for four-dimensional measurement. To our knowledge, freehand ultrasound has not previously been applied to analyzing the movement of a complex structure in three-dimensional space during movement; as such this study represents a novel application of the technology. Proof of concept is supported by

the incremental increases in scapular rotations with humeral elevation. Future studies should implement a system without the sampling frequency restrictions we faced in this study and test for reliability of determining scapular rotation in dynamic trails. A part of these studies should also include determining the actual number of abduction-adduction repetitions required to achieve a dense scapular border. Additionally, larger samples sizes should be employed to determine between group differences in the context of the high between subject variability we have found as described in Chapters 1-3.

5.0   CONCLUSIONS

Altered scapular movement has been linked by a multitude of studies to shoulder pathologies including impingement, bursitis, rotator cuff tears, and adhesive capsulitis. With the inconsistent success of surgical interventions, increased emphasis has been placed on prevention and interventions which correct altered scapular kinematics. In order to identify individuals at risk and evaluate the efficacy of these programs, it is essential to have a reliable method for measuring scapular kinematics. Existing methods with high accuracy are invasive (bone pins), expose individuals to radiation (radiography, fluoroscopy), or may not allow for testing in functional positions (MRI). Attempts have been made in more recent years to use skin based methods (electromagnetic tracking) to evaluate scapular movement. Unfortunately, in comparison studies, skin based methods all show error as a result of skin motion artifacts. Additionally, adipose tissue and muscle between the skin and bone have also been found to affect measurements. The goal of this study was to apply the non-invasive technique of freehand three-dimensional ultrasound to evaluate scapular movement. Ultrasound is an excellent modality for identifying bone surfaces as unlike soft tissue, bone appears very clear and echogenic in images. The addition of motion capture allows for scanning of irregular surfaces, such as the scapula. Freehand three-dimensional ultrasound offers the benefits of relatively low cost, non-invasiveness, and no exposure to radiation.

Calibration of our system resulted in a low RMSE when comparing known to measured dimensions of a scanned phantom. The results of the calibration in conjunction with the high inter- and intra-rater reliabilities we found for manual point identification of the scapular border in ultrasound images, led us to conclude the system was ready to apply to determining scapular position of static postures. For these trials we scanned along the spine and medial border of the scapula while the participant held their arm at rest or elevated in the sagittal, frontal or scapular planes. We evaluated 22 able-bodied individuals without reported shoulder pain 3 times in each testing position. Visual examination of the reconstructed scapular borders showed agreement between trials and differences in scapular position between testing positions, which is what we would have expected. Consistency across trials was supported by the high reliability for all rotations in all testing positions (ICC: 0.62-0.946). Our SEM was less than 2° for all pairings of testing position and scapular rotation. Further, MDC was less than 1° internal/external rotation and anterior/posterior tilting and less than or equal to 3° for upward/downward rotation. The magnitude and direction of some of our rotations did not agree with previous studies. As some of these studies used skin based systems it may be possible that our method is in fact more accurate as we are able to directly visualize the bone. Our SEM and MDC are comparable to other studies which have used bone pins or electromagnetic tracking, leading us to conclude this is an appropriate application of this technology. Comparing elevated testing positions we saw increases in upward rotation and posterior tilting as we would have expected.

We compared our freehand three-dimensional ultrasound measures of rotation to landmark digitization in each of the static postures. We did not find excellent agreement between the two measures. We attribute these differences to poor palpation of bony landmarks. Difficulty was noted during trials with palpation, particularly for the root of the spine and inferior angle.

We believe varying amounts of muscle and tissue as well changes in muscle tension with elevation exacerbated the lack of the raters experience with palpating these bony landmarks. While we found high reliability between trials for our technique, consideration should be given to future studies that validate our methods against a known gold standard.

One caveat of our repeatability testing is we tested 16 wheelchair users prior to testing any able-bodied controls. We found decreased reliability among manual wheelchair users compared to able-bodied controls. As discussed in Chapter 3 this difference could be because the error is inherently higher among this group based on differences in body composition between groups. One reason this is not likely the case is we saw many different body types among both wheelchair users and age matched controls. As diagnoses ranged from SCI (both paraplegia and tetraplegia) to multiple sclerosis and amputation, the group included individuals with a range of BMIs and muscular builds. Using number of points in the reconstructed scapular border as a performance measure, we found a learning effect with increased performance over time. While the reliability across trials for wheelchair users was reasonable, it appears more precise results could have been achieved if these subjects had been tested after a better mastery of ultrasound scanning had been achieved.

Between group differences in scapular kinematics in static testing positions were not found. We believe this is because there was a lack of differences in pathology between groups. Using the WUSPI as an established measure for evaluating shoulder pain, participants in our study showed comparatively lower scores than previous studies among wheelchair users. A large portion of our wheelchair participants took part in athletic events at the NVWG. Pain or pathology may prohibit participation in athletic events and as such the event may have had a screening effect. Further, the protocol required overhead reaching which may be painful for

individuals with shoulder impingement or other pathology. Based on this inclusion criterion, it is possible we attracted subjects with less pathology. Further, there were no between group differences for any of the clinical measures. As dichotomized PESS and USPRS scores resulted in differences in scapular kinematics, we believe that differences in these measures would have resulted in between group differences.

Previous studies of scapular position in static testing have not used resting postures to predict scapular kinematics with arm elevation. Controlling for trunk posture, our study found increased internal rotation at rest was associated with increased internal rotation and decreased posterior tilting with the arm elevated. Increased downward rotation at rest was related to increased downward rotation in the elevated position. Lastly, increased posterior tilting at rest was related to increased posterior tilting and decreased internal rotation with the arm elevated. This would lead us to conclude that someone with increased internal rotation, downward rotation and anterior at rest is more likely to have scapular positioning associated with pathology in the elevated testing position. The relationship between scapular positioning with the rest and elevated could help decrease the number of testing positions required in the future.

Unlike static trials, we only completed one trial for each of tests of dynamic movement. As each trial took 7.5 minutes and required a 2 minute rest period between trials, we were concerned that multiple trials would extend the protocol length and cause fatigue. Additional limitations include the dynamic sampling frequency of the frame grabber used to collect ultrasound data. Based on this variability as well as our limited sampling frequency to begin with (~10Hz), we simplified our data for each adduction-abduction arm movement and used spline fitting and time-normalization to determine one representative point on the scapular border for each angle of humeral elevation. These methods limit our scapular border data to at most 20

135

representative points. Despite this limitation, we were able to create a reconstructed scapular border at intermediate angles of humeral elevation (30°, 45°, 60° and 75°) to determine scapular position. We believe proof of concept is illustrated through the pattern of increased internal rotation, upward rotation and posterior tilting as arm elevation increased during dynamic trials.

Future studies should seek to avoid the technological limitations of this study as related to ultrasound data collection. A system with a higher and constant sampling frequency (such as newer ultrasound machines with built in DVR that can record video at 60Hz) would increase the amount of data and eliminate the need for time normalization. As such, similar to the reconstructed border pulled to match the max elevation of the static trials, an arm angle of interest could be selected and points pulled directly. This increased amount of data could also allow us to determine the actual number of adduction-abduction repetitions that were required, potentially decreasing the time required for each trial. Once these changes are made, repeatability testing of dynamic measures should be performed to determine reliability.

No differences were found with loading or between groups for dynamic trials but this is likely due to the small sample size (n=18). Additionally, only about 90° of humeral elevation was achieved. Future studies should include a larger sample size and include a larger range of motion as other studies have found differences with loading or between groups are intensified at higher angles of arm elevation.

Overall, these studies demonstrate that freehand three-dimensional ultrasound is a reliable method for measuring scapular kinematics in static testing positions. While this study did not validate our methods with an existing gold standard, the high intra-rater reliability and low standard error of measurement indicate these methods would be compatible with longitudinal studies. The effectiveness of treatment of altered scapular movement has been questioned,

particularly among wheelchair users.[18] Studies which evaluate the physical therapy interventions that collect baseline and post-intervention data could use the static methods presented in this study to evaluate changes in scapular movement.

Further these studies demonstrate proof of concept that dynamic movement can also be evaluated using these methods. Future studies should establish reliability of measures for raters for all subject groups before making comparisons between groups. Additionally, while our methods result in scapular rotations that agree with previous literature, proper validation with an acceptable gold standard should be considered. Reliability of dynamic testing between multiple trials should also be completed.

Lastly, for both static and dynamic methods, an automated method of detecting the scapular border should be investigated. Manually processing ultrasound images is a time consuming process and not likely to be compatible with a clinical environment. Automated methods could reduce processing time and provide more immediate feedback to clinicians. Additionally, methods could also be expanded to create a full three-dimensional reconstruction of the scapula, rather than just the spine and medial border. Such methods may provide an even more thorough understanding of scapular movement. Automating these processes could make freehand three-dimensional ultrasound a viable clinical tool. While a 10-camera motion capture system may not be practical in terms of cost or space for a clinic, other motion capture systems could be implemented. Electromagnetic sensors like the 3Space Fastrak System[4] could be attached simply to the trunk, upper arm and ultrasound probe. These sensors reduce most of the space requirements of the Vicon system and are considerably lower in cost. The largest expense of the system would then be the ultrasound machine and with the increased use of ultrasound for

---

[4] Polhemus Navigation, Colchester, VT

diagnostic applications, many clinics are now equipped with ultrasound machines. As such, this technology could be a low cost system to integrate into the clinical environment.

These methods also have the potential to evaluate other joints. Static positions of almost any bone that can be imaged with ultrasound could be evaluated. For dynamic positions, joints which could be gated by repetitive movement could be evaluated. In other words, we gated scapular movement by humeral elevation, extracting points corresponding to arm angle. An example of another potential application is the patellofemoral joint. Movement of the joint is difficult to quantify and existing quantitative methods share many of the shortcomings of technology to evaluate scapular movement. With this application as the patella is a sesamoid bone, its surface does not have features which are as distinct as the scapula. As such, a complete three-dimensional reconstruction may be more useful to characterize the surface and track movement.

APPENDIX A

ULTRASOUND VIDEO PROCESSING

A.1   READ ULTRSOUND VIDEO, WRITE INTO FRAMES

```matlab
function [] = segment_vid( subjects )
% Segment video into frames, input for this function are
        % subjects=[_,_,_], subject_type.xls
            subject_type=xlsread('subject_type');

            subjects = [13]
            for i=1:length(subjects)
                subj_type=subject_type(subjects(i));
                disp(subj_type)
                    for rr = 1:subj_type_tr
                        [folder] = det_trial(rr,subj_type);
                        disp(folder)
                        subjnum = num2str(subjects(i));
                        subjfolder = ['C:\Documents and
                        Settings\law93\Desktop\NVWG\SCAP',subjnum];
                        cd(subjfolder)
                        pathtovid=[folder,'.avi'];
                            if ~exist('index')
                              [count] =
                              write_frames(subjfolder,folder,pathtovid); % If
                              index not given, write images to disk
                            else
                                disp('here')
                                count = index;
                            end
                    end
            end
        end

function [] = write_syncframes( subjects )
% create sync_frame files that start from us sync point
        % inputs for this function are subjects=[_,_,_], subject_type.xls,
```

```matlab
% syncframes.xls
    subject_type=xlsread('subject_type');
    for i=1:length(subjects)
            [mainfolder,subjfolder,subj_type,subj_type_tr,sync_frame,
            subjnum1] = get_subj_info( subjects(i) );
               for rr=1:subj_type_tr
                    [namefile]=det_trial(rr,subj_type);
                    disp(namefile)
                    cd([subjfolder,'\',namefile]);
                    framesync=sync_frame(rr,1);
                    framestop=sync_frame(rr,2);
                    mkdir('sync_frames');
                    [num] =
                    sync_frames(framesync,framestop,subjfolder,namefile);
                end
        end
    end
```

A.2   SELECT SCAPULAR BORDER IN ULTRASOUND IMAGES

```matlab
function [] = pick_points ( subject,freq )
% Pick points in US images
        % freq is the sampling frequency of vicon/10Hz epiphan sampling
          (freq)
            subject=9;
            cd('C:\Documents and Settings\law93\Desktop\NVWG');
            [mainfolder,subjfolder,subj_type,subj_type_tr,sync_frame,
            subjnum1] = get_subj_info( subject )
            cd(subjfolder);
            spine_point=[];
            for rr=1:subj_type_tr
                    figure; imshow('syncframe1.jpeg');  %show an image
                    from trial
                    imgdepth1 = input('What is the image depth?', 's');
                imgdepth=str2num(imgdepth1); %report depth of image
                [namefile]=det_trial(rr,subj_type);
                framesync=sync_frame(rr,1);
                framestop=sync_frame(rr,2);
                j=[framesync:framestop];
                cd([subjfolder,'\',namefile,'\sync_frames']);
                disp([subjfolder,namefile])
                [spine_point]= pick_point(j,imgdepth,subjfolder,namefile);
                %writes x,y coordinates to file
end


function [spine_point]= pick_point(j,imgdepth,subjfolder,namefile);
%This function runs through each ultrasound image, allow the user to select
the x-y coordinate of the scapular border in each image
    close all
```

```matlab
    %Width and origin of us image depend on pixels, set them according to
    %entered depth
    if imgdepth==3
        width=51.158;       %mm
        origin=[163.5,207.5];  %pixels
        conversion=169.67;   %pixel to cm
    elseif imgdepth==4
        width=50.859;        %mm
        origin=[227.5,172.5];  %pixels
        conversion=145.5;   %pixel to cm
    elseif imgdepth==5
        width=50.94839;     %mm
        origin=[301.5,174.5];
        conversion=116.0001;   %pixel to cm
    elseif imgdepth==6
        width=51.10342;     %mm
        origin=[350.5,174.5];
        conversion=96.66677;   %pixel to cm
    elseif imgdepth==7
        width=50.93109;     %mm
        origin=[386.5,174.5];
        conversion=82.85723;   %pixel to cm
    else
        disp 'error'
    end

    frame=[];
    figure; imshow(['frame',num2str(12), '.jpeg']);
    disp('Crop the image')
    cropping=ginput(1);
    X1=origin(1);
    Y1=origin(2);
    X2=cropping(1);
    Y2=cropping(2);
    close all

    spine_point=[];
    for i=1:length(j)%1:num-1
        jk=i;
        frame=j(i);
        disp(frame);
        img=imread(['frame',num2str(frame), '.jpeg']);
        crop_img=img(Y1:Y2,X1:X2);
        figure; imshow(crop_img)
        point_select=ginput(1);
        point_selecta=point_select/conversion;
        spine_point=[spine_point;point_selecta];
        close all
    %
    end
    xlswrite('spine_points',spine_point);

end

function [spine_points_wrow] = nopoint2zero(main_dir,subj_type)
```

141

```matlab
%This function removes the top-left dummy click when no point is present and
replaced it with (0,0)
    if subj_type==1
        for k=1:8
            if k==1
                currdir=[main_dir,'\rest1'];
                namefile='spine_points_wrow_rest1';
            elseif k==2
                currdir=[main_dir,'\rest2'];
                namefile='spine_points_wrow_rest2';
            elseif k==3
                currdir=[main_dir,'\sag1'];
                namefile='spine_points_wrow_sag1';
            elseif k==4
                currdir=[main_dir,'\sag2'];
                namefile='spine_points_wrow_sag2';
            elseif k==5
                currdir=[main_dir,'\front1'];
                namefile='spine_points_wrow_front1';
            elseif k==6
                currdir=[main_dir,'\front2'];
                namefile='spine_points_wrow_front2';
            elseif k==7
                currdir=[main_dir,'\scap1'];
                namefile='spine_points_wrow_scap1';
            else
                currdir=[main_dir,'\scap2'];
                namefile='spine_points_wrow_scap2';
            end
             cd(currdir);
                spine_point=xlsread('spine_points.xls');
                spine_points_wrow=[];
                for i=1:length(spine_point);
                    if spine_point(i,1)>0.5
                        spine_point_wrow=[i,spine_point(i,:)];
                    else
                        spine_point_wrow=[i,0,0];
                    end
                    spine_points_wrow=[spine_points_wrow;spine_point_wrow];
                end
                cd(main_dir);
                xlswrite(namefile,spine_points_wrow);
    else
        for k=1:12
            if k==1
                currdir=[main_dir,'\rest1'];
                namefile='spine_points_wrow_rest1';
            elseif k==2
                currdir=[main_dir,'\rest2'];
                namefile='spine_points_wrow_rest2';
            elseif k==3
                currdir=[main_dir,'\rest3'];
                namefile='spine_points_wrow_rest3';
            elseif k==4
                currdir=[main_dir,'\sag1'];
                namefile='spine_points_wrow_sag1';
            elseif k==5
```

```matlab
                currdir=[main_dir,'\sag2'];
                namefile='spine_points_wrow_sag2';
            elseif k==6
                currdir=[main_dir,'\sag3'];
                namefile='spine_points_wrow_sag3';
            elseif k==7
                currdir=[main_dir,'\front1'];
                namefile='spine_points_wrow_front1';
            elseif k==8
                currdir=[main_dir,'\front2'];
                namefile='spine_points_wrow_front2';
             elseif k==9
                currdir=[main_dir,'\front3'];
                namefile='spine_points_wrow_front3';
            elseif k==10
                currdir=[main_dir,'\scap1'];
                namefile='spine_points_wrow_scap1';
            elseif k==11
                currdir=[main_dir,'\scap2'];
                namefile='spine_points_wrow_scap2';
            else
                currdir=[main_dir,'\scap3'];
                namefile='spine_points_wrow_scap3';
            end


        cd(currdir);
        spine_point=xlsread('spine_points.xls'); spine_points_wrow=[];
        for i=1:length(spine_point);
            if spine_point(i,1)>0.5
                spine_point_wrow=[i,spine_point(i,:)];
            else
                spine_point_wrow=[i,0,0];
            end
            spine_points_wrow=[spine_points_wrow;spine_point_wrow];
        end
        cd(main_dir);
        xlswrite(namefile,spine_points_wrow);
    end
end


end
```

A.3   OPTICAL CHARACTER RECOGNITION OF ULTRASOUND TIME STAMP

```matlab
function [times,tally,jj] = optrec(sync_info,foldername);

    %store numbers
```

```matlab
digmid_twodig=[865.5000;  881.5000;  907.5000;  921.5000;  947.5000;
962.5000];
digmid_onedig=[865.5000;  890.5000;  905.5000;  931.5000;  946.5000];
digmid_twodig = ceil( digmid_twodig );
digmid_onedig = ceil( digmid_onedig );

zero=im2double(im2bw(imread('zero.jpg')));
one=im2double(im2bw(imread('one.jpeg')));
two=im2double(im2bw(imread('two.jpeg')));
three=im2double(im2bw(imread('three.jpeg')));
four=im2double(im2bw(imread('four.jpeg')));
five=im2double(im2bw(imread('five.jpeg')));
six=im2double(im2bw(imread('six.jpeg')));
seven=im2double(im2bw(imread('seven.jpeg')));
eight=im2double(im2bw(imread('eight.jpg')));
nine=im2double(im2bw(imread('nine.jpeg')));

base_numbers = zeros( 18, 13, 10 );
base_numbers( :, :, 1 ) = zero;
base_numbers( :, :, 2 ) = one;
base_numbers( :, :, 3 ) = two;
base_numbers( :, :, 4 ) = three;
base_numbers( :, :, 5 ) = four;
base_numbers( :, :, 6 ) = five;
base_numbers( :, :, 7 ) = six;
base_numbers( :, :, 8 ) = seven;
base_numbers( :, :, 9 ) = eight;
base_numbers( :, :, 10 ) = nine;

jj=sync_info(1,1)-14:sync_info(1,2);
times=[];
tally=[];
tic;

checkneg=0;
checkstart=0;
start=[];
if jj(1)<1
    checkstart=find(jj==1);
    jj=jj(checkstart:length(jj));
    checkneg=1;
end

cd(foldername)
for i=jj
    disp(i)
    img=imread(['frame',num2str(i), '.jpeg']);
    region=img(130:147,1005:1022);
    if mean(mean(region))>50    %twodig
        [time]=det_num_twodig(base_numbers,digmid_twodig,img);
    else    %one dig
        [time]=det_num_onedig(base_numbers,digmid_onedig,img);
    end
    times=[times;time'];

end
```

144

```matlab
    [tally,times] = frame_counter(times,jj,checkneg,checkstart);


end


function [tally,times] = frame_counter(times,jj,checkneg,checkstart);

    % note, instead with OCR read in frames from sync point (or sync point -
    % 15)
    % times=xlsread('times_single');

    if checkneg==0  %this is the case where the sync frame is before 15
        %pull from sync minus 14
        syncdig=times(15);
        firstenv=[];
        aa=times(1:30);
        firstenv=find(aa==syncdig);

        tally=[];
        current=times(max(firstenv)+1);
        count=0;
        j=2;
        tally(1,2)=max(firstenv)-15+1;
        tally(1)=max(firstenv)+1-min(firstenv); %num of frames in envelope
        tally(1,3)=times(max(firstenv));
        tally(1,4)=jj(15);   %this is the frame there is an issue with
        tally(1,5)=jj(15)-jj(1);    %this is the row of the times file that
        corresponds with the frame
        for i=max(firstenv)+1:length(times);%max(firstenv)+1:length(times);
            if times(i)==current
                count=count+1;
                tally(j,1)=count;
                tally(j,3)=times(i);
                if j==2;
                    tally(j,4)=tally(1,2)+tally(j-1,4);
                else
                    tally(j,4)=tally(j-1,1)+tally(j-1,4);
                end
            else
                current=times(i);
                count=1;
                j=j+1;
            end
        end
        times(1,2)=tally(1,4)-14;

    else %this is the case  where the sync frame is before 15
        syncdig=times(checkstart);
        firstenv=[];
        aa=times(1:30);
        firstenv=find(aa==syncdig);

        tally=[];
```

145

```matlab
        current=times(max(firstenv)+1);
        count=0;
        j=2;
        tally(1,2)=max(firstenv)-checkstart+1;
        tally(1)=max(firstenv)+1-min(firstenv);
        tally(1,3)=times(max(firstenv));
        tally(1,4)=jj(checkstart);
        for i=max(firstenv)+1:length(times);%max(firstenv)+1:length(times);
            if times(i)==current
                count=count+1;
                tally(j,1)=count;
                tally(j,3)=times(i);
                if j==2;
                    tally(j,4)=tally(1,2)+tally(j-1,4);
                else
                    tally(j,4)=tally(j-1,1)+tally(j-1,4);
                end
            else
                current=times(i);
                count=1;
                j=j+1;
            end
        end
        times(1,2)=tally(1,4)-(checkstart-1);

    end

    for i=2:length(tally)
        tally(i,5)=tally(i,4)-jj(1);
    end

    for i=2:length(times)
        times(i,2)=times(i-1,2)+1;
    end


end
```

146

APPENDIX B

IDENTIFY SCAPULAR LANDMARKS WITH DIGITIZER

```matlab
function [AA_G,TS_G,AI_G,Rg2sc,Rg2tr,Rtr2sc,IR_UP_POST,Rsc2tr] =
Digitizer(scaplcs,trial,dynamic_mm);
%process digitizer data

    clear;
    subject = 25;
    cd(['C:\Documents and
Settings\law93\Desktop\NVWG\SCAP',num2str(subject)])
    AA_Gall=[]; AI_Gall=[]; TS_Gall=[];
    for rr=1:4

        digname = ['digitizer_times_scap',num2str(subject)];
        digfile = xlsread(digname);

        if rr==1
            viconfile = ('digrest.csv');
        elseif rr==2
            viconfile = ('digsag.csv');
        elseif rr==3
            viconfile = ('digfront.csv');
        else
            viconfile = ('digscap.csv');
        end
        Dynamic = ReadViconNexus(viconfile,
[('C7');('T8');('STERN');('XYP');('digitizer1');('digitizer2');('digitizer3')
;('digitizer4');('digitizer5');('digitizer6')]);
        [Dynamic] = filter_dig(Dynamic);   %temporarily OMITTED FILTER
        [Dynamic]=convert2cm_dig(Dynamic);

        C7=mean(Dynamic.C7cm(1000:1500,:));
T8=mean(Dynamic.T8cm(1000:1500,:));
STERN=mean(Dynamic.Sternumcm(1000:1500,:));
XYP=mean(Dynamic.xyphoidcm(1000:1500,:));
        [Rg2tr, Vg2tr] = TrunkCoord_ISB(STERN, XYP, C7, T8);

        AA1=digfile(rr,1);
```

147

```
        AA2=digfile(rr,2);
        TS1=digfile(rr,3);
        TS2=digfile(rr,4);
        AI1=digfile(rr,5);
        AI2=digfile(rr,6);

AA=mean([Dynamic.digitizer4cm(AA1:AA2,:),Dynamic.digitizer5cm(AA1:AA2,:),Dyna
mic.digitizer6cm(AA1:AA2,:)]);

TS=mean([Dynamic.digitizer4cm(TS1:TS2,:),Dynamic.digitizer5cm(TS1:TS2,:),Dyna
mic.digitizer6cm(TS1:TS2,:)]);

AI=mean([Dynamic.digitizer4cm(AI1:AI2,:),Dynamic.digitizer5cm(AI1:AI2,:),Dyna
mic.digitizer6cm(AI1:AI2,:)]);

        TipDigitizer=[189.2554/10;19.05/10;-15.9363/10];


        land=AA;
        %determine landmark in 3d space
        [Rdigitizer, Vdigitizer] = DigitizerCoord2(land(1:3), land(4:6),
land(7:9));
        [DigitizerOrigin, DigitizerY, DigitizerX] = CoordG2L(Rdigitizer,
Vdigitizer, land(1:3), land(4:6), land(7:9));
        [ProbeOriginG, ProbeYG, ProbeXG, AA_G] = CoordL2G(Rdigitizer,
Vdigitizer, DigitizerOrigin, DigitizerY, DigitizerX, TipDigitizer');

        land=TS;
        %determine landmark in 3d space
        [Rdigitizer, Vdigitizer] = DigitizerCoord2(land(1:3), land(4:6),
land(7:9));
        [DigitizerOrigin, DigitizerY, DigitizerX] = CoordG2L(Rdigitizer,
Vdigitizer, land(1:3), land(4:6), land(7:9));
        [ProbeOriginG, ProbeYG, ProbeXG, TS_G] = CoordL2G(Rdigitizer,
Vdigitizer, DigitizerOrigin, DigitizerY, DigitizerX, TipDigitizer');

        land=AI;
        %determine landmark in 3d space
        [Rdigitizer, Vdigitizer] = DigitizerCoord2(land(1:3), land(4:6),
land(7:9));
        [DigitizerOrigin, DigitizerY, DigitizerX] = CoordG2L(Rdigitizer,
Vdigitizer, land(1:3), land(4:6), land(7:9));
        [ProbeOriginG, ProbeYG, ProbeXG, AI_G] = CoordL2G(Rdigitizer,
Vdigitizer, DigitizerOrigin, DigitizerY, DigitizerX, TipDigitizer');


            axis_tech1 = (AA_G-TS_G)/norm(AA_G-TS_G); %z (right)
            axis_tech2 = cross(axis_tech1,(AI_G-
TS_G))/norm(cross(axis_tech1,(AI_G-TS_G)));      %x (forward)
            axis_tech3 = cross( axis_tech1, axis_tech2 ); %y (up)
            Rscap = [axis_tech2', axis_tech3', axis_tech1'];
            Vscap = AA_G;
        trunkorient = inv([0 0 1; 1 0 0; 0 1 0]) * Rg2tr;
        trunk(rr,:)=EulerYXY(trunkorient, 'ZXY');
        Rtr_sc(rr,:) = EulerYXY(( Rg2tr )' * ( Rscap ),'YXZ');
```

```matlab
            scaprest = [AA_G;TS_G;AI_G;AA_G];
            trunkrest = [C7;T8;XYP;STERN;C7];

    if rr==1
        pointsG3=xlsread('pointsG3_ENVrest2.xls');
    elseif rr==2
      pointsG3=xlsread('pointsG3_ENVsag2.xls');
    elseif rr==3
      pointsG3=xlsread('pointsG3_ENVfront1.xls');
    else
      pointsG3=xlsread('pointsG3_ENVscap1.xls');
    end

    f=figure; hold on;

plot3(scaprest(:,1),scaprest(:,2),scaprest(:,3),'MarkerSize',20,'Marker','.',
'LineStyle','-','MarkerEdgeColor','g')

plot3(pointsG3(:,1),pointsG3(:,2),pointsG3(:,3),'MarkerSize',20,'Marker','.',
'LineStyle','none','MarkerEdgeColor','m')
    xlabel('global x','FontSize',15); ylabel('global y','FontSize',15);
zlabel('global z','FontSize',15);
    view(0,0);
    figname=[num2str(3*rr-2),'.fig'];
    saveas(f,figname)
    view(0,90);
    figname=[num2str(3*rr-1),'.fig'];
    saveas(f,figname)
    view(90,0);
    figname=[num2str(3*rr),'.fig'];
    saveas(f,figname)

    end




    kk = figure; hold on;
        for i=1:12%subj_type_tr
            a1 = subplot(4,3,i);%subj_type_tr/4,i);
            name=[num2str(i),'.fig'];
%            name=[namefile,'_2stdev.fig'];
            f_c = openfig(name);
                axes_to_be_copied = findobj(f_c,'type','axes');
                title_to_be_copied = findobj(f_c,'type','title');
                chilred_to_be_copied = get(axes_to_be_copied,'children');
                [az,el] = view;
                copyobj(chilred_to_be_copied,a1);
```

```matlab
            set(a1,'Xlim',get(axes_to_be_copied,'XLim')) %[-20 -15])%
            set(a1,'Ylim',get(axes_to_be_copied,'YLim'))
            set(a1,'Zlim',get(axes_to_be_copied,'ZLim'))
            view(a1,[az,el])
            close(f_c);
    end
for i=1:3
    subplot(4,3,i);
    xlabel('global x'); zlabel('global z'); ylabel('global y');
    title('rest','FontSize',15);
end
for i=4:6
    subplot(4,3,i);
    xlabel('global x'); zlabel('global z'); ylabel('global y');
    title('sag','FontSize',15);
end
for i=7:9
    subplot(4,3,i);
    xlabel('global x'); zlabel('global z'); ylabel('global y');
    title('front','FontSize',15);
end
for i=10:12
    subplot(4,3,i);
    xlabel('global x'); zlabel('global z'); ylabel('global y');
    title('scap','FontSize',15);
end
% set(kk,'units','normalized','outerposition',[0 0 1 1])

cd('C:\Documents and Settings\law93\Desktop\NVWG');
sumtitl=['dig_and_points3g_all_SCAP',num2str(subject)];
pause;
saveas(kk,sumtitl);
close all;

scaptrunk=xlsread(['scap_trunk_ENV_SCAP',num2str(subject)]);
scapmod=[scaptrunk(1:3,:);mean(scaptrunk(1:3,:));Rtr_sc(1,:);...
    scaptrunk(4:6,:);mean(scaptrunk(4:6,:));Rtr_sc(2,:);...
    scaptrunk(7:9,:);mean(scaptrunk(7:9,:));Rtr_sc(3,:);...
    scaptrunk(10:12,:);mean(scaptrunk(10:12,:));Rtr_sc(4,:)];
titlescap=['scap_rot_point_dig_SCAP',num2str(subject)];
xlswrite(titlescap,scapmod);

trunk1=xlsread(['trunk_pos_ENV_SCAP',num2str(subject)]);
trunkmod=[trunk1(1:3,:);mean(trunk1(1:3,:));trunk(1,:);...
    trunk1(4:6,:);mean(trunk1(4:6,:));trunk(2,:);...
    trunk1(7:9,:);mean(trunk1(7:9,:));trunk(3,:);...
    trunk1(10:12,:);mean(trunk1(10:12,:));trunk(4,:)];
titletrunk=['trunk_point_dig_SCAP',num2str(subject)];
xlswrite(titletrunk,trunkmod);


% WRITE SUMMARY FILE


cd('C:\Documents and Settings\law93\Desktop\NVWG')
```

```matlab
subjects11=[19:21,23,25:27,29,30,32,33,36:41,43:46]; %19:21[23

rot1a=[]; rot1b=[]; rot2a=[]; rot2b=[]; rot3a=[]; rot3b=[];
for p=1:length(subjects11);
    subject=subjects11(p)
    file1=xlsread(['scap_rot_point_dig_SCAP',num2str(subject)]);
        rot11a=file1(:,1);
        rot21a=file1(:,2);
        rot31a=file1(:,3);
        rot1a=[rot1a,rot11a];
        rot2a=[rot2a,rot21a];
        rot3a=[rot3a,rot31a];
    file2=xlsread(['trunk_point_dig_SCAP',num2str(subject)]);
        rot11b=file1(:,1);
        rot21b=file1(:,2);
        rot31b=file1(:,3);
        rot1b=[rot1b,rot11b];
        rot2b=[rot2b,rot21b];
        rot3b=[rot3b,rot31b];
end
xlswrite('scap_rot_point_dig_all_rot1a',rot1a);
xlswrite('scap_rot_point_dig_all_rot2a',rot2a);
xlswrite('scap_rot_point_dig_all_rot3a',rot3a);

xlswrite('trunk_point_dig_all_rot1a',rot1b);
xlswrite('trunk_point_dig_all_rot2a',rot2b);
xlswrite('trunk_point_dig_all_rot3a',rot3b);
end
```

151

APPENDIX C

VICON DATA PROCESSING

C.1   IDENTIFY SYNC IN VICON

```
function [sync_vicon] = sync_vicon_static( subject )
% Determine sync for vicon
        sync_frame=[];
        [mainfolder,subjfolder,subj_type,subj_type_tr,sync_frame, subjnum1]
        = scap_programs.General.get_subj_info ( subject );
          cd(subjfolder);
              for rr=7:subj_type_tr
                  [namefile]=det_trial(rr,subj_type);
                  viconfile=[namefile,'.csv'];
                  Dynamic = ReadViconNexus(viconfile,
                  [('C7');('T8');('STERN');('XYP');('ACROM'); ('LATEL');
                ('MEDEL'); ('UA1');('UA2');('UA3');('ProbeRIGHT');
                ('ProbeLEFT'); ('ProbeBACK');('ProbeTOP');]);
                  Dynamic = ReadViconNexus(viconfile,
                [('C7');('T8');('STERN');('XYP');('ACROM'); ('LATEL');
                ('MEDEL');
                ('UA1');('UA2');('UA3');('ProbeRIGHT');('ProbeLEFT');('Prob
                eBACK');('ProbeTOP');]);
                  [Dynamic] = filter_dyn(Dynamic);
                  [Dynamic]=convert2cm(Dynamic);
                  [sync_vicon]=process_vicon_new(Dynamic);
                  sync_frame(rr,3)=sync_vicon;
              end
          xlswrite('sync_frames.xls',sync_frame);
        end

function [sync_vicon]=process_vicon_new(Dynamic)
% This function allows for identification of the sync in vicon

    marker1move=[]; marker1move2=[];
```

```matlab
    time=[1:length(Dynamic.ProbeLEFT)];
    procfig=figure; plot(time,Dynamic.ProbeLEFT(:,3));
    pause    %allow time to zoom
    disp('select Figure 1')
    marker1move1=ginput(1)    %selects row of start
    close(procfig);

    procfig=figure; plot(time,Dynamic.ProbeRIGHT(:,3)); %plot (time,x) of
marker 2
    disp('select Figure 2')
    pause
    marker1move2=ginput(1)    %selects row of start
    close(procfig);

    markers=[]; start_vicon=[];
    markers=[marker1move1(1),marker1move2(1)];
    sync_vicon=round(mean(markers))

end
```

C.2   COMBING VICON AND ULTRASOUND DATA FOR STATIC TRIAL

```matlab
function [] = static_points3space( subject,vicon_freq )
% This function combines the 2D US points with the vicon data

        clear; clc; close all; subject=5;
        [mainfolder,subjfolder,subj_type,subj_type_tr,sync_frame,
        subjnum1] = scap_programs.General.get_subj_info ( subject );
        vicon_freq=120;
        subjnum1=num2str(subject)
        cd(subjfolder)
        zones=[];
            for rr=1:subj_type_tr
                [namefile]=det_trial(rr,subj_type);
                foldername=['C:\Documents and
                Settings\law93\Desktop\NVWG\SCAP',subjnum1,'\',namefile];
                viconfile=[namefile,'.csv'];
                hinner = figure(2);
                    %houter = figure(2);
                cd(subjfolder)   %vicon is stored in main subject folder
                Dynamic=[]; Dyn=[];
                Dynamic = ReadViconNexus(viconfile,
            [('C7');('T8');('STERN');('XYP');('ACROM'); ('LATEL');
            ('UA1');('UA2');('UA3');('ProbeRIGHT');('ProbeLEFT');('Prob
            eBACK');('ProbeTOP');]);
                [Dynamic] = filter_dyn(Dynamic);
                [Dynamic]=convert2cm(Dynamic);
                  sync_vicon=sync_frame(rr,3);
                  cd(foldername); tally=xlsread('tally');
```

153

```matlab
                        [Dyn,zones]=downsample(Dynamic,sync_vicon,vicon_freq,tall
                        y,rr,zones);
                        xlswrite('zones',zones);
                        cd(subjfolder); [angles] = AngleTrial(Dyn);
                        ultrasoundfile=['spine_points_wrow_',namefile,'_ima'];
                        [spine_point]=xlsread(ultrasoundfile);
                        static_mm=xlsread('beam_attach3');
                        zone=zones(rr,:);

                    [point3space]=transformStatic(hinner,zone,subjnum1,namefile
                    ,Dyn,spine_point,static_mm);
                        filename=['points3space_ENV_ima_',namefile];
                        xlswrite(filename,point3space);
                        [title1]=plotcurrent(subjnum1,namefile,point3space);%
                end
            for rr=1:subj_type_tr
                    [namefile]=det_trial(rr,subj_type);
                    [title1]=plotcurrent2(subjnum1,namefile);
            end
            close all;
        end


function
[point3space,pointcalc1,rows,angles_round1]=transformStatic(hinner,zone,subjn
um1,namefile,Dyn,spine_point,static_mm);
%this function combines ultrasound and vicon data
     %static calibration data
    static=static_mm(1,:)/(10);

    point_xy=[]; point_xyG=[]; point_xyattach=[];
    point3space1=[]; point3space=[];
    pt1a=[]; pt2a=[]; pt3a=[]; pt4a=[];
    point1a=[];point2a=[];point3a=[];point4a=[];point5a=[];point6a=[];
    stern3space1=[]; xyp3space1=[]; c73space1=[]; t83space1=[];
    stern3space=[]; xyp3space=[]; c73space=[]; t83space=[];
    sternA=[]; c7A=[]; t8A=[]; xypA=[];

    looptil=[];
    if length(spine_point) >= length(Dyn.xyphoid)
        looptil=length(Dyn.xyphoid);
    else
        looptil=length(spine_point);
    end


    pointcalc1=[]; point3space=[];
    point3space2=[]; point3space1=[];
    rows=[];
    sternA=[]; xypA=[]; c7A=[]; t8A=[];
    point1a=[]; point3a=[];
    countk=0;
    for i=1:looptil
    if i <= zone(1) || i >= zone(4) || i >= zone(2) && i<=zone(3)
        countk1=countk+1
```
154

```matlab
else
    if spine_point(i,2)> 0
        [pt1,pt2,pt3,pt4,pt5,pt6,pt7,pt8] = loadstatpt(static);
        [Rbeam, Vbeam] = BeamCoord(pt5,pt6,pt7,pt8);
        %static LCS for beam
         point_xy1=[spine_point(i,2:3),0];
        %pts in US space
        [point_xyG1] = CoordL2G(Rbeam, Vbeam, point_xy1);
        %xy in global

        [RattachS, VattachS] = AttachCoord(pt1,pt3,pt4);
        %Static attachment LCS
        [point_xyattach1] = CoordG2L(RattachS, VattachS, point_xyG1);
        %xy in attachment LCS from static calibration

        point1=[]; point2=[]; point3=[]; point4=[];
        %Dynamic attachment LCS

point1=Dyn.ProbeRight(i,:);%[dynamic_ds(j(i),2),dynamic_ds(j(i),3),dyna
mic_ds(j(i),4)];        %probe right

point2=Dyn.ProbeTop(i,:);%[dynamic_ds(j(i),11),dynamic_ds(j(i),12),dyna
mic_ds(j(i),13)];     %probe top

point3=Dyn.ProbeLeft(i,:);%[dynamic_ds(j(i),5),dynamic_ds(j(i),6),dynam
ic_ds(j(i),7)];        %probe left

point4=Dyn.ProbeBack(i,:);%[dynamic_ds(j(i),8),dynamic_ds(j(i),9),dynam
ic_ds(j(i),10)];        %probe back

        [RattachD, VattachD] = AttachCoord(point1,point3,point4);
        %current LCS of attachment during trial
        [pointcalc] = CoordL2G(RattachD, VattachD,point_xyattach1);
        %xy in global

%          PROBE_RIGHT_TRIAL(k,:)=point1;
        %%
        pointcalc1=[pointcalc1;pointcalc];
        %%
        %9/25 ADDED W/R TO TRUNK
        [Rg2tr, Vg2tr] = TrunkCoord_ISB(Dyn.Sternum(i,:),
        Dyn.xyphoid(i,:), Dyn.C7(i,:), Dyn.T8(i,:));
        [point3space1] = CoordG2L(Rg2tr, Vg2tr, pointcalc);
            [point11,point21,point31,point41] = CoordG2L(Rg2tr, Vg2tr,
        point1,point2,point3,point4);
        [stern3space1, xyp3space1, c73space1, t83space1] =
        CoordG2L(Rg2tr, Vg2tr, Dyn.Sternum(i,:), Dyn.xyphoid(i,:),
        Dyn.C7(i,:), Dyn.T8(i,:));

        %trunk orientation during trial
        trunk_angs(i,:)=EulerYXY(Rg2tr, 'ZXY');

        %add a timestamp
        point3space2=[point3space1,i];
```

155

```matlab
        point3space=[point3space;point3space2];
        point1a=[point1a;point11];
        point2a=[point2a;point21];
        point3a=[point3a;point31];
        point4a=[point4a;point41];
        stern3space=[stern3space;stern3space1];
        xyp3space=[xyp3space;xyp3space1]; c73space=[c73space;c73space1];
        t83space=[t83space;t83space1];

        %pull 3 space trunk coordinates8
        sternA=[sternA;Dyn.Sternum(i,:)];
        c7A=[c7A;Dyn.C7(i,:)];
        t8A=[t8A;Dyn.T8(i,:)];
        xypA=[xypA;Dyn.xyphoid(i,:)];
        rows=[rows;i];
        end
    end
    end
    t1=(point1a-point3a)/2;
    for i=2:length(t1)
        vel_t1(i)=sqrt((t1(i,1)-t1(i-1,1))^2 + (t1(i,2)-t1(i-1,2))^2 +
(t1(i,3)-t1(i-1,3))^2)/(point3space(i,4)-point3space(i-1,4));
    end
    for i=2:length(point3space)
        vel_point3space(i)=sqrt((point3space(i,1)-point3space(i-1,1))^2 +
(point3space(i,2)-point3space(i-1,2))^2 + (point3space(i,3)-point3space(i-
1,3))^2)/(point3space(i,4)-point3space(i-1,4));
    end


end
```

C.3   CONVERT TO GLOBAL COORDINATE SYSTEM

```matlab
classdef RotBtwnPointClouds < handle

methods (Static)
    mainfolder=('C:\Documents and Settings\law93\Desktop\NVWG');
    cd(mainfolder);
    subject_type=xlsread('subject_type'); subj_type=subject_type(subject);
    [subj_type_tr] = scap_programs.General.getnumtrials ( subj_type );

    subjects11=[1:2,4:11,13:18,22,28,31,34,35,42]; %1


    for p=1:length(subjects11);
        subject=subjects11(p)

        subjnum1=num2str(subject);
```

```matlab
        subjfolder=['C:\Documents and
Settings\law93\Desktop\NVWG\SCAP',subjnum1];
        cd(subjfolder);
        subj_type=subject_types(subject);

        if subject==1
            t=[1:6,8];
        elseif subject==16
            t=[1:4,6:8];
        elseif subject==18
            t=[1:2,4:8];
        elseif subject==31;
            t=[1:5,8];
        elseif subject==42;
            t=[1:5,7:8];
        else
            t=[1:8];
        end

        trunk=[]; scapG=[]; Rtr_sc=[];
        for s=1:length(t)
            rr=t(s);
            [namefile] = det_trial(rr,subj_type);
            disp(['subject ',subjnum1,' ',namefile]);
            viconfile=[namefile,'.csv'];                        %get trunk LCS
            Dynamic=[]; Dyn=[]; Dynamic = ReadViconNexus(viconfile,
            [('C7');('T8');('STERN');('XYP');('ACROM'); ('LATEL'); ('MEDEL');
            ('UA1');('UA2');('UA3');('ProbeRIGHT');('ProbeLEFT');('ProbeBACK'
            );('ProbeTOP');]);
            [Dynamic] = filter_dyn(Dynamic);
            [Dynamic]=convert2cm(Dynamic);
            C7=mean(Dynamic.C7cm(1000:2000,:));
            T8=mean(Dynamic.T8cm(1000:2000,:));
            STERN=mean(Dynamic.Sternumcm(1000:2000,:));
            XYP=mean(Dynamic.xyphoidcm(1000:2000,:));
            [Rg2tr, Vg2tr] = TrunkCoord_ISB(STERN, XYP, C7, T8);
            trunk(rr,:)=EulerYXY(Rg2tr, 'ZXY');

            points3  = xlsread(['points3space_ENV',namefile,'.xls']);
            pointsG=[];
            for i=1:length(points3)
                    pointsG(i,:)=[CoordL2G(Rg2tr,
                    Vg2tr,points3(i,1:3)),points3(i,4)];
            end
            f=figure; hold on;
plot3(pointsG(:,1),pointsG(:,2),pointsG(:,3),'MarkerSize',10,'Marker','.','Li
neStyle','none','MarkerEdgeColor','b')
                xlabel('xaxis');
                ylabel('yaxis');
                zlabel('zaxis');
                view(90,0);
    %         pause;
            close(f)
            name=['pointsG3_ENV',namefile];
            xlswrite(name,pointsG);
        end
```

```matlab
    end


    clear; clc; close all;
    mainfolder=('C:\Documents and Settings\law93\Desktop\NVWG');
    cd(mainfolder);
    subject_types=xlsread('subject_type'

    subjects11=[31,34,35,42];

    for p=1:length(subjects11);
    subject=subjects11(p)

    subj_type=subject_types(subject);
    [subj_type_tr] = scap_programs.General.getnumtrials ( subj_type );
    subjnum1=num2str(subject);
    subjfolder=['C:\Documents and
Settings\law93\Desktop\NVWG\SCAP',subjnum1];
    cd(subjfolder);

    %accommodate missing trials
    if subject==1
        t=[1:6,8];
    elseif subject==16
        t=[1:4,6:8];
    elseif subject==18
        t=[1:2,4:8];
    elseif subject==31;
        t=[1:5,8];
    elseif subject==42;
        t=[1:5,7:8];
    else
        t=[1:8];
    end
            proc=1;
            midfile=xlsread('midline_select.xls');
            Nsign = xlsread('Nsign.xls');
            dir = xlsread('dir.xls');
            D = xlsread('D.xls');

    Rtr_sc=[]; trunk=[];
    for s=1:length(t)
        rr=t(s);
        C7=[]; T8=[]; STERN=[]; XYP=[];
        [namefile] = det_trial(rr,subj_type);
        disp(namefile);
        name=['pointsG3_ENV',namefile,'.xls'];
        pointsG=xlsread(name);

        [ Rscap, Vscap,midline_select(rr,:) ] = getscaplcs(
pointsG,Nsign(rr),dir(rr),proc,rr,midfile,D(rr) );    %get LCS data
        scapG(rr,:)=EulerYXY(Rscap, 'ZXY');

        viconfile=[namefile,'.csv'];                                %get trunk
LCS
```

```matlab
        Dynamic=[]; Dyn=[]; Dynamic = ReadViconNexus(viconfile,
[('C7');('T8');('STERN');('XYP');('ACROM'); ('LATEL');
('UA1');('UA2');('UA3');('ProbeRIGHT');('ProbeLEFT');('ProbeBACK');('ProbeTOP
');]);
            Dynamic.MEDEL=ones(length(Dynamic.C7),3);
        [Dynamic] = filter_dyn(Dynamic);  %temporarily OMITTED FILTER
        [Dynamic]=convert2cm(Dynamic);
        C7=mean(Dynamic.C7cm(1000:2000,:));
T8=mean(Dynamic.T8cm(1000:2000,:));
STERN=mean(Dynamic.Sternumcm(1000:2000,:));
XYP=mean(Dynamic.xyphoidcm(1000:2000,:));
        [Rg2tr, Vg2tr] = TrunkCoord_ISB(STERN, XYP, C7, T8);
        trunkorient = inv([0 0 1; 1 0 0; 0 1 0]) * Rg2tr;
        trunk(rr,:)=EulerYXY(trunkorient, 'ZXY');


         Rtr_sc(rr,:) = EulerYXY(inv( Rg2tr ) * ( Rscap ),'YXZ');
        close all;
    end
    xlswrite('midline_select',midline_select);
    cd('C:\Documents and Settings\law93\Desktop\NVWG');
    tru=['trunk_pos_ENV_SCAP',num2str(subject)];
    sca=['scap_trunk_ENV_SCAP',num2str(subject)];
    xlswrite(tru,trunk);
    xlswrite(sca,Rtr_sc);
    end

    subjects11=[1:2,4:11,13:18,22,28,31,34:35,42];

subjects11=[19,40,24,25,38,26,44,32,21,30,27,33,37,43,20,46,45,23,39,41,36,29
];


    cd('C:\Documents and Settings\law93\Desktop\NVWG')

    rot1a=[]; rot1b=[]; rot2a=[]; rot2b=[]; rot3a=[]; rot3b=[];
    for p=1:length(subjects11);
        subject=subjects11(p)

        file2=xlsread(['trunk_pos_ENV_SCAP',num2str(subject)]);
            rot11b=file2(:,1);
            rot21b=file2(:,2);
            rot31b=file2(:,3);
            rot1b=[rot1b,[subject;rot11b]];
            rot2b=[rot2b,[subject;rot21b]];
            rot3b=[rot3b,[subject;rot31b]];
    end
    xlswrite('scap_trunk_ENV_rot1_mwu',rot1a);
    xlswrite('scap_trunk_ENV_rot2_mwu',rot2a);
    xlswrite('scap_trunk_ENV_rot3_mwu',rot3a);

    xlswrite('trunk_pos_ENV_rot1_mwu',rot1b);
    xlswrite('trunk_pos_ENV_rot2_mwu',rot2b);
    xlswrite('trunk_pos_ENV_rot3_mwu',rot3b);
```

```matlab
    xlswrite('trunk_pos_ENV_rot1_ab',rot1b);
    xlswrite('trunk_pos_ENV_rot2_ab',rot2b);
    xlswrite('trunk_pos_ENV_rot3_ab',rot3b);

    xlswrite('trunk_point_dig_rot1_ab',rot1b);
    xlswrite('trunk_point_dig_rot2_ab',rot2b);
    xlswrite('trunk_point_dig_rot3_ab',rot3b);

    if proc==2;
        xlswrite('midline_select',midline_select);
    end
    xlswrite('trunk_pos',trunk);
    xlswrite('scap_trunk_postrim',Rtr_sc);

    xlswrite('Nsign',Nsign);
    xlswrite('dir',dir);
    xlswrite('D',D);

end
```

C.4   FIT LOCAL COORDINATE SYSTEM TO SCAPULAR BORDER

```matlab
function [ Rscap1,Vscap1,midline_select ] = getscaplcs(
pointsG,Nsign,dir,proc,rr,midfile,D )
%fit LCS to scapular border
    spiN1=[]; spiP1=[]; medN1=[]; medP1=[];
        %fit plane, get normal and spine regression
            figure; xlabel('x global'); ylabel('y global'); zlabel('z
            global');
            [Err, N1,P1,Xfit1] = ldubs.Project.planeProjection( pointsG );

            [spi1,med1,midline_select]=pull_med_spine(Xfit1,dir,proc,rr,midfi
            le);
                h=figure;
                [Err,spiN1,spiP1] = ldubs.Project.lineProjection( spi1 );
                [Err,medN1,medP1] = ldubs.Project.lineProjection( med1 );
                [P_intersect1,distances1] = lineIntersect3D([spiP1;medP1],
                [[spiN1'+spiP1];[medN1'+medP1]]);
            %LCS for scapula
            axis_tech1 = -D*spiN1; %z (right)
            axis_tech2 = Nsign*N1;      %x (forward)
            axis_tech3 = cross( axis_tech1, axis_tech2 ); %y (up)
            Rscap1 = [axis_tech2, axis_tech3, axis_tech1];
            Vscap1 = spiP1 + 3*axis_tech1';
            z1 = spiP1 + axis_tech1';
            z2 = spiP1 + 3*axis_tech1';
            x1 = P1 + axis_tech2';
            x2 = P1 + 5*axis_tech2';
```

```matlab
plot3(z1(:,1),z1(:,2),z1(:,3),'MarkerSize',30,'Marker','.','LineStyle','none'
,'MarkerEdgeColor','m');

plot3(z2(:,1),z2(:,2),z2(:,3),'MarkerSize',30,'Marker','.','LineStyle','none'
,'MarkerEdgeColor','r');

plot3(x1(:,1),x1(:,2),x1(:,3),'MarkerSize',30,'Marker','.','LineStyle','none'
,'MarkerEdgeColor','m');

plot3(x2(:,1),x2(:,2),x2(:,3),'MarkerSize',30,'Marker','.','LineStyle','none'
,'MarkerEdgeColor','r');

plot3(P_intersect1(1),P_intersect1(2),P_intersect1(3),'MarkerSize',30,'Marker
','.','LineStyle','none','MarkerEdgeColor','g');
            xlabel('x'); ylabel('y'); zlabel('z');
%           view(0,0);
            pause;

%           close(h);

End



function
[spine,med,midline_select]=pull_med_spine(pointset,dir,proc,rr,midfile);

if dir==1;
    h1=figure; hold on;
    %for y-z view
    view(90,0)
    if proc==2;

plot3(pointset(:,1),pointset(:,2),pointset(:,3),'MarkerSize',12,'Marker','.',
'LineStyle','none','MarkerEdgeColor','b');
        xlabel('x'); ylabel('y');zlabel('z');
        midline=ginput3d(2);
    elseif proc==1;
        midline = [midfile(rr,1:3);midfile(rr,4:6)];
    end
    m=(midline(1,3)-midline(2,3))/(midline(1,2)-midline(2,2));
    b=midline(1,3)-m*midline(1,2);
    %divide up data set
    spine=[]; med=[];
    for i=1:length(pointset)
        yline=m*pointset(i,2)+b;
        if pointset(i,3) > yline
            spine=[spine;pointset(i,:)];
        else
            med=[med;pointset(i,:)];
        end
    end
    h2=figure; hold on;
    if length(spine)>1
```

161

```matlab
plot3(spine(:,1),spine(:,2),spine(:,3),'MarkerSize',12,'Marker','.','LineStyl
e','none','MarkerEdgeColor','m');
    end
    if length(med)>1

plot3(med(:,1),med(:,2),med(:,3),'MarkerSize',12,'Marker','.','LineStyle','no
ne','MarkerEdgeColor','g');
    end


elseif dir==2;
    h1=figure; hold on;
    %for xy view
    if proc==2;
        view(0,90)

plot3(pointset(:,1),pointset(:,2),pointset(:,3),'MarkerSize',12,'Marker','.',
'LineStyle','none','MarkerEdgeColor','b');
        xlabel('x'); ylabel('y');zlabel('z');
        midline=ginput3d(2);
    elseif proc==1;
        midline = [midfile(rr,1:3);midfile(rr,4:6)];
    end
    m=(midline(1,2)-midline(2,2))/(midline(1,1)-midline(2,1));
    b=midline(1,2)-m*midline(1,1);
    %divide up data set
    spine=[]; med=[];
    for i=1:length(pointset)
        yline=m*pointset(i,1)+b;
        if pointset(i,2) > yline
            spine=[spine;pointset(i,:)];
        else
            med=[med;pointset(i,:)];
        end
    end
    h2=figure; hold on;
    if length(spine)>1

plot3(spine(:,1),spine(:,2),spine(:,3),'MarkerSize',12,'Marker','.','LineStyl
e','none','MarkerEdgeColor','m');
    end
    if length(med)>1

plot3(med(:,1),med(:,2),med(:,3),'MarkerSize',12,'Marker','.','LineStyle','no
ne','MarkerEdgeColor','g');
    end


else
    disp('you need to say a direction')
end
%     pause;
%     close(h1);
%     close(h2);
midline_select=[midline(1,:),midline(2,:)];


end
```

C.5   DETERMINE ARM POSITION


```matlab
function [] = determine_arm_pos()

clear; clc; close all;
mainfolder=('C:\Documents and Settings\law93\Desktop\NVWG');
cd(mainfolder);
subject_types=xlsread('subject_type');%consider pulling vicon freq as well

subjects11=[19,40,24,25,38,26,44,32,21,30,27,33,37,43,20,46,45,23,39,41,36,29
];

for p=1:length(subjects11);
    subject=subjects11(p)
    subj_type=subject_types(subject);
    [subj_type_tr] = scap_programs.General.getnumtrials ( subj_type );
    subjnum1=num2str(subject);
    title=['arm_ang__DIG_SCAP',num2str(subject)];
     armang=[]; armstd=[];

    subjfolder=['C:\Documents and
Settings\law93\Desktop\NVWG\SCAP',subjnum1];
    cd(subjfolder);
     vicon_freq=120;

    for rr=1:4
        if rr==1
            namefile='digrest';
        elseif rr==2
            namefile='digsag';
        elseif rr==3
            namefile='digfront';
        else
            namefile='digscap';
        end
        disp(namefile)
        viconfile=[namefile,'.csv'];
        Dynamic=[]; Dyn=[];
        Dynamic =
ReadViconNexus(viconfile,[('C7');('T8');('STERN');('XYP');('ACROM');
('LATEL'); ('MEDEL');
('UA1');('UA2');('UA3');('ProbeRIGHT');('ProbeLEFT');('ProbeBACK');('ProbeTOP
');]);
        [angles] = AngleTrial1(Dynamic);
        plot(angles)
        st=round(ginput(2));
        armang(rr)=mean(angles(st(1,1):st(2,1)));
        armstd(rr)=std(angles(st(1,1):st(2,1)));
    end
    cd(mainfolder)
    out=[armang',armstd'];
    xlswrite(title,out);
end
```

APPENDIX D

DYNAMIC TRIALS

D.1   PROCESS DYNAMIC DATA

```matlab
function [] = determine_arm_pos()

clear; clc; close all;
mainfolder=('C:\Documents and Settings\law93\Desktop\NVWG');
cd(mainfolder);
subject_types=xlsread('subject_type');%consider pulling vicon freq as well

subjects11=[19,40,24,25,38,26,44,32,21,30,27,33,37,43,20,46,45,23,39,41,36,29
];

for p=1:length(subjects11);
    subject=subjects11(p)
    subj_type=subject_types(subject);
    [subj_type_tr] = scap_programs.General.getnumtrials ( subj_type );
    subjnum1=num2str(subject);
    title=['arm_ang__DIG_SCAP',num2str(subject)];
     armang=[]; armstd=[];

    subjfolder=['C:\Documents and
Settings\law93\Desktop\NVWG\SCAP',subjnum1];
    cd(subjfolder);
     vicon_freq=120;

    for rr=1:4
        if rr==1
            namefile='digrest';
        elseif rr==2
            namefile='digsag';
        elseif rr==3
            namefile='digfront';
        else
```

```matlab
            namefile='digscap';
        end
        disp(namefile)
        viconfile=[namefile,'.csv'];
        Dynamic=[]; Dyn=[];
        Dynamic =
ReadViconNexus(viconfile,[('C7');('T8');('STERN');('XYP');('ACROM');
('LATEL'); ('MEDEL');
('UA1');('UA2');('UA3');('ProbeRIGHT');('ProbeLEFT');('ProbeBACK');('ProbeTOP
');]);
        [angles] = AngleTrial1(Dynamic);
        plot(angles)
        st=round(ginput(2));
        armang(rr)=mean(angles(st(1,1):st(2,1)));
        armstd(rr)=std(angles(st(1,1):st(2,1)));
    end
    cd(mainfolder)
    out=[armang',armstd'];
    xlswrite(title,out);
end

function [] = dynamic_NEW

    clear; clc; close all; subject=13;
    [mainfolder,subjfolder,subj_type,subj_type_tr,sync_frame, subjnum1] =
scap_programs.General.get_subj_info ( subject );
    vicon_freq=120;
    subjnum1=num2str(subject)
    cd(subjfolder)

    rr=11
    [namefile]=det_trial(rr,subj_type);
    disp(namefile)
    cd(['C:\Documents and
Settings\law93\Desktop\NVWG\SCAP',num2str(subject),'\',namefile])

    sync_vicon=593;
    spine_point=xlsread(['spine_points_wrow_',namefile]);%,'_ml']);
                vicon_freq=120;
                    viconfile=[namefile,'.csv'];
                    hinner = figure(2);
                        %houter = figure(2);
                    Dynamic=[]; Dyn=[];
                    Dynamic = ReadViconNexus(viconfile,
[('C7');('T8');('STERN');('XYP');('ACROM'); ('LATEL'); ('MEDEL');
('UA1');('UA2');('UA3');('ProbeRIGHT');('ProbeLEFT');('ProbeBACK');('ProbeTOP
');]);
                     [Dynamic] = filter_dyn(Dynamic);
                    [Dynamic]=convert2cm(Dynamic);
                    tally=xlsread('tally');

[Dyn]=downsampledyn(Dynamic,sync_vicon,vicon_freq,tally);
                    static_mm=xlsread('beam_attach3');

[point3space]=transformDynamic_315(hinner,subjnum1,namefile,Dyn,spine_point,s
tatic_mm);
```

```matlab
                C7=mean(Dynamic.C7cm(1000:2000,:));
T8=mean(Dynamic.T8cm(1000:2000,:));
STERN=mean(Dynamic.Sternumcm(1000:2000,:));
XYP=mean(Dynamic.xyphoidcm(1000:2000,:));
                [Rg2tr, Vg2tr] = TrunkCoord_ISB(STERN, XYP, C7, T8);
                trunk=EulerYXY(Rg2tr, 'ZXY');
                pointsG=[];
                for i=1:length(point3space)
                    pointsG(i,:)=CoordL2G(Rg2tr, Vg2tr,point3space(i,1:3));
                end
                pointsG=[pointsG,point3space(:,4)];
                    figure; hold on;
                    for i=1:length(pointsG)
                        if pointsG(i,1)==0
                            a=1;
                        else

plot3(pointsG(i,1),pointsG(i,2),pointsG(i,3),'MarkerSize',10,'Marker','.','Li
neStyle','none','MarkerEdgeColor','r')
                        end
                    end
                xlabel('xaxis');ylabel('yaxis');zlabel('zaxis');
                xlswrite('pointsG',pointsG);


                        [angles] = AngleTrial(Dyn);
                        xlswrite('angles',angles);

    figure; plot(angles)
    updowntimes=[];
    for i=1:20
        pause;
        ti=ginput(4)
        updowntimes1=ti(:,1)';
        updowntimes=[updowntimes;round(updowntimes1)];
    end
    updowntimes=round(updowntimes);
    xlswrite('updowntimes',updowntimes);



    angles=xlsread('angles');
    point3space=xlsread('pointsG');
    pointsG=point3space(:,1:3);
    updowntimes=xlsread('updowntimes.xls');
    pGflap=[];
    for u=1:20
        start = updowntimes(u,1);
        stop=updowntimes(u,2);

    %angles
        ang=angles(start:stop);
        ang_t = 0:100/(length(ang)-1):100;
        ang_t2 = [1:100];
        ang_s = interp1(ang_t,ang,ang_t2,'spline');
```

```matlab
    %points
        point_rows_start=min(find(point3space(:,4)==start));
            if length(point_rows_start)==0
                point_rows_start=min(find(abs(point3space(:,4)-
start)==min(abs(point3space(:,4)-start)))+1);
                %determine what part of segment is represented by pointsG
                diffstart = point3space(point_rows_start,4) - start;
            else
                diffstart=0;
            end
        point_rows_stop=max(find(point3space(:,4)==stop));
            if length(point_rows_stop)==0
                point_rows_stop=max(find(abs(point3space(:,4)-
stop)==min(abs(point3space(:,4)-stop)))+1);
                %determine what part of segment is represented by pointsG
                diffstop = point3space(point_rows_stop,4) - stop;
            else
                diffstop=0;
            end
        startadj=round(100*diffstart/(stop-start));
            bufferfront=ones(startadj,3);
        stopadj=round(100*diffstop/(stop-start));
            bufferend=ones(stopadj,3);
        midadj=100-startadj-stopadj;
        if point3space(point_rows_start,4)>= stop
            pGflap(u,:)=[1 1 1 1 1 1 1 1 1 1 1 1 u];
            disp(['u ',num2str(u),' is outside of window']);
        else
            pG=pointsG(point_rows_start:point_rows_stop,:);
            CS = cat(1,0,cumsum(sqrt(sum(diff(pG,[],1).^2,2))));
            pGs = interp1(CS, pG, [linspace(0,CS(end),midadj)],'cubic');

            pGall = [bufferfront;pGs;bufferend];
            figure, hold on
            plot3(pG(:,1),pG(:,2),pG(:,3),'.b-')
            plot3(pGs(:,1),pGs(:,2),pGs(:,3),'.r-')

            a30len=abs(ang_s-30);
                a30=find(a30len==min(a30len));
            a45len=abs(ang_s-45);
                a45=find(a45len==min(a45len));
            a60len=abs(ang_s-60);
                a60=find(a60len==min(a60len));
            a75len=abs(ang_s-75);
                a75= a75len==min(a75len);


pGflap(u,:)=[pGall(a30,:),pGall(a45,:),pGall(a60,:),pGall(a75,:),u];%,pGs(a90
,:)];

        end
    % pause;
    close all
    end

    flap30=[]; flap45=[]; flap60=[]; flap75=[];
```
167

```matlab
for i=1:length(pGflap)
    if pGflap(i,1)>1
        flap30=[flap30;pGflap(i,[1:3,13])];
    end
    if pGflap(i,4)>1
        flap45=[flap45;pGflap(i,[4:6,13])];
    end
    if pGflap(i,7)>1
        flap60=[flap60;pGflap(i,[7:9,13])];
    end
    if pGflap(i,10)>1
        flap75=[flap75;pGflap(i,[10:12,13])];
    end
end

xlswrite('flap30',flap30);
xlswrite('flap45',flap45);
xlswrite('flap60',flap60);
xlswrite('flap75',flap75);

%pull appropriate add-abd movements
spine1 = [1:10];
medial1 = [11:20];
ss30=intersect(flap30(:,4),spine1);
    spi30=[];
    for y=1:length(ss30)
        spi30(y,:)=flap30(find(flap30(:,4)==ss30(y)),:);
    end
ss45=intersect(flap45(:,4),spine1);
    spi45=[];
    for y=1:length(ss45)
        spi45(y,:)=flap45(find(flap45(:,4)==ss45(y)),:);
    end
ss60=intersect(flap60(:,4),spine1);
    spi60=[];
    for y=1:length(ss60)
        spi60(y,:)=flap60(find(flap60(:,4)==ss60(y)),:);
    end
ss75=intersect(flap75(:,4),spine1);
    spi75=[];
    for y=1:length(ss75)
        spi75(y,:)=flap75(find(flap75(:,4)==ss75(y)),:);
    end

mm30=intersect(flap30(:,4),medial1);
    med30=[];
    for y=1:length(mm30)
        med30(y,:)=flap30(find(flap30(:,4)==mm30(y)),:);
    end
mm45=intersect(flap45(:,4),medial1);
    med45=[];
    for y=1:length(mm45)
        med45(y,:)=flap45(find(flap45(:,4)==mm45(y)),:);
    end
mm60=intersect(flap60(:,4),medial1);
    med60=[];
```

```matlab
        for y=1:length(mm60)
            med60(y,:)=flap60(find(flap60(:,4)==mm60(y)),:);
        end
    mm75=intersect(flap75(:,4),medial1);
        med75=[];
        for y=1:length(mm75)
            med75(y,:)=flap75(find(flap75(:,4)==mm75(y)),:);
        end

    % Save either loaded or unloaded trial
    xlswrite('spi30',spi30);
    xlswrite('spi45',spi45);
    xlswrite('spi60',spi60);
    xlswrite('spi75',spi75);
    xlswrite('med30',med30);
    xlswrite('med45',med45);
    xlswrite('med60',med60);
    xlswrite('med75',med75);

    xlswrite('spi30L',spi30);
    xlswrite('spi45L',spi45);
    xlswrite('spi60L',spi60);
    xlswrite('spi75L',spi75);
    xlswrite('med30L',med30);
    xlswrite('med45L',med45);
    xlswrite('med60L',med60);
    xlswrite('med75L',med75);

    h=figure;
    [Err,spiN1,spi1] = ldubs.Project.lineProjection( spi30,'k' );
    [Err,spiN1,med1] = ldubs.Project.lineProjection( med30,'k' );
    [Err,spiN1,spi1] = ldubs.Project.lineProjection( spi45,'r' );
    [Err,spiN1,med1] = ldubs.Project.lineProjection( med45,'r' );
    [Err,spiN1,spi1] = ldubs.Project.lineProjection( spi60,'b' );
    [Err,spiN1,med1] = ldubs.Project.lineProjection( med60,'b'  );
    [Err,spiN1,spi1] = ldubs.Project.lineProjection( spi75,'g'  );
    [Err,spiN1,med1] = ldubs.Project.lineProjection( med75,'g'  );

plot3(flap30(:,1),flap30(:,2),flap30(:,3),'MarkerSize',20,'Marker','.','LineS
tyle','none','MarkerEdgeColor','k')

plot3(flap45(:,1),flap45(:,2),flap45(:,3),'MarkerSize',20,'Marker','.','LineS
tyle','none','MarkerEdgeColor','r')

plot3(flap60(:,1),flap60(:,2),flap60(:,3),'MarkerSize',20,'Marker','.','LineS
tyle','none','MarkerEdgeColor','b')

plot3(flap75(:,1),flap75(:,2),flap75(:,3),'MarkerSize',20,'Marker','.','LineS
tyle','none','MarkerEdgeColor','g')
    xlabel('xaxis');ylabel('yaxis');zlabel('zaxis');
    view(0,0)

    saveas(h,'dynamic_by_ang')


end
```

D.2   PULL DYNAMIC MAX ELEVATION DATA

```matlab
function [] = pull_elev_pts
% PULL ELEVATED POINTS

clear; clc; close all; subject=34;
rr=11
    [mainfolder,subjfolder,subj_type,subj_type_tr,sync_frame, subjnum1] =
scap_programs.General.get_subj_info ( subject );
    vicon_freq=120;
    subjnum1=num2str(subject)
    cd(['C:\Documents and
Settings\law93\Desktop\NVWG\SCAP',num2str(subject)])
scapG = xlsread('pointsG3_ENVscap1');
% % %
    [namefile]=det_trial(rr,subj_type);
    disp(namefile)
    cd(['C:\Documents and
Settings\law93\Desktop\NVWG\SCAP',num2str(subject),'\',namefile])


angles=xlsread('angles');
pointsG=xlsread('pointsG');
figure; plot(angles);

humelev = 77;
maxelev1 = find(round(angles)==humelev);
maxelev2 = find(round(angles)==humelev+2);
maxelev3 = find(round(angles)==humelev+1);
maxelev=[maxelev1;maxelev2;maxelev3];

maxpt=[];
for i=1:length(maxelev3)
    maxpt=[maxpt;pointsG(find(pointsG(:,4)==maxelev3(i)),1:3)];
end
xlswrite('maxpt_dynscap',maxpt)

g=figure; hold on;
plot3(maxpt(:,1),maxpt(:,2),maxpt(:,3),'MarkerSize',20,'Marker','.','LineStyl
e','none','MarkerEdgeColor','c')
plot3(scapG(:,1),scapG(:,2),scapG(:,3),'MarkerSize',20,'Marker','.','LineStyl
e','none','MarkerEdgeColor','b')
view(0,0)
xlabel('xaxis');ylabel('yaxis');zlabel('zaxis');
title=['maxpt_',namefile];
xlswrite(title,maxpt);
cd(['C:\Documents and Settings\law93\Desktop\NVWG\SCAP',num2str(subject)])
saveas(g,title)

%rotation for maxpt
clear; clc; close all; subject=13;
rr=11
```

```matlab
[mainfolder,subjfolder,subj_type,subj_type_tr,sync_frame, subjnum1] = 
scap_programs.General.get_subj_info ( subject );
cd(subjfolder);
    maxpt=xlsread('maxpt_dynscap');
[namefile]=det_trial(rr,subj_type);
disp(namefile)
    cd([subjfolder,'\',namefile]);
    Rg2tr=xlsread('Rg2tr');


close all;
dir=1; proc=2; midfile=[]; D=-1; Nsign=1;
[Err, N1,P1,Xfit1] = ldubs.Project.planeProjection( maxpt );
    [spi1,med1,midline_select]=pull_med_spine(Xfit1,dir,proc,rr,midfile);
    [Err,spiN1,spiP1] = ldubs.Project.lineProjection( spi1,'b' );
        axis_tech1 = -D*spiN1; %z (right)
        axis_tech2 = Nsign*N1;      %x (forward)
        axis_tech3 = cross( axis_tech1, axis_tech2 ); %y (up)
        Rscap = [axis_tech2, axis_tech3, axis_tech1];
        z1 = spiP1 + axis_tech1';
        z2 = spiP1 + 3*axis_tech1';
        x1 = P1 + axis_tech2';
        x2 = P1 + 5*axis_tech2';

plot3(z1(:,1),z1(:,2),z1(:,3),'MarkerSize',30,'Marker','.','LineStyle','none'
,'MarkerEdgeColor','m');

plot3(z2(:,1),z2(:,2),z2(:,3),'MarkerSize',30,'Marker','.','LineStyle','none'
,'MarkerEdgeColor','r');

plot3(x1(:,1),x1(:,2),x1(:,3),'MarkerSize',30,'Marker','.','LineStyle','none'
,'MarkerEdgeColor','m');

plot3(x2(:,1),x2(:,2),x2(:,3),'MarkerSize',30,'Marker','.','LineStyle','none'
,'MarkerEdgeColor','r');
        xlabel('x'); ylabel('y'); zlabel('z');
        Rtr_sc = EulerYXY(inv( Rg2tr ) * ( Rscap ),'YXZ')
        xlswrite('Nsign_max',Nsign); xlswrite('dir_max',dir);
xlswrite('D_max',D);
        xlswrite('Rtr_sc_max',Rtr_sc);


end
```

D.3   FIT LOCAL COORDINATE SYSTEM TO DYNAMIC DATA

```matlab
function [] = scap_rot_dynamic()
% DETERMINE SCAPULAR ROTATION FOR DYNAMIC TRIALS

    clear; clc; close all;
    subject = 34
```

```matlab
    subj_type=1;
    rr=12
        [namefile]=det_trial(rr,subj_type);
         disp(namefile)
         cd(['C:\Documents and
Settings\law93\Desktop\NVWG\SCAP',num2str(subject),'\',namefile])
        viconfile=[namefile,'.csv'];
        Dynamic=[]; Dyn=[]; Dynamic = ReadViconNexus(viconfile,
[('C7');('T8');('STERN');('XYP');('ACROM'); ('LATEL');
('UA1');('UA2');('UA3');('ProbeRIGHT');('ProbeLEFT');('ProbeBACK');('ProbeTOP
');]);
            Dynamic.MEDEL=ones(length(Dynamic.C7),3);
        [Dynamic] = filter_dyn(Dynamic);
        [Dynamic]=convert2cm(Dynamic);
        C7=mean(Dynamic.C7cm(1000:2000,:));
T8=mean(Dynamic.T8cm(1000:2000,:));
STERN=mean(Dynamic.Sternumcm(1000:2000,:));
XYP=mean(Dynamic.xyphoidcm(1000:2000,:));
        [Rg2tr, Vg2tr] = TrunkCoord_ISB(STERN, XYP, C7, T8);
        xlswrite('Rg2tr',Rg2tr);
        Rg2tr=xlsread('Rg2tr');

    flap30=xlsread('flap30');
    flap45=xlsread('flap45');
    flap60=xlsread('flap60');
    flap75=xlsread('flap75');
    if rr==11
        spi30=xlsread('spi30');
        spi45=xlsread('spi45');
        spi60=xlsread('spi60');
        spi75=xlsread('spi75');
    elseif rr==15
        spi30=xlsread('spi30');
        spi45=xlsread('spi45');
        spi60=xlsread('spi60');
        spi75=xlsread('spi75');
    elseif rr==12
        spi30=xlsread('spi30L');
        spi45=xlsread('spi45L');
        spi60=xlsread('spi60L');
        spi75=xlsread('spi75L');
    elseif rr==16
        spi30=xlsread('spi30L');
        spi45=xlsread('spi45L');
        spi60=xlsread('spi60L');
        spi75=xlsread('spi75L');
    else
        disp('error');
    end

    dir=1; proc=2; midfile=[]; D=1; Nsign=1;
    [Err, N1,P1,Xfit1] = ldubs.Project.planeProjection( flap30 );
        [Err,spiN1,spiP1] = ldubs.Project.lineProjection( spi30,'b' );
            axis_tech1 = -D*spiN1; %z (right)
            axis_tech2 = Nsign*N1;      %x (forward)
            axis_tech3 = cross( axis_tech1, axis_tech2 ); %y (up)
```

```matlab
            Rscap = [axis_tech2, axis_tech3, axis_tech1];
            z1 = spiP1 + axis_tech1';
            z2 = spiP1 + 3*axis_tech1';
            x1 = P1 + axis_tech2';
            x2 = P1 + 5*axis_tech2';

plot3(z1(:,1),z1(:,2),z1(:,3),'MarkerSize',30,'Marker','.','LineStyle','none'
,'MarkerEdgeColor','m');

plot3(z2(:,1),z2(:,2),z2(:,3),'MarkerSize',30,'Marker','.','LineStyle','none'
,'MarkerEdgeColor','r');

plot3(x1(:,1),x1(:,2),x1(:,3),'MarkerSize',30,'Marker','.','LineStyle','none'
,'MarkerEdgeColor','m');

plot3(x2(:,1),x2(:,2),x2(:,3),'MarkerSize',30,'Marker','.','LineStyle','none'
,'MarkerEdgeColor','r');
            xlabel('x'); ylabel('y'); zlabel('z');
            Rtr_sc_30 = EulerYXY(inv( Rg2tr ) * ( Rscap ),'YXZ')
            xlswrite('Nsign30',Nsign); xlswrite('dir30',dir);
xlswrite('D30',D);

    dir=1; proc=2; midfile=[]; D=1; Nsign=1;
    [Err, N1,P1,Xfit1] = ldubs.Project.planeProjection( flap45 );
        [Err,spiN1,spiP1] = ldubs.Project.lineProjection( spi45,'b' );
            axis_tech1 = -D*spiN1; %z (right)
            axis_tech2 = Nsign*N1;      %x (forward)
            axis_tech3 = cross( axis_tech1, axis_tech2 ); %y (up)
            Rscap = [axis_tech2, axis_tech3, axis_tech1];
            z1 = spiP1 + axis_tech1';
            z2 = spiP1 + 3*axis_tech1';
            x1 = P1 + axis_tech2';
            x2 = P1 + 5*axis_tech2';

plot3(z1(:,1),z1(:,2),z1(:,3),'MarkerSize',30,'Marker','.','LineStyle','none'
,'MarkerEdgeColor','m');

plot3(z2(:,1),z2(:,2),z2(:,3),'MarkerSize',30,'Marker','.','LineStyle','none'
,'MarkerEdgeColor','r');

plot3(x1(:,1),x1(:,2),x1(:,3),'MarkerSize',30,'Marker','.','LineStyle','none'
,'MarkerEdgeColor','m');

plot3(x2(:,1),x2(:,2),x2(:,3),'MarkerSize',30,'Marker','.','LineStyle','none'
,'MarkerEdgeColor','r');
            xlabel('x'); ylabel('y'); zlabel('z');
            Rtr_sc_45 = EulerYXY(inv( Rg2tr ) * ( Rscap ),'YXZ')
            xlswrite('Nsign45',Nsign); xlswrite('dir45',dir);
xlswrite('D45',D);

    dir=1; proc=2; midfile=[]; D=1; Nsign=1;
    [Err, N1,P1,Xfit1] = ldubs.Project.planeProjection( flap60 );
        [Err,spiN1,spiP1] = ldubs.Project.lineProjection( spi60,'b' );
            axis_tech1 = -D*spiN1; %z (right)
            axis_tech2 = Nsign*N1;      %x (forward)
            axis_tech3 = cross( axis_tech1, axis_tech2 ); %y (up)
```

```matlab
            Rscap = [axis_tech2, axis_tech3, axis_tech1];
            z1 = spiP1 + axis_tech1';
            z2 = spiP1 + 3*axis_tech1';
            x1 = P1 + axis_tech2';
            x2 = P1 + 5*axis_tech2';

plot3(z1(:,1),z1(:,2),z1(:,3),'MarkerSize',30,'Marker','.','LineStyle','none'
,'MarkerEdgeColor','m');

plot3(z2(:,1),z2(:,2),z2(:,3),'MarkerSize',30,'Marker','.','LineStyle','none'
,'MarkerEdgeColor','r');

plot3(x1(:,1),x1(:,2),x1(:,3),'MarkerSize',30,'Marker','.','LineStyle','none'
,'MarkerEdgeColor','m');

plot3(x2(:,1),x2(:,2),x2(:,3),'MarkerSize',30,'Marker','.','LineStyle','none'
,'MarkerEdgeColor','r');
            xlabel('x'); ylabel('y'); zlabel('z');
            Rtr_sc_60 = EulerYXY(inv( Rg2tr ) * ( Rscap ),'YXZ')
            xlswrite('Nsign60',Nsign); xlswrite('dir60',dir);
xlswrite('D60',D);

    dir=1; proc=2; midfile=[]; D=1; Nsign=1;
    [Err, N1,P1,Xfit1] = ldubs.Project.planeProjection( flap75 );
        [Err,spiN1,spiP1] = ldubs.Project.lineProjection( spi75,'b' );
            axis_tech1 = -D*spiN1; %z (right)
            axis_tech2 = Nsign*N1;      %x (forward)
            axis_tech3 = cross( axis_tech1, axis_tech2 ); %y (up)
            Rscap = [axis_tech2, axis_tech3, axis_tech1];
            z1 = spiP1 + axis_tech1';
            z2 = spiP1 + 3*axis_tech1';
            x1 = P1 + axis_tech2';
            x2 = P1 + 5*axis_tech2';

plot3(z1(:,1),z1(:,2),z1(:,3),'MarkerSize',30,'Marker','.','LineStyle','none'
,'MarkerEdgeColor','m');

plot3(z2(:,1),z2(:,2),z2(:,3),'MarkerSize',30,'Marker','.','LineStyle','none'
,'MarkerEdgeColor','r');

plot3(x1(:,1),x1(:,2),x1(:,3),'MarkerSize',30,'Marker','.','LineStyle','none'
,'MarkerEdgeColor','m');

plot3(x2(:,1),x2(:,2),x2(:,3),'MarkerSize',30,'Marker','.','LineStyle','none'
,'MarkerEdgeColor','r');
            xlabel('x'); ylabel('y'); zlabel('z');
            Rtr_sc_75 = EulerYXY(inv( Rg2tr ) * ( Rscap ),'YXZ')
            xlswrite('Nsign75',Nsign); xlswrite('dir75',dir);
xlswrite('D75',D);

    Rtr_sc = [Rtr_sc_30;Rtr_sc_45;Rtr_sc_60;Rtr_sc_75]
    xlswrite('Rtr_sc',Rtr_sc);


    subjects = [4,6,7,9,15,18,28,31,24,25,38,26,27,37,46,23,39];
    scap30=[]; scap45=[]; scap60=[]; scap75=[];
```

```matlab
    scap30L=[]; scap45L=[]; scap60L=[]; scap75L=[];
    for y = 1:length(subjects)
        subject = subjects(y)
        cd(['C:\Documents and
Settings\law93\Desktop\NVWG\SCAP',num2str(subject),'\dynscap'])
        scap = xlsread('Rtr_sc');
            scap30(y,:) = [subject,scap(1,:)];
            scap45(y,:) = [subject,scap(2,:)];
            scap60(y,:) = [subject,scap(3,:)];
            scap75(y,:) = [subject,scap(4,:)];
        cd(['C:\Documents and
Settings\law93\Desktop\NVWG\SCAP',num2str(subject),'\dynscapLOADED'])
        scapL = xlsread('Rtr_sc');
            scap30L(y,:) = [subject,scapL(1,:)];
            scap45L(y,:) = [subject,scapL(2,:)];
            scap60L(y,:) = [subject,scapL(3,:)];
            scap75L(y,:) = [subject,scapL(4,:)];
    end
    dynscap=[scap30,scap30L;scap45,scap45L;scap60,scap60L;scap75,scap75L];
    cd('C:\Documents and Settings\law93\Desktop\NVWG');
    xlswrite('DYNAMIC_scap_trunk1',dynscap)

end
```

E.1   PESS

Each test is scored from 0 to 2, where "0" indicated the sign or symptom of pain is definitely absent, "1" indicates the sign or symptom of pain is equivocally present, and "2" indicates the sign or symptom of pain is definitely present.

1) **Biceps tendon/bicipittal groove tenderness**. Palpation of the biceps tendon and bicipittal groove is best achieved with the arm in ten degrees of internal rotation

2) **Supraspinatus tendon/greater tuberosity tenderness**. Palpation of the greater tuberosity and supraspinatus insertion is best achieved by slightly extending and internally rotation the arm. The graeter tuberosity can be found distal to the anterolateral border of the acromion.

3) **Acromioclaivicular joint tenderness**. Pain with palpation of the acromioclavicular joint

4) **Resisted external and 5) internal rotation**. The subject isometrically attempts rotation against resistance while keeping the palm facing medially and elbow flexed at ninety degrees

6) **Supraspinatus Test**. Resistance is applied with the patient's arm abducted to ninety degrees, forward flexed to thirty degrees, and pronated. The test is positive if pain or weakness are present during resistance.

7) **Painful Arc Test**. Pain between sixty and one hundred-twenty degrees of active shoulder abduction in the coronal plane

8) **Neer's Impingement Sign**. With the examiners opposite hand on the trapezius, the patient's arm is forcibly elevated through forward flexion by the examiner causing a jamming of the greater tuberosity against the anterioinferior border of the acromion. The test is positive if it produces pain

9) **Hawkins-Kennedy Impingement Sign**. Slightly flexed at the elbow, the patient's arm is first elevated forward to ninety degrees and then forcibly medially rotated. This pushes the supraspinatus tendon against `the anterior surface of the coracoacromial ligament. The test is positive if the maneuver produces pain

10) **O'Brien's Active Compression Test for Acromioclavicular Joint Pathology and 11) Labral Pathology**. While seated the patient is asked to forward flex the affected arm to ninety degrees with the elbow in full extension. The patient then adducts the arm ten to fiftenn degrees medial to the sagittal plane of the body and fully pronates the arm so the thumb points downward, the examiner, standing behind the patient, then applies a downward force to the arm; the maneuver is repeated with the palm fully supinated. The test is positive if pain is elicited during the first maneuver, and reduced or eliminated during the second maneuver. The test for acromioclavicular joint is positive if the test elicits pain localized to that location, and the test is positive for the labrum if there is pain or painful clicking described deep within the shoulder.

Biceps Tendinosis/Tendinopathy

0 = normal fibrillar pattern and echogenicity

1 = mild loss of fibrillar pattern and/or echogenicity

2 = moderate loss of fibrillar pattern and/or echogenicity

3 = Complete or near complete loss of fibrillar pattern

4 = Clear longitudinal tear

5 = Partial rupture

6 = Full rupture/absence of tendon

Supraspinatus Tendinosis/Tendinopathy

0 = normal fibrillar pattern and echogenicity

1 = mild loss of fibrillar pattern and/or echogenicity

2 = moderate loss of fibrillar pattern and/or echogenicity

3 = Complete or near complete loss of fibrillar pattern

4 = Clear tear partial thickness

5 = Clear tear full thickness

Greater Tuberosity Cortical Surface

0 = Smooth hypoechoic cortical surface

1 = Mild cortical irregularity or hypoechoic surface

2 = Moderate cortical irregularity

3 = cortical irregularity or pitting

Dynamic Supraspinatus Impingement

0 = No evidence of impingement

1 = Mild impingement: slight irregularity in motion with or without crepitus

2 = Moderate impingement: moderate to marked irregularity in motion with or without crepitus/clear tendon contact with acromion

3 = marked impingement: lack of full ROM/greater tuberosity contact with acromion

Dynamic Subscap/Biceps/Coracoid Impingement

0 = No evidence of impingement; smooth motion without crepitus

1 = Mild impingement: slight irregularity in motion with or without crepitus

2 = Moderate impingement: moderate to marked irregularity in motion with or without crepitus/clear tendon contact with coracoid

3 = marked impingement: lack of full ROM or clear biceps contact with coracoid process

BIBLIOGRAPHY

1. Chakravarty K, Webley M. Disorders of the shoulder: an often unrecognised cause of disability in elderly people. *BMJ: British Medical Journal.* 1990;300(6728):848.

2. Wanklyn P, Forster A, Young J. Hemiplegic shoulder pain (HSP): natural history and investigation of associated features. *Disability & Rehabilitation.* 1996;18(10):497-501.

3. Ludewig PM, Cook TM. Alterations in shoulder kinematics and associated muscle activity in people with symptoms of shoulder impingement. *Physical therapy.* 2000;80(3):276-291.

4. Holmström E, Lindell J, Moritz U. Low back and neck/shoulder pain in construction workers: occupational workload and psychosocial risk factors. Part 2: Relationship to neck and shoulder pain. *Spine.* 1992;17(6):672.

5. Lo Y, Hsu Y, Chan K. Epidemiology of shoulder impingement in upper arm sports events. *British journal of sports medicine.* 1990;24(3):173-177.

6. Bayley JC, Cochran T, Sledge C. The weight-bearing shoulder. The impingement syndrome in paraplegics. *The Journal of bone and joint surgery. American volume.* 1987;69(5):676.

7. van der Windt DAWM, Thomas E, Pope DP, et al. Occupational risk factors for shoulder pain: a systematic review. *Occupational and environmental medicine.* 2000;57(7):433-442.

8. Gellman H, Sie I, Waters RL. Late complications of the weight-bearing upper extremity in the paraplegic patient. *Clinical Orthopaedics and related research.* 1988(233):132.

9. Nichols P, Norman P, Ennis J. Wheelchair user's shoulder? Shoulder pain in patients with spinal cord lesions. *Scandinavian journal of rehabilitation medicine.* 1979;11(1):29.

10. Curtis KA, Drysdale GA, Lanza RD, Kolber M, Vitolo RS, West R. Shoulder pain in wheelchair users with tetraplegia and paraplegia. *Archives of physical medicine and rehabilitation.* 1999;80(4):453-457.

11. Pentland W, Twomey L. The weight-bearing upper extremity in women with long term paraplegia. *Spinal Cord.* 1991;29(8):521-530.

12. Silfverskiold J, Waters RL. Shoulder pain and functional disability in spinal cord injury patients. *Clinical orthopaedics and related research.* 1991;272:141.

13. Samuelsson K, Tropp H, Gerdle B. Shoulder pain and its consequences in paraplegic spinal cord-injured, wheelchair users. *Spinal cord.* 2004;42(1):41-46.

14. Gerhart K, Bergstrom E, Charlifue S, Menter R, Whiteneck G. Long-term spinal cord injury: Functional changes over time. *Archives of physical medicine and rehabilitation.* 1993;74(10):1030.

15. Ballinger DA, Rintala DH, Hart KA. The relation of shoulder pain and range-of-motion problems to functional limitations, disability, and perceived health of men with spinal cord injury: a multifaceted longitudinal study. *Archives of physical medicine and rehabilitation.* 2000;81(12):1575-1581.

16. Robinson M, Hussey R, Ha C. Surgical decompression of impingement in the weightbearing shoulder. *Archives of physical medicine and rehabilitation.* 1993;74(3):324-327.

17. Goldstein B, Young J, Escobedo EM. Rotator Cuff Repairs in Individuals With Paraplegia1. *American journal of physical medicine & rehabilitation.* 1997;76(4):316.

18. Subbarao J, Klopfstein J, Turpin R. Prevalence and impact of wrist and shoulder pain in patients with spinal cord injury. *The journal of spinal cord medicine.* 1995;18(1):9.

19. Paletta GA, Warner JJP, Warren RF, Deutsch A, Altchek DW. Shoulder kinematics with two-plane x-ray evaluation in patients with anterior instability or rotator cuff tearing. *Journal of Shoulder and Elbow Surgery.* 1997;6(6):516-527.

20. Kibler WB. The role of the scapula in athletic shoulder function. *The American journal of sports medicine.* 1998;26(2):325-337.

21. Mell AG, LaScalza S, Guffey P, et al. Effect of rotator cuff pathology on shoulder rhythm. *Journal of Shoulder and Elbow Surgery.* 2005;14(1):S58-S64.

22. Deutsch A, Altchek DW, Schwartz E, Otis JC, Warren RF. Radiologic measurement of superior displacement of the humeral head in the impingement syndrome. *Journal of Shoulder and Elbow Surgery.* 1996;5(3):186-193.

23. Lukasiewicz A, McClure P, Michener L, Pratt N, Sennett B. Comparison of 3-dimensional scapular position and orientation between subjects with and without shoulder impingement. *The Journal of orthopaedic and sports physical therapy.* 1999;29(10):574.

24. Warner J, Micheli LJ, Arslanian LE, Kennedy J, Kennedy R. Scapulothoracic motion in normal shoulders and shoulders with glenohumeral instability and impingement syndrome. A study using Moire topographic analysis. *Clinical orthopaedics and related research.* 1992(285):191.

25. Lin J, Lim HK, Yang JL. Effect of shoulder tightness on glenohumeral translation, scapular kinematics, and scapulohumeral rhythm in subjects with stiff shoulders. *Journal of Orthopaedic Research.* 2006;24(5):1044-1051.

26. Endo K, Ikata T, Katoh S, Takeda Y. Radiographic assessment of scapular rotational tilt in chronic shoulder impingement syndrome. *Journal of orthopaedic science.* 2001;6(1):3-10.

27. Hébert L, Moffet H, McFadyen B, St-Vincent G. A method of measuring three-dimensional scapular attitudes using the optotrak probing system. *Clinical Biomechanics.* 2000;15(1):1-8.

28. Lin J, Hanten WP, Olson SL, et al. Functional activities characteristics of shoulder complex movements: exploration with a 3-D electromagnetic measurement system. *J Rehabil Res Dev.* 2005;42:199-210.

29. Illyés Á, Kiss RM. Kinematic and muscle activity characteristics of multidirectional shoulder joint instability during elevation. *Knee Surgery, Sports Traumatology, Arthroscopy.* 2006;14(7):673-685.

30. Ogston JB, Ludewig PM. Differences in 3-dimensional shoulder kinematics between persons with multidirectional instability and asymptomatic controls. *The American journal of sports medicine.* 2007;35(8):1361-1370.

31. von Eisenhart-Rothe R, Matsen III F, Eckstein F, Vogl T, Graichen H. Pathomechanics in atraumatic shoulder instability: scapular positioning correlates with humeral head centering. *Clinical orthopaedics and related research.* 2005;433:82.

32. Fayad F, Roby-Brami A, Yazbeck C, et al. Three-dimensional scapular kinematics and scapulohumeral rhythm in patients with glenohumeral osteoarthritis or frozen shoulder. *Journal of Biomechanics.* 2008;41(2):326-332.

33. Rundquist PJ. Alterations in scapular kinematics in subjects with idiopathic loss of shoulder range of motion. *The Journal of orthopaedic and sports physical therapy.* 2007;37(1):19.

34. CAROLYN MS, JAMES DM, WILLIAM SM. Occupational risk factors associated with soft tissue disorders of the shoulder: a review of recent investigations in the literature. *Ergonomics.* 1993;36(6):697-717.

35. Sommerich CM, McGlothlin JD, Marras WS. Occupational risk factors associated with soft tissue disorders of the shoulder: a review of recent investigations in the literature. *Ergonomics.* 1993;36(6):697-717.

36. Nygren A, Berglund A, Von Koch M. Neck-and-shoulder pain, an increasing problem. Strategies for using insurance material to follow trends. *Scandinavian journal of rehabilitation medicine. Supplement.* 1995;32:107.

37.   Meislin RJ, Sperling JW, Stitik TP. Persistent shoulder pain: epidemiology, pathophysiology, and diagnosis. *American journal of orthopedics (Belle Mead, NJ).* 2005;34(12 Suppl):5.

38.   Croft P, Pope D, Silman A. The clinical course of shoulder pain: prospective cohort study in primary care. Primary Care Rheumatology Society Shoulder Study Group. *BMJ: British Medical Journal.* 1996;313(7057):601.

39.   Bot SDM, van der Waal JM, Terwee CB, et al. Predictors of outcome in neck and shoulder symptoms: a cohort study in general practice. *Spine.* 2005;30(16):E459.

40.   Winters J, Sobel J, Groenier K, Arendzen J, Meyboom-de Jong B. The long-term course of shoulder complaints: a prospective study in general practice. *Rheumatology.* 1999;38(2):160-163.

41.   Chard M, Sattelle L, Hazleman B. The long-term outcome of rotator cuff tendinitis—a review study. *Rheumatology.* 1988;27(5):385-389.

42.   Vecchio P, Kavanagh R, Hazleman B, King R. Community survey of shoulder disorders in the elderly to assess the natural history and effects of treatment. *Annals of the rheumatic diseases.* 1995;54(2):152-154.

43.   Williams R, Westmorland M. Occupational cumulative trauma disorders of the upper extremity. *The American Journal of Occupational Therapy.* 1994;48(5):411-420.

44.   Neer CS. Anterior acromioplasty for the chronic impingement syndrome in the shoulder A preliminary report. *The Journal of Bone and Joint Surgery (American).* 1972;54(1):41-50.

45.   Rockwood CA, Lyons F. Shoulder impingement syndrome: diagnosis, radiographic evaluation, and treatment with a modified Neer acromioplasty. *The Journal of bone and joint surgery. American volume.* 1993;75(3):409.

46.   Brox JI, Staff PH, Ljunggren AE, Brevik JI. Arthroscopic surgery compared with supervised exercises in patients with rotator cuff disease (stage II impingement syndrome). *British medical journal.* 1993;307(6909):899-903.

47.   Bongers PM. The cost of shoulder pain at work. *Bmj.* 2001;322(7278):64-65.

48.   Van der Windt D, Koes BW, Boeke A, Deville W, De Jong BA, Bouter LM. Shoulder disorders in general practice: prognostic indicators of outcome. *The British Journal of General Practice.* 1996;46(410):519.

49.   Culham E, Peat M. Functional anatomy of the shoulder complex. *Journal of Orthopaedic and Sports Physical Therapy.* 1993;18:342-342.

50.   Ludewig PM, Reynolds JF. The association of scapular kinematics and glenohumeral joint pathologies. *The Journal of orthopaedic and sports physical therapy.* 2009;39(2):90.

51.   Lin J, Hanten WP, Olson SL, et al. Shoulder dysfunction assessment: self-report and impaired scapular movements. *Physical therapy.* 2006;86(8):1065-1074.

52.   Hébert L, Moffet H, McFadyen BJ, Dionne CE. Scapular behavior in shoulder impingement syndrome. *Archives of physical medicine and rehabilitation.* 2002;83(1):60-69.

53.   Laudner KG, Myers JB, Pasquale MR, Bradley JP, Lephart SM. Scapular dysfunction in throwers with pathologic internal impingement. *The Journal of orthopaedic and sports physical therapy.* 2006;36(7):485.

54.   McClure PW, Michener LA, Karduna AR. Shoulder function and 3-dimensional scapular kinematics in people with and without shoulder impingement syndrome. *Physical therapy.* 2006;86(8):1075-1090.

55.   Vermeulen H, Stokdijk M, Eilers P, Meskers C, Rozing P, Vlieland TPMV. Measurement of three dimensional shoulder movement patterns with an electromagnetic tracking device in patients with a frozen shoulder. *Annals of the rheumatic diseases.* 2002;61(2):115-120.

56.   Neer CS. Impingement lesions. *Clinical Orthopaedics and related research.* 1983;173:70.

57.   Rathbun JB, Macnab I. The microvascular pattern of the rotator cuff. *J Bone Joint Surg Br.* 1970;52(3):540-553.

58.   Fu FH, HARNER CD, KLEIN AH. Shoulder impingement syndrome: a critical review. *Clinical orthopaedics and related research.* 1991;269:162.

59.   Zuckerman JD, Kummer FJ, Cuomo F, Simon J, Rosenblum S, Katz N. The influence of coracoacromial arch anatomy on rotator cuff tears. *Journal of Shoulder and Elbow Surgery.* 1992;1(1):4-14.

60.   Jobe F, Bradley J. The diagnosis and nonoperative treatment of shoulder injuries in athletes. *Clinics in sports medicine.* 1989;8(3):419.

61.   Solem-Bertoft E, Thuomas K, Westerberg CE. The influence of scapular retraction and protraction on the width of the subacromial space. An MRI study. *Clinical orthopaedics and related research.* 1993(296):99.

62.   Graichen H, Stammberger T, Bonel H, et al. Three-dimensional analysis of shoulder girdle and supraspinatus motion patterns in patients with impingement syndrome. *Journal of orthopaedic research.* 2001;19(6):1192-1198.

63.   Freedman L, MUNRO RR. Abduction of the arm in the scapular plane: scapular and glenohumeral movements a roentgenographic study. *The Journal of Bone and Joint Surgery (American).* 1966;48(8):1503-1510.

64. Poppen N, Walker P. Normal and abnormal motion of the shoulder. *J Bone Joint Surg Am.* 1976;58(2):195-201.

65. Högfors C, Peterson B, Sigholm G, Herberts P. Biomechanical model of the human shoulder joint--II. The shoulder rhythm. *Journal of Biomechanics.* 1991;24(8):699-709.

66. Kondo M, Tazoe S, Yamada M. Changes of the tilting angle of the scapula following elevation of the arm. *Surgery of the Shoulder. Philadelphia, Pa: BC Decker Inc.* 1984:12-16.

67. Graichen H, Stammberger T, Bonel H, et al. Magnetic resonance based motion analysis of the shoulder during elevation. *Clinical orthopaedics and related research.* 2000;370:154.

68. Harryman DT, Sidles JA, Harris SL, Matsen FA. Laxity of the normal glenohumeral joint: a quantitative in vivo assessment. *Journal of Shoulder and Elbow Surgery.* 1992;1(2):66-76.

69. Koh T, Grabiner M, Brems J. Three-dimensional in vivo kinematics of the shoulder during humeral elevation. *Journal of applied biomechanics.* 1998;14:312-326.

70. Doody S, Freedman L, Waterland J. Shoulder movements during abduction in the scapular plane. *Archives of physical medicine and rehabilitation.* 1970;51(10):595.

71. Youdas JW, Carey JR, Garrett TR, Suman VJ. Reliability of goniometric measurements of active arm elevation in the scapular plane obtained in a clinical setting. *Archives of physical medicine and rehabilitation.* 1994;75(10):1137.

72. Ludewig PM CT, Nawoczenski DA. Three-dimensional scapular orientation and muscle activity at selected positions of humeral elevation. *J Orthop Sports Phys Ther.* 1996;24(2):57-65.

73. van der Helm FCT, Pronk GM. Three-dimensional recording and description of motions of the shoulder mechanism. *Journal of biomechanical engineering.* 1995;117:27.

74. McQuade K, Wei SH, Smidt G. Effects of local muscle fatigue on three-dimensional scapulohumeral rhythm. *Clinical Biomechanics.* 1995;10(3):144-148.

75. Cook TM, Ludewig P. Three-dimensional scapular orientation and muscle activity at selected positions of humeral elevation. *Journal of Orthopaedic Sports Physical Therapy.* 1996;24(2):57.

76. Karduna AR, McClure PW, Michener LA, Sennett B. Dynamic measurements of three-dimensional scapular kinematics: a validation study. *Journal of biomechanical engineering.* 2001;123:184.

77. Moriwaki M. Analysis of three-dimensional motion of the scapula and the glenohumeral joint]. *Nihon Seikeigeka Gakkai zasshi.* 1992;66(7):675.

78. Johnson G, Stuart P, Mitchell S. A method for the measurement of three-dimensional scapular movement. *Clinical Biomechanics.* 1993;8(5):269-273.

79. Karduna AR. Direct 3-dimensional measurement of scapular kinematics during dynamic movements in vivo. *J Shoulder Elbow Surg.* 2001.

80. McQuade K, Smidt G. Dynamic scapulohumeral rhythm: the effects of external resistance during elevation of the arm in the scapular plane. *The Journal of orthopaedic and sports physical therapy.* 1998;27(2):125.

81. Prager RW, Gee A, Berman L. Stradx: real-time acquisition and visualization of freehand three-dimensional ultrasound. *Medical Image Analysis.* 1999;3(2):129-140.

82. Guerra F, Isla A, Aguilar R, Fritz E. Use of free-hand three-dimensional ultrasound software in the study of the fetal heart. *Ultrasound in obstetrics & gynecology.* 2000;16(4):329-334.

83. Hashimoto S, Goto H, Hirooka Y, et al. An evaluation of three-dimensional ultrasonography for the measurement of gallbladder volume. *The American journal of gastroenterology.* 1999;94(12):3492-3496.

84. Gee A, Prager R, Treece G, Berman L. Engineering a freehand 3D ultrasound system. *Pattern Recognition Letters.* 2003;24(4):757-777.

85. Leroy A, Mozer P, Payan Y, Troccaz J. Rigid registration of freehand 3D ultrasound and CT-scan kidney images. *Medical Image Computing and Computer-Assisted Intervention– MICCAI 2004.* 2004:837-844.

86. Fu FH, HARNER CD, KLEIN AH. Shoulder impingement syndrome: a critical review. *Clinical Orthopaedics and Related Research.* 1991;269:162-173.

87. Bourne DA, Choo AM, Regan WD, MacIntyre DL, Oxland TR. Three-dimensional rotation of the scapula during functional movements: an in vivo study in healthy volunteers. *Journal of Shoulder and Elbow surgery.* 2007;16(2):150-162.

88. McClure PW. Direct 3-dimensional measurement of scapular kinematics during dynamic movements in vivo. *J Shoulder Elbow Surg.* 2001.

89. van Andel C, van Hutten K, Eversdijk M, Veeger D, Harlaar J. Recording scapular motion using an acromion marker cluster. *Gait & posture.* 2009;29(1):123-128.

90. Brochard S, Lempereur M, Rémy-Néris O. Accuracy and reliability of three methods of recording scapular motion using reflective skin markers. *Proceedings of the Institution of Mechanical Engineers, Part H: Journal of Engineering in Medicine.* 2011;225(1):100-105.

91. Finley MA, Rodgers MM. Prevalence and identification of shoulder pathology in athletic and nonathletic wheelchair users with shoulder pain: a pilot study. *Journal of rehabilitation research and development.* 2004;41(3B):395-402.

92. Meskers C, Vermeulen H, De Groot J, Van der Helm F, Rozing P. 3D shoulder position measurements using a six-degree-of-freedom electromagnetic tracking device. *Clinical Biomechanics.* 1998;13(4):280-292.

93. Bourne D, Choo A, Regan W, MacIntyre D, Oxland T. Accuracy of digitization of bony landmarks for measuring change in scapular attitude. *Proceedings of the Institution of Mechanical Engineers, Part H: Journal of Engineering in Medicine.* 2009;223(3):349-361.

94. Wu G vdHF, Veeger HE, Makhsous M, Van Roy P, Anglin C, Nagels J,, Karduna AR MK, Wang X, Werner FW, Buchholz B. ISB recommendation on definitions of joint coordinate systems of various joints

for the reporting of human joint motion--Part II: shoulder, elbow, wrist and

hand. *J Biomech.* May 2005;38(5):981-992.

95. Ephiphan. Technical Specifications. 2013; http://www.epiphan.com/products/dvi-frame-grabbers/dvi2usb-duo/specifications/. Accessed 3/28/2013.

96. Landis JR, Koch GG. The measurement of observer agreement for categorical data. *biometrics.* 1977:159-174.

97. Laumann U. Kinesiology of the shoulder joint. *Shoulder Replacement*: Springer; 1987:23-31.

98. Van der Helm F, Pronk GM. Three-dimensional recording and description of motions of the shoulder mechanism. *Journal of Biomechanical Engineering.* 1995;117(1):27.

99. Inman VT, Abbott LC. Observations on the function of the shoulder joint. *The Journal of Bone & Joint Surgery.* 1944;26(1):1-30.

100. Bayley JC, Cochran TP, Sledge CB. The weight-bearing shoulder. The impingement syndrome in paraplegics. *Journal of Bone and Joint Surgery - Series A.* 1987;69(5):676-678.

101. Curtis K, Roach K, Applegate E, et al. Reliability and validity of the wheelchair user's shoulder pain index (WUSPI). *Spinal Cord.* 1995;33(10):595-601.

102. Brose SW, Boninger ML, Fullerton B, et al. Shoulder ultrasound abnormalities, physical examination findings, and pain in manual wheelchair users with spinal cord injury. *Archives of physical medicine and rehabilitation.* 2008;89(11):2086-2093.

103. Curtis K, Roach K, Applegate EB, et al. Development of the wheelchair user's shoulder pain index (WUSPI). *Spinal Cord.* 1995;33(5):290-293.

104. Curtis K, Tyner T, Zachary L, et al. Effect of a standard exercise protocol on shoulder pain in long-term wheelchair users. *Spinal cord.* 1999;37(6):421-429.

105. Finley MA, Lee RY. Effect of sitting posture on 3-dimensional scapular kinematics measured by skin-mounted electromagnetic tracking sensors. *Archives of physical medicine and rehabilitation.* 2003;84(4):563-568.

106. Burnham RS, May L, Nelson E, Steadward R, Reid DC. Shoulder pain in wheelchair athletes The role of muscle imbalance. *The American journal of sports medicine.* 1993;21(2):238-242.

107. Cook TM, Ludewig P. Translations of the humerus in persons with shoulder impingement symptoms. *Journal of Orthopaedic & Sports Physical Therapy.* 2002;32(6):248.

108. Fayad F, Hoffmann G, Hanneton S, et al. 3-D scapular kinematics during arm elevation: effect of motion velocity. *Clinical Biomechanics.* 2006;21(9):932-941.

109. Pascoal AG, van der Helm FF, Pezarat Correia P, Carita I. Effects of different arm external loads on the scapulo-humeral rhythm. *Clinical Biomechanics.* 2000;15:S21-S24.

110. Kon Y, Nishinaka N, Gamada K, Tsutsui H, Banks SA. The influence of handheld weight on the scapulohumeral rhythm. *Journal of Shoulder and Elbow surgery.* 2008;17(6):943-946.

111. Michiels I, Grevenstein J. Kinematics of shoulder abduction in the scapular plane: on the influence of abduction velocity and external load. *Clinical Biomechanics.* 1995;10(3):137-143.

112. Myers JB, Laudner KG, Pasquale MR, Bradley JP, Lephart SM. Scapular position and orientation in throwing athletes. *The American journal of sports medicine.* 2005;33(2):263-271.